Graduate School Form 9
(Revised 6/03)

PURDUE UNIVERSITY
GRADUATE SCHOOL
Thesis Acceptance

This is to certify that the thesis prepared

By Gustavo J. Rodriguez

Entitled

Molecular Insights Into the Translocation Mechanism for Substrates by the Serotonin Transporter

Complies with University regulations and meets the standards of the Graduate School for originality and quality

For the degree of Doctor of Philosophy

Signed by the final examining committee:

Chair

Approved by: Vincent J. Davisson 02/27/04
Head of the Graduate Program Date

This thesis ☐ is ☒ is not to be regarded as confidential.

Major Professor

Format Approved by:

Chair, Final Examining Committee or Department Thesis Format Advisor

MOLECULAR INSIGHTS INTO THE TRANSLOCATION MECHANISM FOR SUBSTRATES BY THE SEROTONIN TRANSPORTER

A Thesis
Submitted to the Faculty
of
Purdue University
by
Gustavo J. Rodríguez

In Partial Fulfillment of the
Requirements for the Degree
of
Doctor of Philosophy

May 2004

To my parents and Hecmary

ACKNOWLEDGMENTS

I want to thank my graduate committee members for all their guidance during this journey, especially Dr. Eric L. Barker for being a great mentor and friend. To Drs. David Nichols, Gregory Hockerman, and William Cramer, my gratitude for all of your advice. I am honored to have great mentors like you on my committee, and I wish the best in your research.

I also want to thank my friends: Med, Dave, Kellie, Matt, Crystal, Melissa, Marla, and our former lab manager, Fred for your friendship. Special thanks to Kellie for her assistance during the process of writing this thesis. For all of you my best wishes in your journeys and I hope that we can meet again to catch up on great times, especially to share more of Matt's stories.

For my family and friends back in Puerto Rico, especially my parents Mercedes and Andres, and my wife Hecmary, thank you for always being there and believing in me. I thank God every second of my life for having the best family that a person could ask for. You were an essential support that helped me to finish this goal. Thank you to Marta Chamorro for showing me the beauty of science and research. You inspired me to follow a career in this business and my Ph.D. is one way to say: "gracias, gracias, gracias". You are the best teacher and mentor that a student could have. To my friends at home, I want to say this to you: "Cuenta conmigo en todo momento para lograr tus metas y sueños, como yo he contado contigo para lograr este".

TABLE OF CONTENTS

Page

Page

LIST OF TABLES

LIST OF FIGURES

Figure Page

Figure Page

LIST OF ABBREVIATIONS

5-HT	Serotonin
SERT	Serotonin transporter
MPP^+	N-methyl-4-phenylpyridinium
MMAI	5-methoxy-6-methyl-2-aminoidan
hSERT	Human serotonin transporter
dSERT	*Drosophila* serotonin transporter
DA	Dopamine
NE	Norepinephrine
DAT	Dopamine transporter
NET	Norepinephrine transporter
GABA	γ-Aminobutyric acid
GAT	γ-Aminobutyric acid transporter
GLYT	Glycine transporter
SGTL	Secondary active Na^+-dependent glucose transporter
GLUT	Facilitated glucose transporter
MDR	Multidrug resistance transporter
CFTR	Cystic fibrosis transmembrane regulator
NBD	Nucleotide binding domain
EAAT	Excitatory amino acid transporter
VMAT	Vesicular monoamine transporter
HEK	Human embryonic kidney cell line
KRH	Krebs-Ringer-HEPES Buffer
PBS/CM	Phosphate buffer saline with calcium and magnesium chloride
SCAM	Substituted-cysteine accessibility method
MTS	Methanethiosulfonate

MTSET	[2-(Trimethylammonium)ethyl] Methanethiosulfonate
MTSES	[2-(trimethylammonium)ethyl] Methanethiosulfonate
TMD	Transmembrane domain
EL	Extracellular loop

ABSTRACT

Rodríguez, Gustavo J. Ph.D., Purdue University, May 2004. Molecular Insights into the Translocation Mechanism for Substrates by the Serotonin Transporter. Major Professor: Eric L. Barker.

The serotonin transporter (SERT) is responsible for regulating the serotonin (5-HT) concentration in the synapse. I used human and *Drosophila* serotonin transporters (hSERT and dSERT, respectively) to explore differences in substrate recognition. hSERT and dSERT showed similar K_m values for 5-HT transport, suggesting similar recognition of 5-HT by the two species variants. Interestingly, another substrate, *N*-methyl-4-phenylpyridinium (MPP^+), was transported only by hSERT. However, MPP^+ inhibited 5-HT uptake in both species variants with similar potencies. Guided by studies using hSERT/dSERT chimeras, the region encompassing transmembrane domains (TMDs) V to IX was implicated in substrate recognition and transport. Residues in the TMDs V to VIII region divergent between hSERT and dSERT as well the two phenylalanines at position 551 and 556 of hSERT were mutated. Mutants V366S, M370L, S375A, T381S, and F556S showed a decrease in transport capacity for 5-HT and MPP^+ uptake in comparison with wild-type. Residues V366, M370, and T381 are predicted to face the same region of TMD VII, whereas S375 is localized on the other side of this α-helix. F556 is predicted to be localized in TMD XI, close to the extracellular side. To further explore the role of these residues in the transport process, I generated cysteine mutants at positions S365, V366, M370, S375, F380, T381, F551 and F556. Pretreatment with the cysteine-modifying reagent MTSET

([2-(trimetylammonium)ethyl]methanethiosulfonate) caused a decrease in transport of [^{3}H]5-HT in V366C, M370C, and F556C mutants. MTSET also disrupted [^{3}H]MPP$^+$ uptake in F556C. Replacement of sodium with lithium did not prevent MTSET from interacting with V366C, M370C, or F556C mutants. However, 5-HT partially protects these sites from MTS interaction in the presence of lithium. My data suggest that V366, M370, and F556 are localized in or near the permeation pathway used for substrate translocation. These studies as well as mutagenesis and SCAM data from monoamine transporters were used to generate models for substrate permeation and TMD arrangement for SERT.

Supported by NIH grant MH60221 and APA Minority Fellowship in Neuroscience.

CHAPTER I

INTRODUCTION

Importance of membrane transport

Cells use different modes of transport to obtain essential molecules and ions from the extracellular environment. Biological transport systems are responsible for keeping the ion balance, pH, and osmolarity within the cell (Copper, 2000). In eukaryotic cells, intracellular transport is necessary to translocate molecules, including mRNA, Ca^{2+}, and ATP, between compartments. Furthermore, prokaryotic and cancer cells depend on translocation processes for their survival, by expelling cytotoxic compounds (Higgins, 1992).

The chemical and physical properties of the lipid membrane limit and control the traffic of water and other small neutral molecules, ions like Na^{+}, K^{+}, Cl^{-}, and Ca^{2+} among others, sugars, peptides and proteins, charged molecules, and lipids (Cooper, 2000). To achieve the balance necessary for their survival, cells depend on several transport mechanisms including passive diffusion, facilitated diffusion, and active transport. Small molecules like O_2 and CO_2 are able to diffuse through the membrane without the assistance of proteins. Cells use membrane proteins that work as channels or transporters to transport charged and hydrophilic structures. Ion channels and some transporters facilitate the diffusion of substrates like sodium and glucose by providing a permeation pathway to cross the membrane. The transport by facilitated diffusion follows a concentration gradient when the solute is translocated down its concentration gradient without the coupling of an external energy source. Transport systems that require a source of energy are classified as primary or

secondary transport. These systems use the hydrolysis of ATP directly or ion gradients indirectly to transport solutes against their concentration.

Modes of substrate transport

Passive diffusion

Passive or simple diffusion is the movement of the solute across the membrane down the electrochemical gradient without the assistance of a transport protein. Passive diffusion does not require any biological energy, but follows Fick's law, which postulates that the water-hydrocarbon interface is stable and the rate of solute transfer is governed solely by the solubility of the solute and its diffusion characteristics in the hydrocarbon domain of the membrane (Sten-Kurdsen, 1978). This theory implies that solutes become physically "dissolved" in the membrane and move by random molecular-molecular motion through the membrane. The random movement across two compartments increases the entropy of the system stabilizing this process. Several factors alter the diffusion of molecules through the membrane including: (1) temperature which affects the random movement of molecules, (2) viscosity that influences the free movement of solutes, (3) size, shape, and electrical charge of the solute, (4) relative solubility of the molecule in the aqueous and lipid regions, (5) solvent flow in the membrane, and (6) the surface of the membrane accessible to solute. Many small lipid-soluble molecules such as oxygen, nitrogen, carbon dioxide, and ammonia are transported by simple diffusion through biological membranes (Cooper, 2000).

Facilitated Diffusion

Hydrophilic molecules and ions are unable to cross the membrane by passive diffusion. Cells use membrane proteins to obtain such essential

components from their environment. Transmembrane proteins involved in facilitated diffusion form water-filled pores in the membrane providing a permeation pathway for ions and molecules. These membrane proteins are classified in two major groups: transporters or permeases and channels. In both cases, the transport of solute follows the concentration gradient allowing the translocation to occur without an external source of energy. Facilitated diffusion shows vectorial transport in a favorable direction and displays saturation kinetics (Stein, 1986).

Ion channels consist of a single or an assembly of proteins that form a pore where ions cross the membrane down their electrochemical gradient (Stein, 1986). These proteins open and close a pore gate in response to various signals. Channel proteins are classified in four major groups: (1) ligand-gated, (2) mechanically-gated, (3) voltage-gated, and (4) light-gated channels. Ion channels are specific and the transport rate is faster than that observed in transporter proteins (Cooper, 2000). In an open stage, the transport rate in channels is limited by the diffusion of ions through the pore, whereas transporter proteins are limited by the conformational changes required to move the substrate from one compartment to another. Among the physiologically relevant characteristics of this transport mechanism, ion movement through the channel produces currents across the membrane important in maintaining membrane potential and propagating action potentials in excitable cells.

Glucose enters the erythrocyte by facilitated diffusion via a specific glucose permease (Cooper, 2000). Typically, sugars are in higher concentration outside the cell. The concentration gradients provide net forces directed from outside to inside the cell. Carrier proteins or transporters bind sugars on the external surface of the membrane and move them into the cell using the energy generated in the concentration gradients.

Active Transport

Frequently, cells need to transport molecules against their concentration gradient. Similar to facilitated diffusion, transporter proteins localized in the cell membrane provide the permeation pathway for these molecules to enter the cell. These proteins are called active transporter proteins and require an external source of energy (i.e. ATP hydrolysis) to transport solutes across the membrane. The two major mechanisms for obtaining the energy necessary for solute movement are ATP hydrolysis or coupling to an ion gradient (Copper, 2000). Active transport systems are classified as primary or secondary active transport.

Primary transporters directly use energy to transport solutes. One of the most important primary transporters in the cell is the Na^+/K^+ ATPase. In animals, the intracellular concentration of sodium is lower than in the extracellular environment. Conversely, the potassium concentration is higher inside the cell than in the extracellular fluids. The Na^+/K^+ ATPase hydrolyzes ATP to pump three ions of sodium outside the cell and translocate two potassium ions into the cytoplasm (Copper, 2000). This process is essential for maintaining the membrane potential and the osmotic balance. ABC (ATP-binding cassette) transporters are another type of primary active carrier. This family of transporter proteins uses the hydrolysis of ATP to transport a wide variety of molecules ranging from ions and xenobiotic compounds to lipids, peptides, and proteins (Higgins, 1992).

Secondary transporters indirectly use energy to transport molecules against their concentration gradient. This group of transporters does not couple substrate translocation with ATP hydrolysis, instead, an ion gradient (generally sodium) enables the translocation of solutes across the membrane. The electrochemical gradient is either generated in the same or opposite direction to the movement of the solute. In either case, the Na^+/K^+ ATPase is necessary for maintaining the electrochemical gradient. Co-transporters or symporters use the gradient generated by moving ions from higher to lower concentrations to

transport the substrate in the same direction of the ion flux (Copper, 2000). An example of a symporter is the active glucose transporter that couples sodium ions to glucose transport into the cell (Gould and Bell, 1990). Counter-transport is the movement of two or more ions or solutes in opposite directions across the membrane. By moving ions down their concentration gradient to generate electrochemical energy (increasing the entropy of the system) these antiporters are able to translocate solutes against their concentration.

The structure of two secondary transport proteins expressed in *Escherichia coli*, the lactose permease (LacZ) and the glycerol-3-phosphate transporter (GlpT), were elucidated at high resolution (Abramson et al., 2003;Huang et al., 2003). Both structures show two domains of six transmembrane helices symmetrically positioned within the transporters, forming the pore for substrate translocation. The GlpT binding site, a centrally positioned substrate-translocation pore, is located closed off from the periplasm by two arginines. Upon substrate binding, the protein adopts a more compact conformation. The proposed mechanism predicts that GlpT operates by a single-binding site alternating-access mechanism through a rocker-switch type of movement, which implies the transport of one molecule of the substrate per turnover cycle. The elucidation of the LacZ structure also supports the alternating-access mechanism suggesting that secondary transporters use similar mechanisms for substrate translocation (Abramson, et al. 2003). The translocation mechanism is proposed to consist of six steps: (i) protonation of LacZ; (ii) binding of lactose; (iii) a conformational change that closes the gate facing the extracellular side and opens the gate to the cytoplasm; (iv) release of lactose into the cytoplasm; (v) release of a proton; and (vi) return of the empty transporter to the outward-facing conformation. The relative positions of the residues determined for the LacZ structure in the protonated inward-facing conformation with bound substrate are consistent with the proposed structure for this state derived from biochemical studies (Kaback et al., 2001).

Transporter Families

Glucose Transporters

Glucose is an important source of energy for living organisms. Cells use membrane proteins that mediate the transport of glucose into the cytoplasm. This process is stereospecific as D-glucose is the endogenous substrate for these proteins. The glucose transporter family is composed of two subgroups: the secondary active Na^+-dependent glucose transporters (SGLT1 and SGLT2) (Turk et al., 1996) and the facilitated glucose transporters (GLUT1-5) (Gould and Bell, 1990).

Sequence analysis of SGLT proteins suggests a topology with fourteen putative α-helices (Turk et al., 1996) with a leucine zipper domain on the extracellular loop that may be involved in formation of oligomers (Fig 1.1A). SGLT proteins transport glucose using a sodium gradient as the driving force for substrate transport (Oulianova and Berteloot, 1996, Fig 1.1B). SGLT1 and SGLT2 however, differ in the ion/substrate stoichiometry for substrate transport. SGLT1 requires one ion of sodium with one molecule of glucose per cycle whereas SGLT2 couples glucose transport with two ions of sodium. The sodium gradient is maintained by the Na^+/K^+ ATPase in the basolateral membrane. This subgroup of transporters is distributed in the mucosal cells of the intestine and the proximal tubular cells of the kidney (Oulianova and Berteloot, 1996). The major role of these proteins is to guarantee an efficient absorption of glucose from the diet as well as minimize the loss of this important nutrient in the urine.

Despite sharing approximately 60% sequence identity, the pharmacology of SGLTI and SGLT2 are vastly different. Glucose translocation by SGLT1 is a high-affinity ($K_m \approx 0.2$ μmol/L), low-capacity ($V_{max} \approx 4.0$ nmol/min per mg of protein) process (Turner and Moran, 1982). The accumulated glucose in mucosal cells is released in the bloodstream by facilitated glucose transporters. This process is nonspecific as SGLT1 also transports galactose with similar

Figure 1.1: Predicted topology of secondary-active glucose transporter (A) and proposed transport mechanism for substrate uptake (B). (A) Topology of the human sodium-dependent glucose transporter. Experimental analysis indicates fourteen transmembrane α-helices, an extracellular N-terminus, a large intracellular loop localized between TMDs XIII and XIV, and the TMD XIV formed by the C-terminus. (B) The proposed mechanism for glucose translocation by SGLT consists of five steps: (1) Sodium binds to the transporter from the external medium; (2) glucose binds to the transporter-sodium complex; (3) the transporter changes to a conformation that faces the cytoplasm and allows glucose release; (4) sodium is released into the cytoplasm; and (5) the empty transporter returns to the conformation facing the extracellular environment to start another cycle.

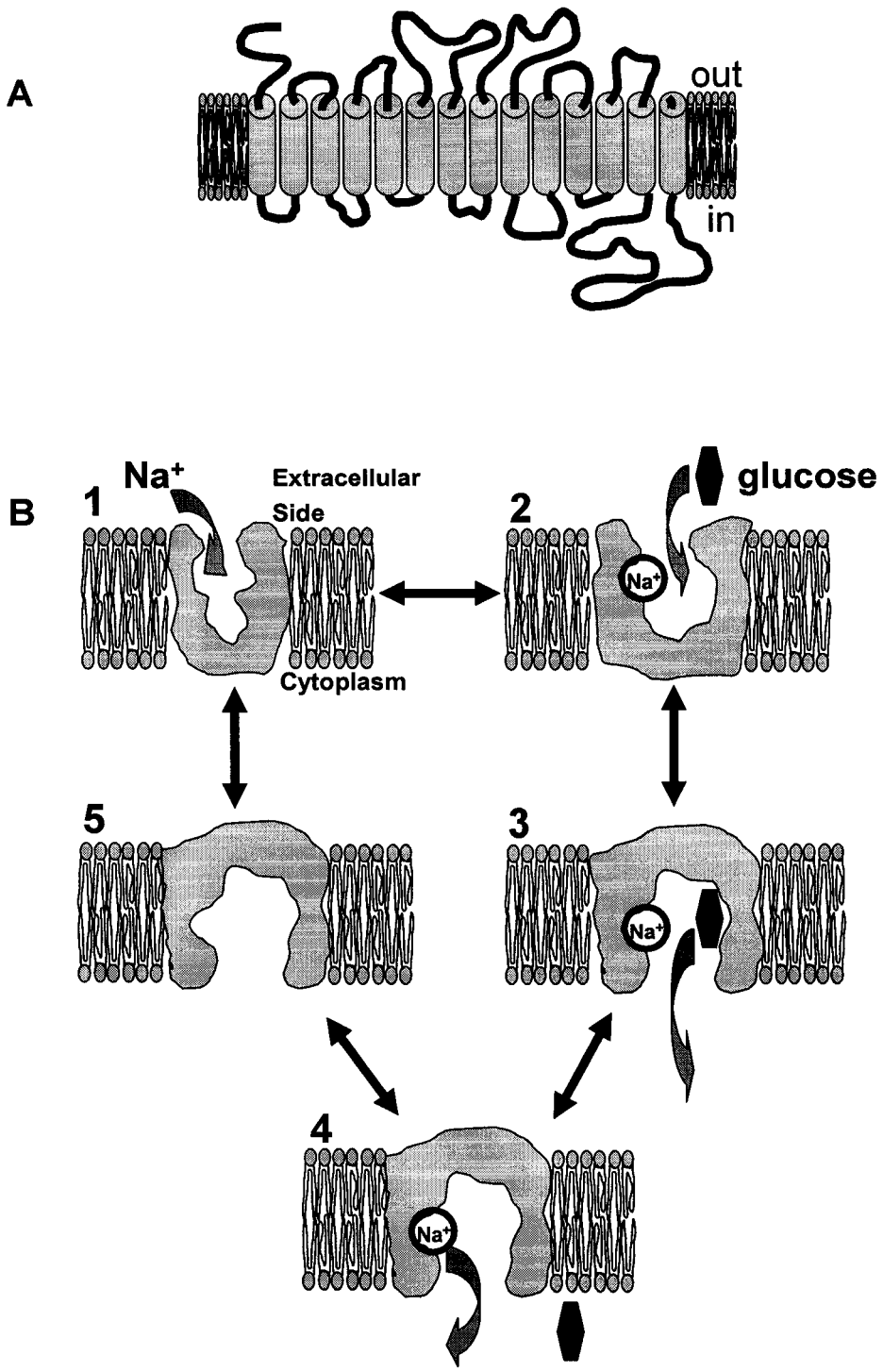
A
out
in
B
1
Na+
Extracellular
Side
Cytoplasm
2
glucose
Na+
3
Na+
4
Na+
5

Figure 1.1

efficiency. The reabsorption of glucose in the kidneys involves SGLT1 and SGLT2. Glucose transport through SGLT2 is a low-affinity ($K_m \approx 10$ mmol/L), high-capacity ($V_{max} \approx 10$ nmol/min per mg of protein) process (Turner and Moran, 1982). SGLT2 expressed in the proximal tube, however, is responsible for the majority of the reabsorption of glucose. The glucose remaining in the kidneys is then absorbed by SGLT1.

The uptake of glucose in other tissues involves facilitated transport. To date, four facilitated transporters (GLUT 1-4) have been cloned and extensively characterized (Olson and Pessin, 1996). Although structurally similar to the other GLUT transporters, GLUT5 is specific for fructose (Burant et al., 1992). Two other GLUT genes have been reported: GLUT6 (Kayano et al., 1990), a nonfunctional pseudogene, and the GLUT7 gene expressed in the endoplasmic reticulum of hepatic cells (Waddell et al., 1992) but more studies need to be performed to definitively include this protein in the glucose transporter family. GLUT1 has been extensively studied and many of its properties also apply to the other isoforms (Walmsley et al., 1998). Hydropathy analysis of the primary sequence of GLUT1 predicts twelve putative transmembrane α-helices (Fig 1.2A). Sequence analysis shows that transmembrane domains (TMDs) III, V, VII, VIII, and XI are amphipathic and may form part of the permeation pathway for glucose transport. Studies in the other GLUT transporter isoforms show similar characteristics. GLUT1 topology reveals cytoplasmic N- and C-termini as well as a large loop between TMDs VI and VII. The only N-glycosylation site is present on a large extracellular loop between TMDs I and II. Site-specific trypsin-digestion, antibodies against the C-terminus, and mutagenesis studies have provided solid evidence supporting the predicted topology (Olson and Pessin, 1996). The structure of GLUT1 has also been studied using different biophysical techniques. Fourier-transforming infrared (FTIR) studies, which analyzes secondary structure of proteins in aqueous environments, demonstrate that GLUT1 (purified and reconstituted in lipid bilayers) is composed mostly of α-

Figure 1.2: Predicted topology (A) and the proposed mechanism of glucose transport (B) by the facilitated glucose transporter. (A) Hydropathy analysis of the primary sequence of GLUT1 predicts twelve putative TMDs with both N- and C-termini intracellulary located and a large extracellular loop with several glycosylation sites between TMDs I and II. (B) Schematic model proposed glucose translocation process by facilitated-transport. Upon glucose binding (1), the transporter changes its conformation to allow the translocation of the substrate (2 and 3). After substrate release, GLUT returns to the original conformation to initiate another cycle (4). Because the driving force for GLUT is the glucose gradient, the direction of the translocation will be determined by the glucose concentration.

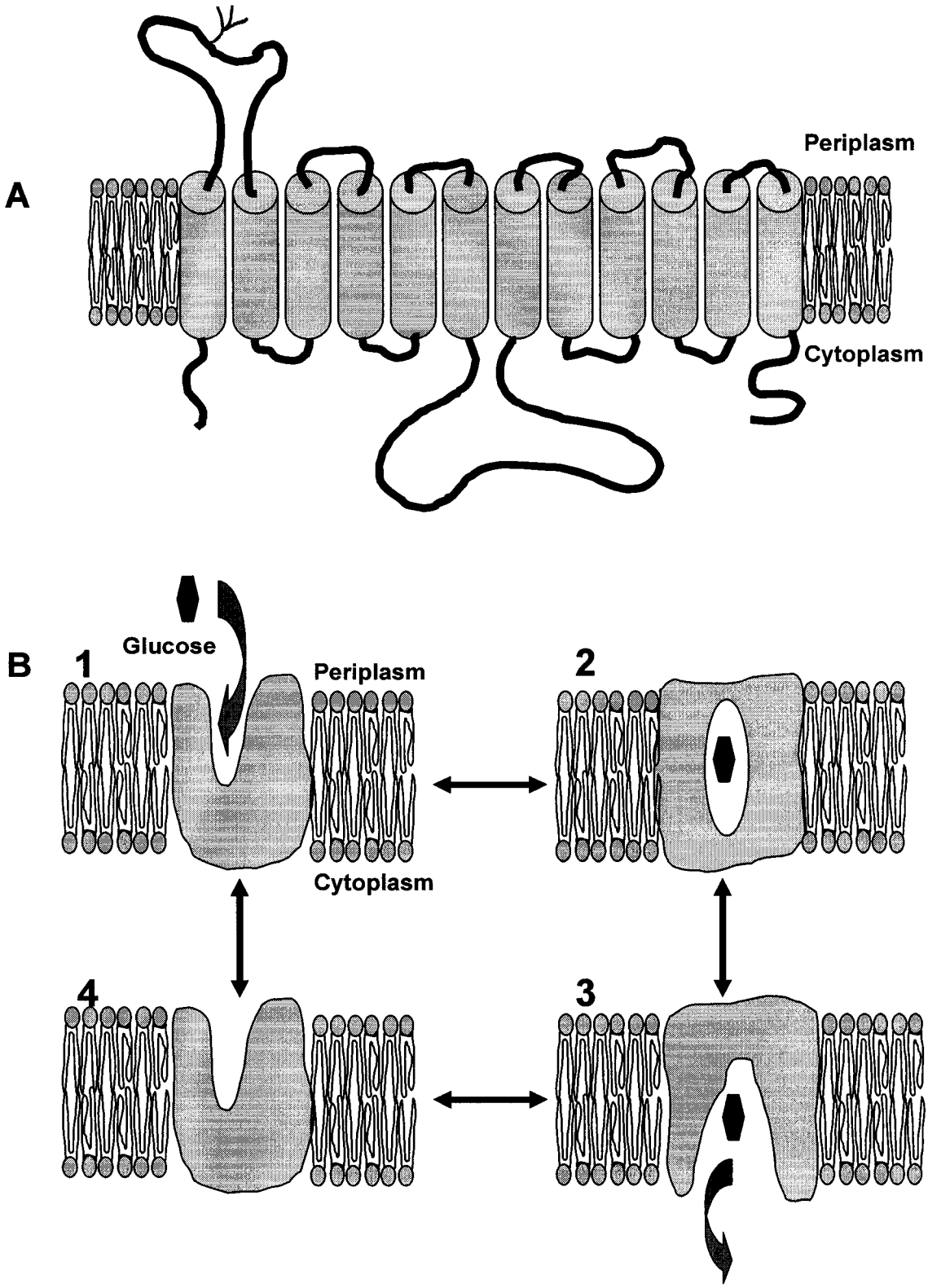

Figure 1.2

helices with some regions of β-sheet, β-turns, and random coil (Alvarez et al., 1987). Polarized FTIR suggests that the α-helices are orientated perpendicular to the planar membrane with a tilt of > 38° from the membrane normal (Chin et al., 1987). Although no β-sheet structure was detected, circular dichroism studies support FTIR results for GLUT1 predicting 82% of the sequence is α-helical (Chin et al., 1987). Hydrogen-deuterium exchange of reconstituted GLUT1 shows that 80% of the protein backbone is accessible to the aqueous environment (Jung et al., 1986;Alvarez et al.,1987). Regions predicted to be α-helical demonstrated slow exchange supporting the hydrophobic environment in the membrane. These studies, although not representative of a three-dimensional structure for GLUT1, support the presence of the predicted hydrophilic pore.

GLUT1 is highly expressed in endothelial cells of the microvasculature of the brain and is responsible for glucose permeation through the blood-brain barrier. This GLUT isoform is also distributed in astrocytes which play an important role in the delivery of glucose to neurons (Brown, 2000). The GLUT1 transport process exhibits simple Michalis-Menton kinetics similar to other facilitated transporters. The most accepted transport model for glucose translocation is the alternating-access (Fig 1.2B). This model predicts a binding site for glucose that may be accessible from either side of the membrane, but not to both sides simultaneously. Upon glucose binding, the transporter changes its conformation to allow the translocation of the substrate. After substrate release, GLUT returns to the original conformation to initiate another cycle. Because the driving force for GLUT is the glucose gradient, the direction of the translocation will be determined by the glucose concentration (Gould and Bell, 1990). Furthermore, GLUTs, like other transporters, exhibit a phenomenon called trans-acceleration. This concept describes the vectorial acceleration of labeled substrate induced by the presence of unlabeled substrate on the opposite site (Lieb, 1982). In GLUTs, the rate of reorientation of the occupied transporter is

faster than when the transporter is empty providing evidence of the trans-acceleration phenomena (Lieb, 1982).

Among the glucose transporter family, GLUT4 is the only member whose activity is regulated by insulin (Elmendorf, 2002;Furtado et al., 2002). Prior to the cloning of GLUT4, studies using adipose tissue demonstrated that insulin increased the number of glucose transporters at the cell surface(Wardzala et al., 1978), subsequently reducing the intracellular pool of glucose transporters relative to control (Cushman and Wardzala, 1980). This insulin-stimulated effect is also observed in skeletal muscle cells (Marette et al., 1992;Li et al., 2001). Interestingly, GLUT4 is highly expressed in muscle and fat tissue (Furtado et al., 2002).

The insulin-mediated regulation of GLUT4 function and trafficking to the plasma membrane has been extensively studied (For review Khan and Pessin, 2002). Insulin binding to its receptor tyrosine kinase initiates a signaling pathway that includes the phosphorylation of several intracellular proteins. Among these proteins is the insulin receptor substrate (IRS). IRS is the docking site for p85, the regulatory subunit of type I phosphatidylinositol 3-kinase (PI3K). PI3K increases the level of phosphatidylinositol 3,4,5-trisphophate (PIP_3) initiating a signal cascade that activates 3'-phosphoinositide-dependent kinase-1 (PDK-1). The protein kinase B/Akt family and protein kinase C isoforms λ and ζ are the downstream targets of the PI3K/PDK-1 signaling cascade. Phosphorylation of these two kinase groups mediates the trafficking of GLUT4 to the surface from an intracellular pool (Elmendorf, 2002;Khan and Pessin, 2002). Despite the vast information regarding this mechanism, further studies are necessary to understand the mechanism of translocation and the protein machinery responsible for the trafficking and insertion of GLUT4 in the membrane. Recent studies reveal a PI3K-independent mechanism of insulin-stimulated GLUT4 translocation. Although less understood, this mechanism involves a series of signaling proteins confined to lipid rafts (Elmendorf, 2002).

The discrepancy in the magnitude of GLUT4 trafficking to the cell membrane and the transport capacity of GLUT4 suggests another mechanism of insulin-mediated GLUT4 regulation in addition to that previously described. In a series of experiments, Klip and coworker found that the inhibition of p38 mitogen activating protein kinase (MAPK) reduces the translocation of glucose (Furtado et al., 2002). The MAPK inhibitors SB202190, and SB203580, which selectively interact with the α and β isoforms of MAPK, respectively, reduced the insulin-stimulated 2-deoxyglucose uptake by 60% without affecting GLUT4 trafficking to the surface supporting the regulation of GLUT4 function by the MAPK pathway (Furtado et al., 2002).

ABC Transporters

ABC transporters represent one of the largest families of transporters found in prokaryotic and eukaryotic organisms (Higgins, 1992;Ames et al., 1992). This family of membrane proteins is involved in translocation of a wide variety of substrates including ions, peptides, sugars, lipids and cytotoxic drugs (Higgins, 1992). Several ABC transporter members possess clinical relevance such as the cystic fibrosis transmembrane regulator (CFTR), the multidrug resistant P-glycoprotein (MDR), ABCA and ABCG transporters (important for cholesterol metabolism), and the rim protein (Higgins, 1992).

CFTR is an interesting member of the ABC transporter family because it is a chloride channel rather than a pump or transporter (McCarty, 2000). CFTR is a polypeptide with two membrane-spanning regions consisting of six α-helices, two nucleotide-binding domains (NBD), and a regulatory domain in the cytoplasm between the first NBD and the second TMD. Mutations in the CFTR gene cause cystic fibrosis (CF), a genetic disease affecting approximately 30,000 children and adults in the United States (from Cystic Fibrosis Foundation website, http://www.cff.org). Most of the mutations detected in CF patients affect the folding of the protein and abolish the sorting and membrane insertion of CFTR.

The most common allele (representing approximately 60% of the cases) is the deletion of the codon that encodes a phenylalanine at position 508 causing the intracellular retention of the protein.

MDR proteins are key components in the ineffectiveness of different agents in the treatment of infections and chemotherapy. Several studies have detected overexpression of MDR proteins in cancer and prokaryotic cells, thus, reflected by an increase in the flux of cytotoxic drugs out of the cell. Charged and polar residues within the membrane-spanning region of the transporter have been implicated in the function of this subgroup of ABC transporters. For example, several charged residues in the BmrR protein, an MDR protein expressed in *Bacillus subtilis*, play an important role in the translocation of substrates. Although the substrates for MDR transporters are highly hydrophobic, all possess either electrical charges or polar regions in their structure that are presumed to interact with the hydrophilic residues in the transporter (Neyfakh, 2002). Recently, electron microscopy of MDR protein revealed a relatively large chamber inside the protein with two gates facing the membrane (Rosenberg et al., 2001). Presumably, the chamber can accommodate a wide variation of structurally-diverse molecules during the transport process. The gate facing the inner side of the pore observed in the MDR structure supports an early observation that substrates are transported from the inner face of the membrane rather than from the cytoplasm (Higgins and Gottesman, 1992). Furthermore, the second gate observed in MDR protein suggests the translocation of substrates to the outer membrane.

The rim protein (ABCR) is a membrane glycoprotein that has been localized to the rims of photoreceptor outer segment discs, but whose function is not well understood (Allikmets et al., 1997a;Biswas and Biswas, 2000;Sun and Nathans, 2000). Mutations in the ABCA 4 gene, which encodes for the ABCR protein, are responsible for a large variety of retinal degenerations including all cases of Stargardt macular dystrophy and fundus flavimaculatus, some forms of cone-rod degeneration and retinitis pigmentosa, and likely increases the risk of

developing age-related macular degeneration (Allikmets et al., 1997a,b). ABCR is hypothesized to transport a complex of retinaldehyde and phosphatidylethanolamine in the retina of the eye.

Recently, several groups have identified four ABC transporters (ABCA1, ABC1, ABCG5, and ABCG8) that modulate cholesterol and lipoprotein metabolism. Mutations in the ABCA1 gene were discovered in patients with Tangier disease, a genetic disorder that affects cholesterol transport. Biochemical and genetic studies implicate ABCA1 in the efflux of phospholipids and cholesterol to apo-A-1, producing pre-β HDL (high density lipoprotein).

Numerous biochemical and biophysical studies have tried to determine the structure of the ABC transporters. The general topology includes twelve TMDs generally in packages of six and two NBD sites (Higgins, 1992, Figure 1.3B). These domains are either found in separate proteins that form a complex that forms the pore (generally in prokaryotes) or are expressed as a full polypeptide. Several ABC transporters exhibit a topology that includes a third membrane-spanning region as determined for the ABCC2 drug-pump. The greatest homology among the ABC transporters is found within the NBD (approximately 30%). NBDs contain three characteristic domains: an approximately twelve residue signature sequence starting with LSGGQ, the Walker A, and the Walker B motifs. Although the function of the signature sequence remains unclear, it is localized in close proximity to the Walker B domain. The Walker A motif, with sequence A/Gx_4GKT/S (where x is any amino acid), was initially identified in various ATP-dependent enzymes (Walker et al., 1982). The Walker B motif (xxxxD, where x is generally a hydrophobic residue) forms a β strand that is followed by an aspartate residue. The motifs are separated from each other by 90–120 amino acids. NBDs are accessible to the cell cytoplasm. The less conserved membrane-spanning region contains between six to twelve α-helices and provides the specificity for substrate recognition (McKeegan et al., 2003). The recent elucidation of the three-dimensional structures of three ABC transporters in *Escherichia coli*, MsbA, BtuCD, and AcrB transporter, have

Figure 1.3: Proposed mechanism of substrate transport and topology of different ABC transporters. (A) General mechanism of substrate efflux through ABC transporters. Substrates localized in the inner layer of the plasma membrane interact with the ABC transporter. Hydrolysis of ATP in the nucleotide-binding domains localized in the cytoplasm generates the energy required to transport substrates to the outer side of the plasma membrane. (B) Topology of different ABC transporters. The general topology includes two membrane-spanning regions and two nucleotide-binding sites. MbsA is an ABC transporter expressed in prokaryotes. MRP1 and MDR1 are two ABC transporters involved in multidrug resistance. CFTR is a chloride channel that belongs to the ABC transporter gene family. Mutations in CFTR are responsible for the development of cystic fibrosis.

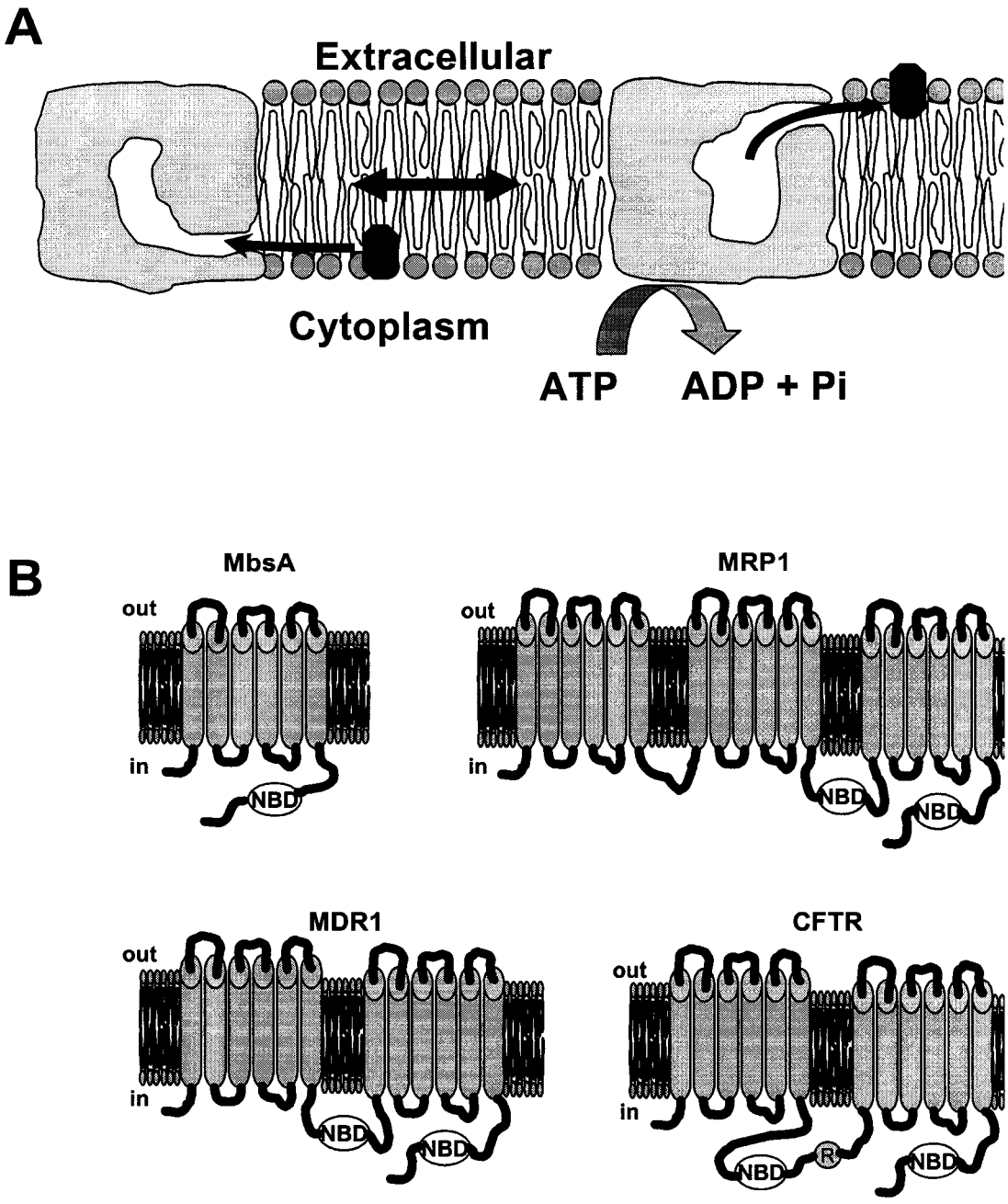
A
Extracellular
Cytoplasm
ATP
ADP + Pi
B
MbsA
out
in
NBD
MRP1
out
in
NBD
NBD
MDR1
out
in
NBD
NBD
CFTR
out
in
NBD
R
NBD

Figure 1.3

provided important insights in understanding the structure and function of this family of proteins. The first two are the transporters for lipid A and vitamin B_{12}, respectively, and the former is a multidrug pump protein (Chang and Roth, 2001;Locher et al., 2002;Murakami et al., 2002). The MsbA transporter is a homodimer with six TMD α-helices whose structure was determined at 4.5 Å resolution by X-ray crystallography. The structure of the vitamin B_{12} transporter, BtuCD, was determined at 3.2 Å resolution and is composed of two membrane subunits and two NBD subunits. AcrB contains twelve transmembrane α-helices consistent with the hydropathy plot-based prediction and topology studies by site-directed chemical modification of cysteine mutants. Crystal structures show that three molecules of ligand bind simultaneously to the extremely large central cavity of 5000 cubic angstroms primarily by hydrophobic, aromatic stacking, and van der Waals interactions. Each ligand uses a slightly different subset of AcrB residues for binding. The bound ligand molecules often interact with each other, stabilizing the binding.

ABC transporters use ATP hydrolysis to generate the energy necessary to transport different substrates across lipid bilayers (Fig 1.3A). Although ATP hydrolysis is clearly the driving force for active transport by ABC transporters, it is not clear how hydrolysis is coupled to the transmembrane transport of solutes. Several lines of research suggest that NBDs in MDR transporters function by an alternating-access mechanism in which the binding and hydrolysis of ATP in one site prevents the hydrolysis of ATP on the other site (McKeegan et al., 2003). Additionally, there are high- and low-affinity substrate-binding sites on the intracellular and extracellular sides of the membrane, respectively, that are exposed alternately to facilitated drug translocation (McKeegan et al., 2003). The transport cycle is initiated by substrate binding to the high-affinity site in the TMD. The substrate-protein interaction likely induces a conformational change that modulates the interaction between the NBD and ATP. The binding and hydrolysis of ATP leads to the translocation of the substrate by closing the intracellular gate and inducing the protein to open the extracellular entry, thus,

changing the high-affinity binding site to a low-affinity binding site facilitating the release of the substrate. Studies performed in LmrA (another MDR expressed in *Lactococcus lactis*) using vanadate-trapping experiments demonstrate that the ADP·Pi transition state reduced affinity for substrates, which could be attributable to the occlusion of the binding site. The binding of ATP, but not ADP triggers the dimerization of the NBDs, suggesting that ATP binding drives the interaction of the two ATPase subunits. The comparison of the ADP-NBD complex and the ATP-bound dimer of MJ0796 and E179Q transporters (two drug-pumps expressed in prokaryotes) indicates that reorientation of the α-helical domain is required to stabilize the interaction with ATP. The binding of ATP to the TMD-substrate state induces the two NBDs to move together, closing the intracellular cavity. ATP hydrolysis could then be used to drive the conformational changes necessary to open the extracellular gate. Structural evidence from E179Q and MJ0796 demonstrates the ability of these proteins to bind ATP in both NBDs simultaneously arguing against the assumption of the alternating-site model that binding of ATP to one NBD prevents the binding of ATP to the second NBD. One possible explanation for the ability of ABC transporters to bind ATP at both NBDs is that the hydrolysis of both ATPs will trigger different events. Evidence from CFTR suggests that the first NBD stabilizes the second NBD for ATP hydrolysis (McKeegan et al., 2003).

Glutamate Transporters

Communication between neurons to propagate specific and well-controlled signaling is essential to their function. Neurotransmitters play a vital role in the transfer of messages between neurons. Depolarization of the presynaptic neuron opens calcium channels at the end of the axon thereby increasing intracellular Ca^{2+} concentrations. Among the signal pathways that this intracellular divalent cation initiates is the calcium-dependent vesicle-mediated release of neurotransmitter in the synapse. The neurotransmitter interacts with

pre- and postsynaptic receptors localized in neuron membranes to propagate the signal. Among the receptors are G-protein coupled receptors and ligand-gated ion channels. The neurotransmitter concentration at the synapse is controlled by different mechanisms including enzyme degradation, diffusion, and uptake into the cell by transporter proteins.

Glutamate is the predominant excitatory neurotransmitter in the central nervous system. The extracellular glutamate concentration is maintained below neurotoxic levels via regulation by the glutamate transporter expressed in glia and neuron cells (Robinson and Dowd, 1997;Dunlop et al., 1999;Danbolt, 2001). Glutamate transporters expressed in glia cells also provide the glutamate necessary for metabolic processes such as glutamate-glutamine cycle (O'Shea, 2002). Dysfunction of glutamate transporters has been implicated in several neurological diseases including epilepsy, stroke, ischemia, amyotrophic lateral sclerosis, and Alzheimer's Disease (Maragakis and Rothstein, 2001).

To date, five high-affinity glutamate transporters, termed excitatory amino acid transporters (EAAT1 or GLAST, EAAT2 or GLT1, EAAT3 or EAAC1, EAAT4, and EAAT5), have been cloned from humans (Storck et al., 1992;Kanai and Hediger, 1992;Pines et al., 1992;Arriza et al., 1993;Fairman et al., 1995;Arriza et al., 1997). EAAT1 and EAAT2 are expressed in glia cells. EAAT3 is widely distributed in neurons. EAAT4 is specifically expressed in the cerebellum, and EAAT5 is localized in retina cells. The EAAT1 sequence contains 573 amino acids with a relative molecular mass of 64 kDa (Danbolt et al., 1990;Danbolt et al., 1992;Storck et al., 1992). Hydropathy studies predict a topology with eight membrane-spanning α-helices with a re-entry loop between TMD VI and VII and another loop, which contains a hydrophilic linker, between TMD VII and VIII (Fig 1.4A). A large extracellular loop between TMD III and IV contains several N-glycosylation sites. Recently, this topology was challenged assigning TMD VII as a re-entry loop (Seal et al., 2001). Kanner and coworkers used the substituted-cysteine accessibility method (SCAM, Javitch, 1998) to experimentally confirm the proposed topology. Cysteine mutants at positions

Figure 1.4: Topology, glutamate transport mechanism and oligomerization of the glutamate transporter. (A) The topology of EAAT includes eight transmembrane domains and two re-entrant loops as well as native N-linked glycosylation sites. (B) Transport and channel activities associated with glutamate transporters. The transporter expressed in the central nervous system couples sodium and potassium gradients to drive the transport of Glu^-. In addition, a variable glutamate-gated chloride-channel activity is associated with the different subtypes of glutamate transporters. (C) Possible Glu^- and chloride translocation paths in the pentameric organization of glutamate transporters. In the first two models, Glu^- and chloride ions use the same pore. Model 1 proposes that the five monomers form a single pore. In model 2, Glu^- and chloride ions use separate paths. Each monomer transports glutamate independently, but the pentameric structure is required for the chloride channel. The last model, proposes that each monomer forms a separate pore.

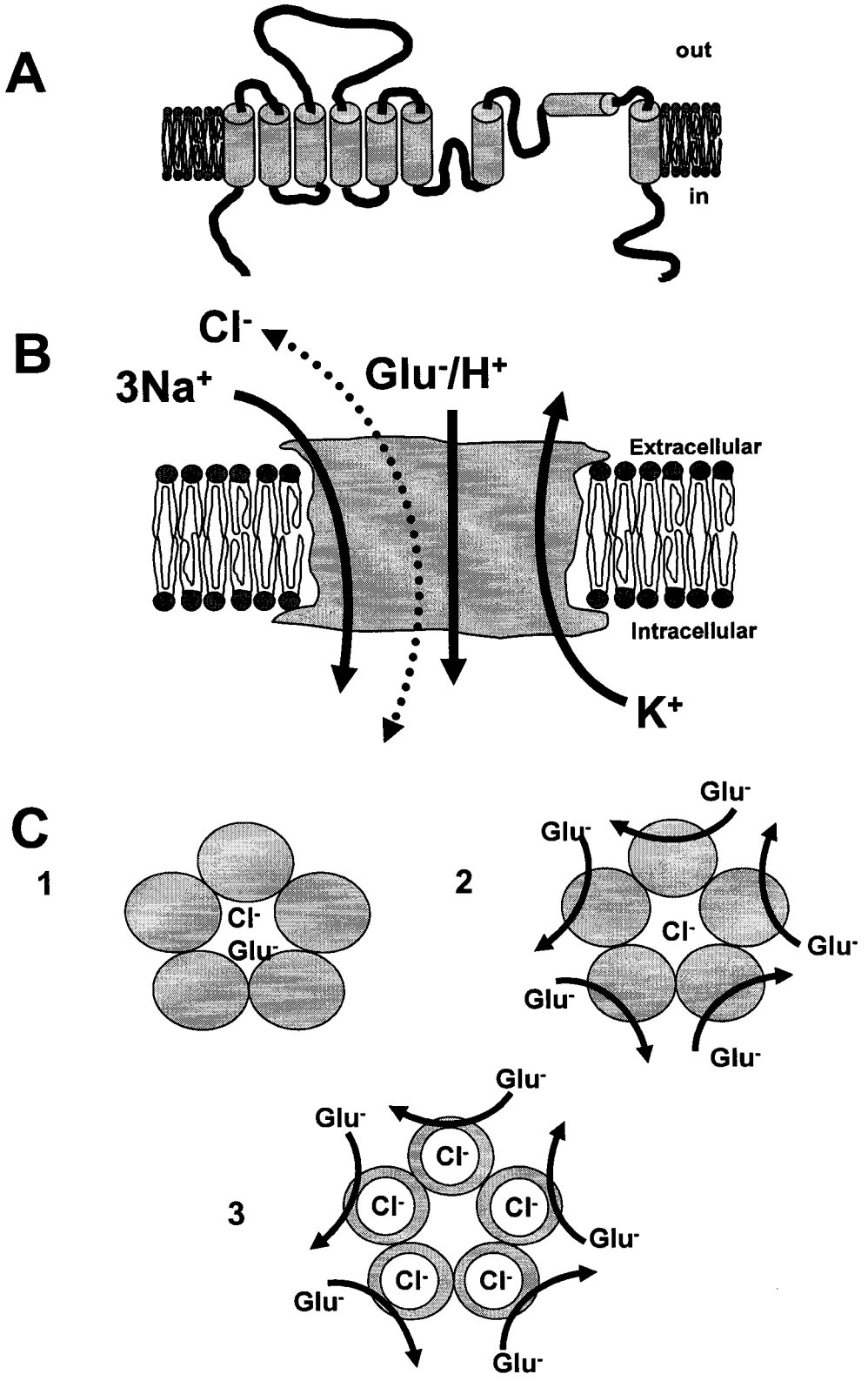
A
out
in
B
Cl-
3Na+
Glu-/H+
Extracellular
Intracellular
K+
C
1
Cl-
Glu-
2
Glu-
Glu-
Cl-
Glu-
Glu-
Glu-
3
Glu-
Glu-
Cl-
Cl-
Cl-
Glu-
Cl-
Cl-
Glu-
Glu-

Figure 1.4

364 and 440 of EAAT1, corresponding to the first and second re-entry loops, respectively, were modified by MTSET ([2-(trimetylammonium)ethyl]methanethiosulfonate), a membrane impermeable sulfhydryl-specific reagent, suggesting these residues are accessible to the aqueous environment (Zhang and Kanner, 1999;Grunewald and Kanner, 2000). Glutamine and EAAT antagonists were able to partially protect these sites suggesting that these residues may be close to the substrate binding site. Another possibility is that a change of protein conformation upon ligand binding buries these residues making them inaccessible to MTSET. EAATs use the inward transport of two or three Na^+ and one H^+, and the outward movement of one K^+ as the driving force for glutamate transport (Zerangue and Kavanaugh, 1996). Although thermodynamically uncoupled to the transport process, recent studies performed with the five human glutamate transporter isoforms in cortex and cerebellum tissue extracts demonstrated the association of EAATs and Cl^- conductance. Mutagenesis studies have shown two residues in TMD VII of EAAT1, Tyr 403 and Glu 404, important for potassium binding that may be close to one of the sodium binding sites (Kavanaugh et al., 1997;Zarbiv et al., 1998). Mutation of Glu 404 for Asp abolished potassium- dependent inward and outward transport of glutamate, but did not show any effects on the sodium-mediated transport or substrate-induced chloride conductance. Tyr 403 is accessible to methanethiosulfonate (MTS) reagents in the presence of sodium and EAAT blockers, but was protected in the presence of EAAT substrates. The same residue was modified in the presence of substrates by *N*-ethylmaleimide, which is highly permeant but unable to modify cysteine residues buried within membrane proteins. These observations suggest that tyrosine 403 is alternately accessible from either side of the membrane, consistent with its role as a structural determinant of the potassium binding site.

Recent mutagenesis studies have identified several residues involved in glutamate binding or in proximity to the substrate binding site. Serine at position 440, which is located in one of the predicted re-entry loops, is implicated in the

coupling of sodium and glutamate (Zhang and Kanner, 1999). This residue was reactive to MTS reagents and protected by substrates and antagonists of EAATs suggesting its proximity to the glutamate binding site. Mutation of arginine for cysteine at position 447 in TMD VIII of EAAT2 abolished glutamate transport but did not affect cysteine translocation (Bendahan et al., 2000). The arginine is conserved among the glutamate transporter family (Conradt and Stoffel, 1995). This mutation affects the transport of di-carboxylic amino acids, but not cysteine, suggesting a possible interaction between Arg 447 and the γ-carboxyl group of glutamate. Another mutant, V449C, is accessible to cysteine-modifying reagents (Seal et al., 2001). Reaction with MTS reagents abolished glutamate transport in both directions without affecting Cl^- conductance suggesting separation between both processes.

The re-entry loops in the topology of the glutamate transporter family are predicted to produce two water-filled pores, one between TMDs VI and VII and a less spacious pore between TMDs VII and VIII (Grunewald et al., 1998;Slotboom et al., 1999;Slotboom et al., 2001a). These re-entry loop structures are commonly present in channel proteins suggesting a possible role in the substrate-induced Cl^- conductance. Several studies have shown the well established chloride-channel activity for different EAATs, but there are significant differences among the EAAT family members. EAAT5, which is highly expressed in vertebrates, has high chloride-channel activity (Arriza et al., 1997), whereas EAATs expressed in glia cells (EAAT1 and EAAT2) are characterized by their low chloride channel-activity (Eliasof et al., 1998). Although the three-dimensional structure of the EAATs remains undetermined, several models have been proposed to accommodate the glutamate transport capacity and the channel-like activity of this family of transporters (Slotboom et al., 2001b). For instance, if the water-filled pores in EAATs are involved in Cl^- conductance, it would provide evidence supporting a similar pathway for both substrate transport and channel activity. Interestingly, recent evidence suggests a pentameric quaternary structure for EAAT3 (Eskandari et al., 2000). This pentameric

structure may form a common pore for both glutamate and Cl^- (Fig 1.4B). Another possible model is that each monomer in the structure works as a single unit (Fig 1.4C). An additional model proposes each monomer transports glutamate independently and the pentameric structure forms the pore for Cl^- conductance (Fig 1.4C). Until more structural studies are available, any of the proposed models are likely to occur. The exceptional ability of EAATs to transport mono- and di-carboxylic amino acids, as well as channel-activity associated with this transporter family, makes structure-function studies of EAATs not only important for elucidating the permeation pathway of glutamate and Cl^-, but also important to understanding the role of both processes in several neurological disorders.

Monoamine Transporters

Neurotransmitters represent a diverse group of chemical compounds ranging from simple amines and amino acids such as γ-aminobutyric acid (GABA), to polypeptides such as the enkephalins. Monoamine neurotransmitters, which include dopamine (DA), norepinephrine (NE), and serotonin (5-hydroxytryptamine, 5-HT), regulate important physiological events such as locomotion, emotions, appetite, metabolism, sleep, and muscle contraction. Plasma membrane transporters for DA, NE, and 5-HT (DAT, NET, and SERT, respectively) belong to the GABA/NET transporter gene family. These transporter proteins are responsible for translocating monoamine neurotransmitter back to the cell. Neurotransmitter accumulated in the cytosol is recycled into vesicles or metabolized. DA and NE, also called catecholamines, are catabolized to inactive compounds through the sequential actions of monoamine oxidase A (MAO-A) and catecholamine-O-methyltransferase (COMT) while the main degradation enzyme for 5-HT is MAO-B (Barker and Blakely, 1995).

5-HT is a monoamine neurotransmitter that plays an essential role in the nervous system. 5-HT is important for physiological processes including smooth muscle tone, memory, appetite, and mood (Jacobs and Fornal, 1995). 5-HT signaling is regulated by a diverse set of mechanisms, including biosynthetic enzymes, secretory proteins, ion channels, pre- and postsynaptic receptors, and transporters. The synaptic concentration of 5-HT is regulated by sodium- and chloride-dependent secondary transporters (Barker and Blakely, 1995) that couple uptake to an electrochemical gradient, thus, facilitating inward translocation of the neurotransmitter (Gu et al., 1994;Rudnick, 1998). Besides a role in the termination of synaptic 5-HT signals, SERT is the target of various clinical drugs such as tricyclic antidepressants (imipramine, amitriptyline) and selective serotonin reuptake inhibitors (fluoxetine, paroxetine, citalopram). Abused drugs such as cocaine and psychoactive amphetamines also alter the 5-HT transport mechanism. SERT antagonists including the tricyclic antidepressants, selective serotonin reuptake inhibitors, and cocaine are thought to inhibit the translocation process by binding to the transporter (White, 1998, Barker and Blakely, 1995). The amphetamines (3,4-methylenedioxymethamphetamine, *p*-chloroamphetamine), like 5-HT itself, are substrates for SERT and induce an outward movement or efflux of 5-HT from the cytoplasm through SERTs (Rudnick and Wall, 1992a,b). Although the molecular mechanism by which the amphetamines promote nonvesicular 5-HT release is not well understood, previous studies suggest that the inward movement of amphetamine leads to reversal of the transport process and results in the net efflux of intracellular 5-HT (Rudnick and Wall, 1993;Wall et al., 1995). This ability has been attributed to the trans-acceleration phenomena exhibited by different transporter proteins (Lieb, 1982).

The mechanism by which monoamine transporters mediate substrate translocation requires sequential binding and co-transport of Na^+ and Cl^- ions (Nelson and Rudnick, 1982;Barker and Blakely, 1995;Gu et al.,1996). The driving force for transporter-mediated substrate uptake is the ion concentration

gradient that is generated by the plasma membrane Na^+/K^+ ATPase. DAT couples two Na^+ ions and one Cl^- ion per cycle whereas SERT and NET couple one ion of sodium and chloride. In the case of SERT, it also couples an outward transport of one ion of potassium per cycle. It is proposed that binding of sodium, chloride, and 5-HT to SERT induces a series of conformational changes that allow the substrate to be transported from the extracellular medium into the cytoplasm. Outward transport of K^+ may be involved in the reorientation of SERT to start another transport cycle.

Substrate transport through SERT has been proposed as a series of conformational changes in which the transporter alternately faces outward and inward allowing one 5-HT molecule to cross the membrane per cycle. Recently, the elucidation of a high-resolution structure for the lactose permease supports the alternating access model for carrier-mediated transport (Abramson et al., 2003), although this model has been challenged for SERT with the discovery of channel-like currents associated with SERTs and other monoamine transporters (Galli et al., 1995;Lin et al., 1996;Petersen and DeFelice, 1999;Adams and DeFelice 2002). These currents are proposed to exist independently of the uptake mechanism (Mager et al., 1994).

Cloning of genes that encode different monoamine transporters has permitted rapid progress in the biophysical analysis of transporters and the examination of structure/function relationship in heterologous systems. Hydropathy analysis of the sequence coding for SERT (Blakely et al., 1991;Hoffman et al., 1991;Ramamoorthy et al., 1993;Corey et al., 1994) predicted twelve α-helical transmembrane domains connected by six extracellular and five intracellular loops with both termini localized in the cytoplasm similar to other members of the GABA/NET transporter family (Guastella et al., 1990;Pacholczyk et al., 1991;Kilty et al., 1991). Cysteine-scanning mutagenesis has been used to confirm the localization of the predicted extracellular and intracellular loops of SERT (Chen et al., 1997a;Chen et al., 1998;Androutsellis-Theotokis and Rudnick, 2002).

Monoamine transporters have a high degree of sequence identity, thus, these proteins are expected to have similar topology. In agreement with predicted topology, Bruss and coworkers found that antibodies directed against the N- and C- termini of NET detected the protein only in permeabilized cells, but antibodies directed against two predicted external loops detected the transporter in intact cells (Bruss et al., 1995). Moreover, Hersch and coworkers localized the N-terminus of DAT to the cytoplasmic face of the plasma membrane, and verified that the second external loop was exposed to the extracellular environment using immunogold electron microscopy (Hersch et al., 1997). Other studies have challenged the proposed topology of the N-terminal region of monoamine transporters. Kanner and coworkers used glycosylation site-scanning method to determine the topology of the N-terminal of GABA and glycine transporters (Bennett and Kanner, 1997;Olivares et al., 1997). They proposed that the first TMD did not span the membrane, but rather this region was localized in the extracellular space. Furthermore, TMD III was determined to span the membrane twice (Bennett and Kanner, 1997;Olivares et al., 1997). These studies, as well as others (Clark, 1997), included several inactive mutants whose topology could be completely different from wild-type, thus, leading to a different topology than the most accepted, as described above.

Several groups have investigated the role of the extracellular loops (EL) in the function of monoamine transporters and how these regions affect ion conductance and substrate translocation. Rudnick and coworkers found that substitution of EL IV, V, or VI in SERT with the equivalent sequence of NET showed a dramatic loss in SERT activity (Chen et al., 1998). Of these, perhaps the most interesting was EL V, where only three residues differ between SERT and NET. A similar approach was used to study the GABA transporter (GAT) family. Substitution of EL V from GAT1 to GAT3 led to the ability to bind β-alanine as an inhibitor. The group postulated that EL IV, EL V, and EL VI formed a binding site for GABA and other substrates in the GABA transporter family (Tamura et al., 1995). Previously, Cao and coworkers demonstrated that

residues in the EL V of SERT are associated with the uncoupled ion flux carried by SERT suggesting that this region may be part of the external gate of SERT (Cao et al., 1997).

Analysis of chimeric proteins, SCAM, and site-directed mutagenesis have been used extensively to identify the binding site for substrates and antagonists as well as to elucidate the transport mechanism for substrates at the molecular level. Chimeric proteins between DAT and NET have been constructed to exploit pharmacological differences among these two monoamine transporters. Giros and coworkers identified a discrete region from TMDs VI to VIII in NET as an important determinant in the affinity of cocaine and tricyclic antidepressants (Roubert et al., 2001). Moreover, their studies implicated TMDs IX to XII for substrate recognition. Buck and Amara used a similar approach to study the substrate translocation mechanism in these transporters. Chimeric studies suggest TMDs IV to VIII are important for substrate translocation and antidepressant recognition (Buck and Amara, 1994;Buck and Amara, 1995). Lee and colleagues developed a series of chimeras between the human and bovine DAT and proposed that TMD III was important for dopamine transport (Lee et al., 1998). Chimeric studies in SERT also revealed regions important for substrate and antagonist interaction (Barker et al., 1994;Barker and Blakely, 1998;Barker et al., 1998;Rodriguez et al., 2003). Barker and coworkers identified the region distal to TMD XI to be important for tricyclic antidepressants using cross-species chimeras between the human and rat SERTs (Barker et al., 1994). Moreover, cross-species chimeras between human and *Drosophila* suggest the portion of SERT encoding TMDs V to IX is important for cocaine and antidepressant binding in agreement to previous studies in DAT and NET (Roman et . al. 2003a and b).

SCAM has been used to determine the packing of α-helices of monoamine transporters (Chen et al., 1997b;Chen and Rudnick, 2000;Henry et al., 2003). Rudnick and coworkers utilized this technique to identify three residues (Ile-172, Tyr-176, and Ile-179) in TMD III of SERT that appear to reside on the same face

of the α-helix and are accessible to modifying sulfhydryl reagents (Chen et al., 1997b). After mutation of these residues to cysteine, interaction with membrane-impermeable MTS reagents blocks substrate transport suggesting that this TMD forms part of the water-filled pore used in substrate translocation. Furthermore, Ile-172 was protected from MTSET inactivation by 5-HT or cocaine, suggesting that this residue resides in or near the binding site for both 5-HT and cocaine. The accessibility of Ile-179 was found to be sensitive to conformational changes that result from substrate binding and translocation (Chen and Rudnick, 2000). Site-directed mutagenesis studies identified another residue in TMD III, Asn-177, involved in ion conductance (Cao et al., 1997). Together, these results indicate that TMD III of SERT is crucial for 5-HT and cocaine binding, and may be located in the permeation pathway.

Recently, Henry and coworkers generated 20 cysteine mutants to scan TMD I of hSERT (Henry et al., 2003). All mutants were generated using a C109A/hSERT mutant to reduce endogenous sensitivity to externally applied MTS reagents. Previously, mutagenesis studies showed that among the eighteen endogenous cysteines in TMDs of rat SERT, only C109 was determined to be accessible to MTS reagents and accounted for the inhibition effect of these compounds (Chen et al., 1997a). Similar studies in hSERT revealed comparable results (Henry et al., 2003). SCAM revealed that the TMD I residues in the external half of the α-helix are accessible to MTS reagents, whereas none of the residues from the middle of the TMD to the cytoplasmic site were MTS sensitive. Additional mutagenesis studies in this region of SERT identified two residues important for substrate recognition and antagonist binding. The first residue, Asp-98, is critical for substrate translocation (Barker et al., 1999). Mutation of Asp-98 to glutamate reduces 5-HT transport capacity and diminishes coupling to extracellular Na^+ and Cl^- with no change in 5-HT K_m value. This mutation also altered binding properties of cocaine, imipramine, and citalopram (Barker et al., 1999). In hDAT, mutation of Asp-79 (Asp-98 in hSERT) to alanine, glycine, or glutamate dramatically reduced uptake of [^{3}H]dopamine and the Parkinsonism-

inducing neurotoxin, 1-methyl-4-phenylpyridinium (MPP^+) (Kitayama et al., 1992). It is proposed that this Asp interacts with the positively-charged amino alkyl side chains of substrates, and this interaction is vital for the transport mechanism. Another mutation in TMD I of hSERT, Y95F, was shown to alter antagonist selectivity (Barker et al., 1998). Moreover, this site is also involved in tryptamine-analog recognition (Adkins et al., 2001). Ravna and coworkers proposed a model for citalopram and cocaine interaction using a hypothetical three-dimensional model of SERT and DAT generated from published site-directed mutagenesis data (Ravna et al., 2003a,b). Tyr-95 in TMD I determines the transporter selectivity of *S*-citalopram for SERT over DAT and NET. A dipole-dipole interaction proposed between the hydroxyl group of Tyr-95 in SERT and the nitrile group of citalopram could not be formed by citalopram in DAT and NET where the corresponding amino acid is a phenylalanine. The tropane ring of cocaine interacts with Tyr-95 in SERT and with the corresponding phenylalanine in NET and DAT. This may explain, in part, the selectivity of citalopram for SERT, whereas cocaine is a nonselective inhibitor for SERT, DAT, and NET.

Other regions in monoamine transporters have been implicated in substrate translocation. Site-directed mutagenesis in TMD VII and XI of DAT identified several residues implicated in MPP^+ transport (Kitayama et al., 1993). Mutation of Ser-350 and Ser-359 in DAT (V-366 and S-375 in hSERT) selectively affects MPP^+ transport. Other residues in TMD XI of DAT, Tyr-533 and Ser-538 (Phe 551 and 556 at hSERT) are also implied in MPP^+ transport (Kitayama et al., 1993). Using these data, Ravna and Edvardsen proposed a model for MPP^+ translocation where TMDs I, VII, and XI form the permeation pathway for this molecule (Ravna and Edvardsen, 2001), although this model remains to be proven.

Because high-resolution structures for monoamine transporters are not available to date, determining the permeation pathway at the molecular level has been challenging. Several lines of evidence indicate that monoamine transporter proteins exist as oligomers rather than single units (Jess et al., 1996;Kilic and

Rudnick, 2000;Schmid et al., 2001b;Torres et al., 2003;Scholze et al., 2002). This phenomenon has been described for other membrane proteins such as receptors tyrosine kinase (Kubar and Van Obberghen, 1989), G-protein coupled receptors (Rios et al., 2001), and glucose transporters (Hebert and Carruthers, 1992;Zottola et al., 1995) among others. In a heterologous expression system, flag-tagged and myc-tagged SERTs were co-immunoprecipitated, providing evidence of inter-protein interaction between SERT monomers (Kilic and Rudnick, 2000). Sitte and colleagues used fusion proteins of SERT with spectral-variants of the green fluorescent protein to study the quaternary structure of SERT. Oligomers were visualized by fluorescence resonance energy transfer (FRET) in living cells, confirming the co-immunoprecipitation studies using tagged SERTs (Schmid et al., 2001a). Hastrup and coworkers identified a cysteine residue in TMD VI of DAT that produces symmetrical crosslinking between two monomers (Hastrup et al., 2003). Recently, mutations of the leucine repeat domain in TMD II of DAT abolished oligomerization and affected protein trafficking to the plasma membrane (Torres et al., 2003). Torres and coworkers proposed that TMD II may be important for transporter assembly, and the oligomerization process is essential for the trafficking of the transporter to the cell surface.

The mechanism for substrate translocation by SERT at the molecular level is not known. SERT is believed to transport substrate using an alternating-access process, similar to the mechanism described earlier for the sodium-dependent glucose transporter (see above). SGLT and SERT transport mechanisms may differ in several steps at the molecular level (Fig 1.1, Fig 1.5). First, SGLT translocates glucose with one Na^+, whereas SERT requires the sequential binding of Na^+, 5-HT, and Cl^- to initiate the transport cycle (Gu et al.,1996). In the case of SERT, Na^+ is not required for 5-HT binding but may induce conformational changes that influence the interaction of Cl^- with SERT. Furthermore, Na^+ in conjunction with Cl^- may induce conformational changes that trigger the translocation process. Second, it is proposed that after glucose is

Figure 1.5: Hypothetical mechanism of 5-HT translocation in SERT. The proposed transport process for 5-HT uptake consist of six steps: (i) Sodium binds to the transporter from the external medium; (ii) 5-HT binds to the transporter-sodium complex; (iii) One Cl^- binds to SERT; (iv) the transporter changes to a conformation that faces the cytoplasm; (v) 5-HT, Na^+, and Cl^- are release into the cytoplasm; (vi) One K^+ binds to the transporter facing the cytoplasmic side and returns to the conformation facing the extracellular environment to start another cycle.

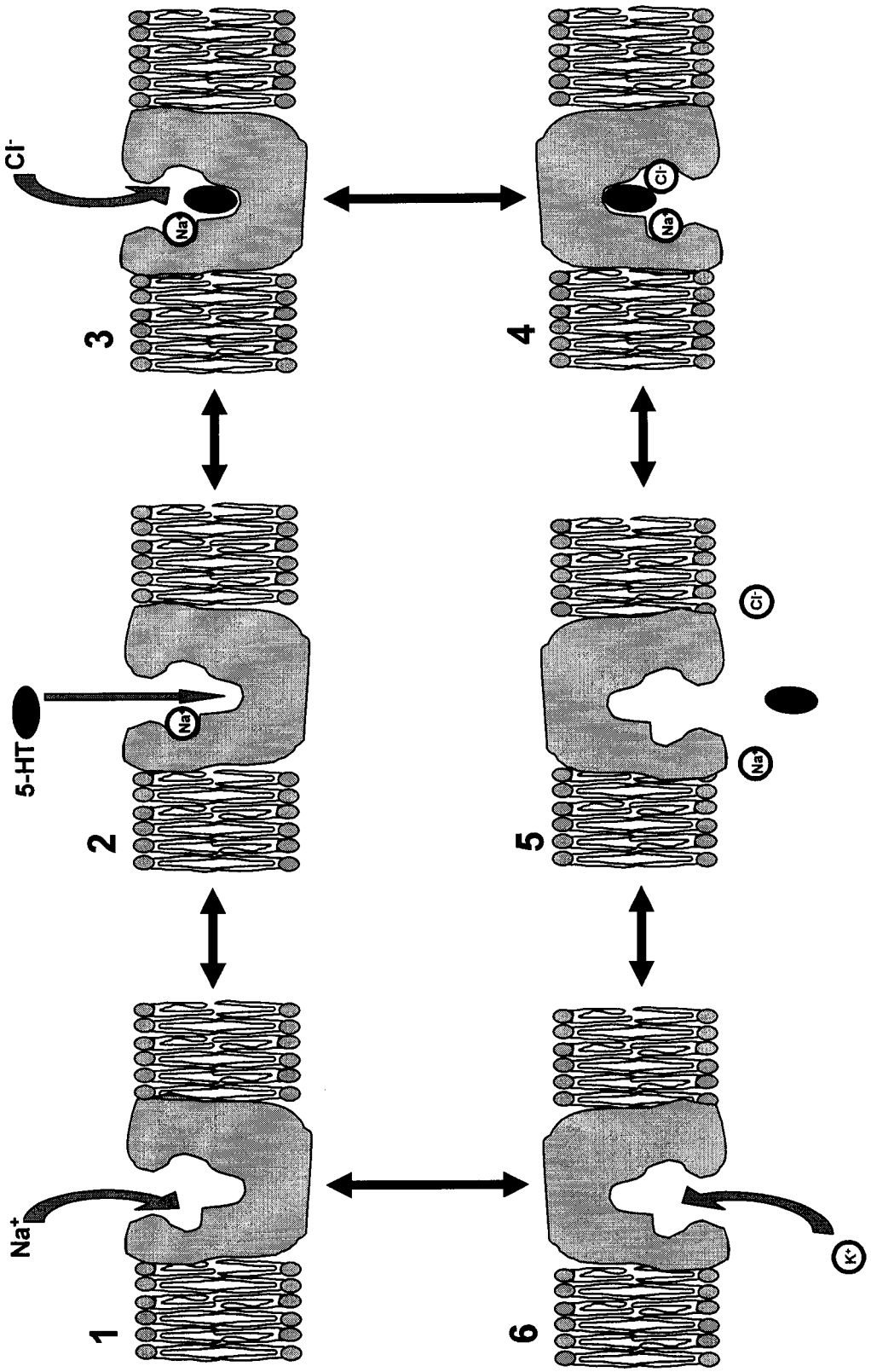

Figure 1.5

released, the empty SGLT returns to a conformation facing the extracellular side to start another cycle, whereas in SERT the release of 5-HT, Cl^-, and Na^+ is followed by the binding of one K^+ to the transporter that is outwardly transported.

The free neurotransmitter in the cytoplasm after either being synthesized or transported back into the cell from the synapse is concentrated into vesicles. This process is mediated by the vesicular monoamine transporters (VMATs). This membrane protein, unlike the monoamine transporters described above, is nonspecific and can transports catecholamines, 5-HT, and histamine (Parsons, 2000). To date, two isoforms have been clone (VMAT1 and VMAT2) that are encoded by two different genes. Whereas VMAT1 is expressed in chromaffin granules, VMAT2 is localized exclusively in neurons (Weihe and Eiden, 2000). These isoforms also demonstrate differences in their pharmacology for inhibitors and substrates. Reserpine is an inhibitor for both isoforms with comparable potency, whereas tetrabenzine exhibits 10-folds greater potency for VMAT2 over VMAT1 (Chaplin et al., 1985). Moreover, both VMAT1 and VMAT2 transport dopamine, norepinephrine, epinephrine, and 5-HT, whereas only VMAT2 transports histamine (Eiden, 2000).

Sequence analysis of VMATs suggests a topology of twelve putative transmembrane domains with a large hydrophilic loop between TMD I and II that contains a N-glycosylation site (Liu et al., 1992). According to the hypothesized model, the N- and C-termini are both localized in the cytoplasm. VMATs are classified as antiporter transporter. These membrane proteins concentrate neurotransmitter into the vesicle against their concentrations using the outward proton gradient (for review see Parsons, 2000). This proton gradient is generated by the H^+-ATPase. The stoichiometry for this process is two protons per neurotransmitter molecule transported into the vesicle (Knoth et al., 1981;Nguyen et al., 1998). Several residues have been implicated in the function and pharmacology of VMATs. The first proton that is release from the vesicle is believed to induce a conformational change in VMAT that exposed the high-affinity binding site for substrates. This site is also a point of recognition for

reserpine. The second proton is necessary for the translocation of substrate into the vesicle.

Mutagenesis studies have implicated several residues important for VMAT function. Schuldiner and colleagues identified a histidine residue in the cytoplasmic loop between TMD X and XI that upon protonation is involved in the conformational change that exposes the high-affinity substrate binding site to the cytoplasm (Shirvan et la., 1994). Other studies focused on aspartic acid residues predicted to lie in the middle of TMDs I, VI, X, and XI for both isoforms. Edwards and coworkers identified an aspartate in TMD XII that forms an ion pair with a conserved lysine residue in TMD II (Merickel et al., 1997). This interaction is thought to increase the affinity for substrate binding but is not necessary for protein function. Mutation of an aspartate in TMD I to alanine or asparigine generates a transporter that can not translocate 5-HT (Merickel et la., 1995). The replacement of the aspartate with glutamate reduced transport capacity, but does not affect the affinity for 5-HT. The mutagenesis data from VMAT isoforms provide insights about the recognition and translocation of substrates but further studies are necessary to establish a direct role of the residues implicated in the function of the VMAT translocation process.

Scope of the Work

The overall aim of my studies is to gain insights into the translocation mechanism for substrates by the serotonin transporter at the molecular level. The two specific aims are:

1- To determine regions in the serotonin transporter important for substrate recognition and translocation. The specific questions that will be addressed are:

A. Do differences exist in substrate recognition and transport between the human and *Drosophila* serotonin transporters?
B. Are there differences in amphetamine-induced substrate efflux and transport between the human and *Drosophila* serotonin transporters?
C. Using cross-species chimeras between human and *Drosophila* serotonin transporters, what regions in SERT are involved in substrate recognition and translocation?

2- To identify residues in the serotonin transporter critical in substrate translocation and or localized within the permeation pathway. The specific questions that will be addressed are:

A. Which transmembrane domains and/or residues form the permeation pathway in SERT?
B. Are these sites accessible to membrane-impermeable MTS reagents?
C. Can substrates or antagonists prevent MTS accessibility?

CHAPTER II

Distinct recognition of substrates by the human and *Drosophila* serotonin transporters.

Introduction

Cloning of SERT from several organisms including rat (Blakely et al., 1991;Hoffman et al., 1991), human (Ramamoorthy et al., 1993), and *Drosophila* (Corey et al., 1994;Demchyshyn et al., 1994) revealed shared sequence identity with other members of the sodium- and chloride-dependent GAT/NET transporter gene family. Despite the sequence homology and similar K_m values for 5-HT transport between SERT species variants, several lines of evidence demonstrate species differences in antagonist recognition (Barker et al., 1994;Barker et al., 1998) and the recognition of tryptamine analogs (Adkins et al., 2001). These studies have revealed that single amino acid substitutions across SERT species variants are sufficient to alter ligand recognition. Amino acids involved with species-specific pharmacologic properties of SERT may play a role in maintaining a favorable conformation for ligand recognition or may directly participate in ligand binding as part of the drug binding pocket.

Limited information is available on the molecular determinants of substrate recognition and translocation by SERT. In the present study, I investigated differences in the properties of SERT substrates between the human and *Drosophila* SERTs (hSERT and dSERT, respectively). hSERT (630 amino acids) and dSERT (622 amino acids) share 51% sequence identity and demonstrate similar K_m values for 5-HT uptake (Demchyshyn et al., 1994). I speculated that hSERT and dSERT might demonstrate marked differences for the transport of

other substrates such as *N*-methyl-4-phenylpyridinium (MPP^+) and the amphetamines, providing opportunities to exploit these species-specific properties in molecular studies to reveal structural information about substrate recognition and permeation. Indeed, hSERT readily transported the neurotoxic compound MPP^+; however, MPP^+ was not transported by dSERT. Moreover, amphetamine analogs were not readily transported by dSERT as determined by 5-HT release assays. Finally, experiments with cross-species chimeras between hSERT and dSERT implicated the region from TMD V to IX of SERT as containing structural components involved with substrate recognition.

Materials and Methods

Materials

HEK-293 cell lines stably expressing hSERT or dSERT were generous gifts from Dr. Randy D. Blakely (Vanderbilt University). [^{3}H]5-Hydroxytryptamine ([^{3}H]5-HT; 122 Ci/mmol) and [^{3}H]citalopram (85 Ci/mmol) were purchased from Amersham Biosciences Inc. (Piscataway, NJ). [^{3}H]Mazindol (21 Ci/mmol) and [^{3}H]MPP$^+$ (78 Ci/mmol) were obtained from PerkinElmer Life Sciences (Boston, MA). Fluoxetine, MPP$^+$, and pargyline were purchased from Sigma/RBI (Natick, MA). Unlabeled 5-HT was obtained from Sigma-Aldrich (St. Louis, MO). Amphetamines were kindly provided by Dr. David Nichols (Purdue University). All other reagents were purchased from commercial sources.

Chimera Construction

The generation of the $H^{1-118}D^{119-627}$ cross-species chimera between hSERT and dSERT using a restriction site-independent method of chimera formation was described previously (Moore and Blakely, 1994;Barker and Blakely, 1998). The resulting cross-species chimera encoded amino acids 1 to 118 from hSERT and 119 to 627 from dSERT. Construction of the $H^{1-281}D^{282-476}H^{477-638}$ chimera was initiated using the QuikChange® mutagenesis kit (Stratagene, La Jolla, CA) to make a silent mutation in the *Drosophila* SERT cDNA that introduced a *Bsi*WI restriction site at position 1419 from the first position of the coding region. The same method was used on the human SERT cDNA to introduce a complementary *Bsi*WI site (from position 1446 of the initiating codon), as well as an *Eco*NI site at position 808 from the first position of the coding region. A complementary *Eco*NI restriction site is native in dSERT (Fig 1A). Mutations were confirmed by restriction enzyme digestion and nucleotide sequencing. Each SERT cDNA was digested with *Eco*NI and *Bsi*WI;

the resulting fragments were gel-purified, and complementary fragments were ligated to yield the chimeric cDNA. The resulting construct encoded amino acids 1 to 281 from hSERT, 282 to 476 from dSERT, and 477 to 638 from hSERT (Fig 2.1A).

HEK-293 cells stably expressing the hSERT/dSERT chimeras were produced as described elsewhere (Qian et al., 1997). Briefly, chimeric cDNAs in pBluescript KSII$^+$ were digested with *Xho*I/*Xba*I and subcloned into pcDNA 3.1 (Invitrogen, Carlsbad, CA). Wild-type HEK-293 cells were transfected with either $H^{1-118}D^{119-627}$/pcDNA 3.1 or $H^{1-281}D^{282-476}H^{477-638}$ /pcDNA 3.1 using a lipid-mediated transfer (Lipofectamine 2000; Invitrogen) as described by the manufacturer. Transfected cells were selected with 600 mg/l geneticin (G418; Invitrogen). Selected colonies were characterized for [^{3}H]5-HT uptake.

HEK-293 cells stably expressing hSERT, dSERT, or chimeras were maintained in Dulbecco's modified Eagle's medium with 10% dialyzed fetal bovine serum supplemented with penicillin, streptomycin, L-glutamine, and G418 (600 mg/l). Cells were grown in a 37°C humidified environment with 5% CO_2.

[^{3}H]-Substrate Uptake Assays

Saturation transport assays were performed in 24-well culture plates precoated with poly-D-lysine. At the time of assay, cells (1 x 10^5 cells per well) were washed once with Krebs/Ringer/HEPES (KRH) buffer (120 mM NaCl, 4.7 mM KCl, 2.2 mM $CaCl_2$, 10 mM HEPES, 1.2 mM KH_2PO_4, 1.2 mM $MgSO_4$, pH 7.4). Cells were incubated with increasing concentrations of substrate for 10 min at 37°C in KRH containing D-glucose (1.8 g/l), L-ascorbic acid (100 µM), and pargyline (100 µM). Fluoxetine (10 µM) was used to define nonspecific uptake. Saturation kinetics were determined using increasing concentrations of [^{3}H]5-HT (0.6-20 µM) or [^{3}H]MPP^+ (12.5–400 µM) with a specific activity diluted to ≈ 0.1 Ci/mmol with unlabeled compound. Assays were terminated by washing three times with KRH buffer and the cells were solubilized using Microscint-20

Figure 2.1: (A) Diagram of wild-type hSERT, dSERT, and cross-species chimeras transporters. Two functional chimeras between hSERT (black) and dSERT (blue) were constructed as described in Materials and Methods. (B) Table of the amphetamine analogs used in these experiments. The table includes name, abbreviation and the chemical structure.

A

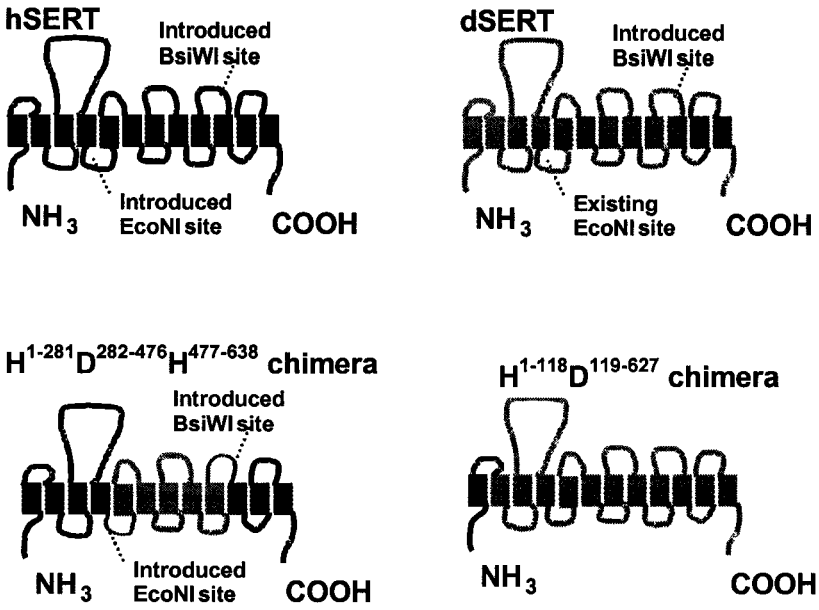

B

Compound name	Abbreviation	Structure
5-methoxy-6-methyl-2-aminoindan	MMAI	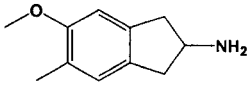
3,4-dichloroamphetamine	DCA	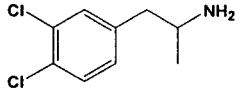
3,4-difluoroamphetamine	DFA	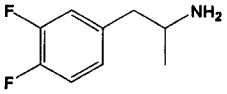
4-trifluoromethamphetamine	TFMA	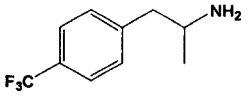
4-methylthioamphetamine	4-MTA	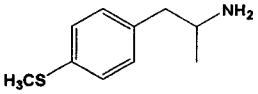
3-methylthioamphetamine	3-MTA	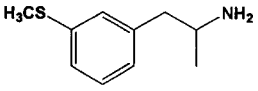
3,4-methylenedioxymethamphetamine	MDMA	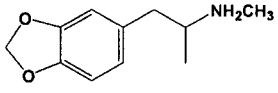

Figure 2.1

scintillation fluid. The amount of remaining radiolabeled substrate was then determined using a PerkinElmer TopCount-NXT Microplate Scintillation and Luminescence Counter. Saturation assays on the substituted amphetamines were not performed because radiolabeled compounds were not available, and furthermore, these compounds are extremely lipophilic, thus preventing accurate determination of the transport kinetics.

For uptake inhibition assays, cells were plated as described for efflux assays. At the time of assay, the plates were washed with KRH buffer, incubated with increasing concentration of drug at 37°C for 10 min, and then treated with [^{3}H]5-HT (20 nM). Cells were incubated another 10 min and uptake was terminated by harvesting into a 96-well GF/B filter plate. Accumulated [^{3}H]5-HT was determined as described above.

[^{3}H]5-HT Efflux Assays

For release assays, cells were plated in tissue culture dishes (150 mm x 20 mm) and incubated at 37°C for 2 days (approximately 90% confluent). Cells were resuspended in KRH/D-glucose (15 ml final volume). Protein concentrations were determined using the Bradford method (Bio-Rad, Hercules, CA), and suspensions were diluted to 0.5 mg/ml with KRH/D-glucose buffer. At the time of assay, 50 µg of protein (100 µl) was incubated with 100 µl of [^{3}H]5-HT (50 nM final concentration) at 37°C for 5 min (hSERT) or 30 min (dSERT, $H^{1-118}D^{119-627}$, and $H^{1-281}D^{282-476}H^{477-638}$) to provide for equivalent loading. The cell suspensions were treated with increasing concentrations of drug in a final volume of 1 ml. Time course experiments revealed that efflux at both hSERT and dSERT reached maximum at 10 min (Fig 2.2). Thus, cells were incubated for 10 min, and then efflux was terminated by harvesting into a 96-well GF/B filter plate. The amount of remaining radiolabeled substrate was determined using liquid scintillation spectrometry as described above.

Figure 2.2: Time-course of [^{3}H]5-HT efflux in HEK-293 cells stably expressing either hSERT (A) or dSERT (B) as described in the Materials and Methods. Cells were incubated with 50 nM [^{3}H]5-HT for 10 minutes (hSERT) or 30 minutes (dSERT) to allow equivalent loading. Cells were washed with KRH to remove labeled 5-HT and incubated at different time points with 10 μM DCA. Results shown represent mean ± standard errors of triplicate determination and are representative of three independent experiments.

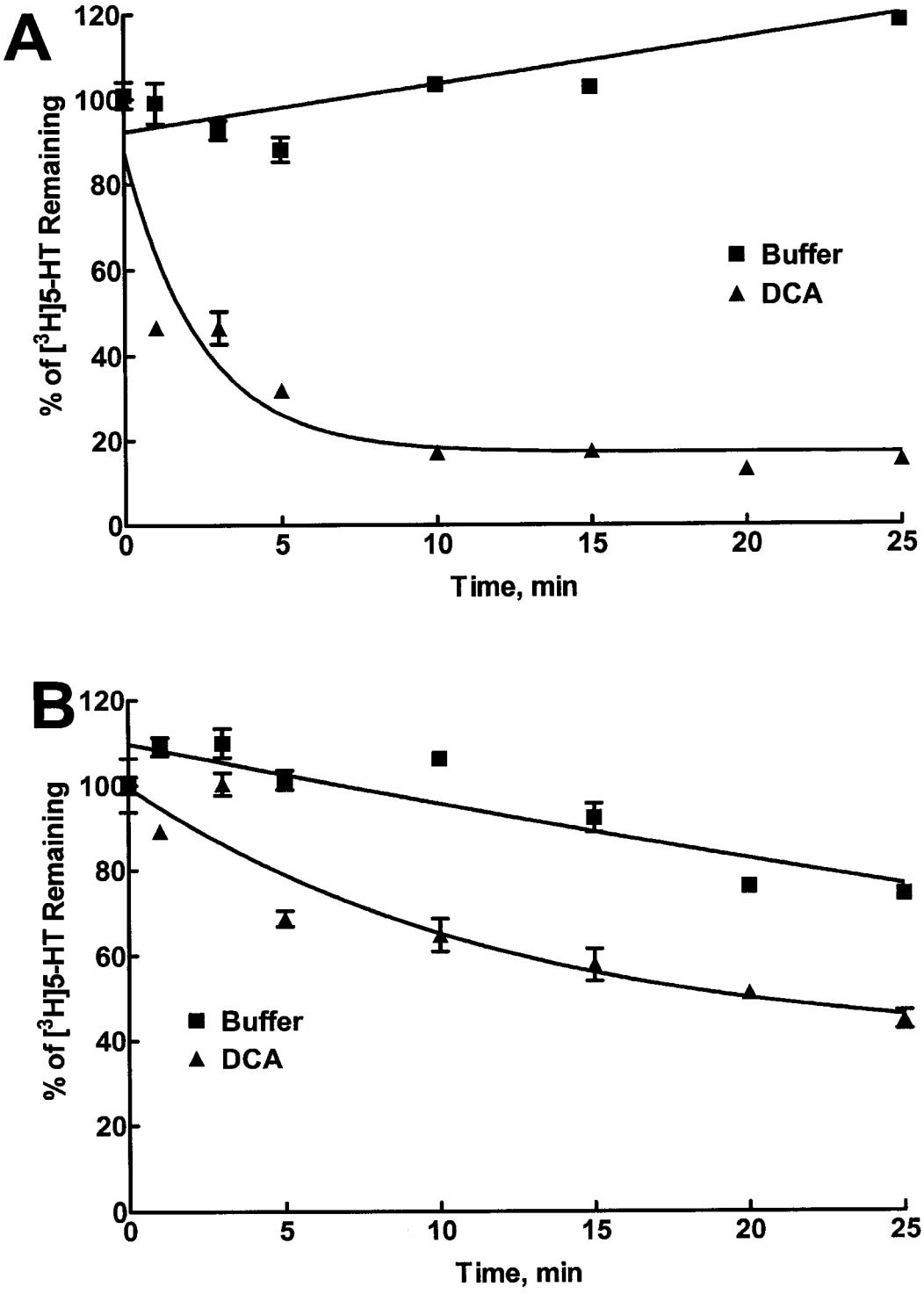
A
120
100
80
60
40
20
0
% of [3H]5-HT Remaining
Buffer
DCA
0
5
10
15
20
25
Time, min
B
120
100
80
60
40
20
0
% of [3H]5-HT Remaining
Buffer
DCA
0
5
10
15
20
25
Time, min

Figure 2.2

Whole-Cell Radioligand Binding Assay

Whole-cell binding experiments were performed in six-well plates (1×10^6 cells per well) precoated with poly-D-lysine. The day after plating, cells were washed once with KRH. A saturating concentration (20 nM) of [^{3}H]citalopram or[^{3}H]mazindol was used as a radiolabeled ligand for hSERT and dSERT, respectively. Radiolabeled ligand and cells were incubated at 4°C for 1 h. After incubation, cells were rapidly washed twice with 1000 µl of KRH, solubilized with 10% sodium dodecyl sulfate solution, and transferred into a scintillation vial. [^{3}H] Ligand was determined using a Beckman LS 1801 liquid scintillation counter (Beckman Coulter, Fullerton, CA). Total binding was established in the presence of KRH buffer. Nonspecific binding was defined as the binding of radiolabeled ligand in the presence of fluoxetine (10 µM). Internal binding was determined in the presence of MPP^+ (400 µM). Specific surface binding was calculated as (total binding – binding in the presence fluoxetine) – (binding in the presence of MPP^+ – binding in the presence of fluoxetine).

Data Analysis

V_{max} and K_m values in saturation experiments were calculated, and efflux EC_{50} values were estimated using nonlinear curve-fitting analysis (Prism 3.0; GraphPad Software Inc., San Diego, CA). All results were expressed as mean ± SEM for at least three experiments performed in triplicate.

Results

Kinetic Analysis of 5-HT Transport for Wild-Type and Cross-Species SERT Chimeras.

Wild-type and chimeric SERTs demonstrated similar K_m values for [^{3}H]5-HT uptake (Table 2.1). In contrast, the 5-HT transport V_{max} value for hSERT (5.3 ± 0.2 x 10^{-17} mol/min/cell) was 2-fold greater than dSERT (2.3 ± 0.1 x 10^{-17} mol/min/cell) and the cross-species chimeras. The similar K_m values suggest that both SERT species recognize 5-HT in a similar way. The differences in V_{max} values between hSERT and dSERT could be the result of different cell surface expression levels in the transfected HEK-293 cells. To address this issue, I determined surface expression of SERTs by whole-cell binding assays carried out at 4°C. [^{3}H]Citalopram and [^{3}H]mazindol were used as radiolabeled ligands for hSERT and dSERT, respectively. Fluoxetine (10 µM) was used to define nonspecific binding for intracellular and plasma membrane pools of SERT, and MPP^+ (400 µM) was used to bind SERT expressed at the plasma membrane. Although I observed that 400 µM MPP^+ was transported by hSERT at 37°C (Table 2.1), inward transport of this concentration of MPP^+ was not detected at 4°C for hSERT (data not shown) or at any temperature for dSERT (see below and Table 2.1), thus validating the use of MPP^+ to define surface expression. hSERT showed nearly 8-fold greater surface expression than dSERT, explaining in part the differences in V_{max} between the two SERT species (Fig 2.3A and B). V_{max} values for hSERT and dSERT from these cells were used to approximate the 5-HT transport turnover number. Turnover number provides an opportunity for direct comparison between the two SERT species without concerns related to cell surface expression. Interestingly, the turnover number for dSERT was almost 2-fold greater than that for hSERT (Fig 2.3C), implying a potential distinction in the transport mechanism between hSERT and dSERT.

Table 2.1: K_m and V_{max} values for 5-HT and MPP^+ uptake in HEK-293 cells stably expressing parental and chimeric SERTs.

		hSERT	dSERT	$H^{1-118}D^{119-627}$	$H^{1-281}D^{282-476}H^{477-638}$
5-HT	K_m (μM)	1.2 ± 0.2	0.9 ± 0.2	1.4 ± 0.2	0.8 ± 0.1
	V_{max} (mol/min/cell) x 10^{-17}	5.3 ± 0.2	2.3 ± 0.1	3.3 ± 0.1	2.4 ± 0.1
MPP^+	K_m (μM)	24.2 ± 0.5	>1000	>1000	>1000
	V_{max} (mol/min/cell) x 10^{-17}	5.7 ± 0.6	ND	ND	ND

Kinetic values of 5-HT and MPP^+ uptake in HEK-293 cells stably transfected wild-type and chimera SERTs. Values represent mean ± standard errors for at least three independent experiments. ND: Not determined due to a lack of uptake at concentrations up to 1 mM.

Figure 2.3: Whole-cell radioligand binding in HEK-293 cells stably transfected with hSERT and dSERT. Assays were performed in six-well plates coated with poly-D-lysine as described in Materials and Methods. A saturating concentration of [^{3}H]citalopram (20 nM) or [^{3}H]mazindol (20 nM) was used for (A) hSERT and (B) dSERT, respectively. Nonspecific binding was defined as the binding of radiolabeled ligand in the presence of 10 µM fluoxetine. Internal binding was determined as the binding of [^{3}H] ligand in the presence of 400 µM and 1 mM MPP^+ for hSERT and dSERT respectively. Specific surface binding was calculated as (total binding – binding in the presence fluoxetine) – (binding in the presence of MPP^+ – binding in the presence of fluoxetine). (C) Turnover numbers for 5-HT transport at hSERT and dSERT were calculated with V_{max} values (Table 2.1) and specific surface binding in units of 5-HT molecules/transporter/min. Bars represent the mean of three independent experiments ± SEM, $^*p < 0.05$ using a two-tailed Student's t-test.

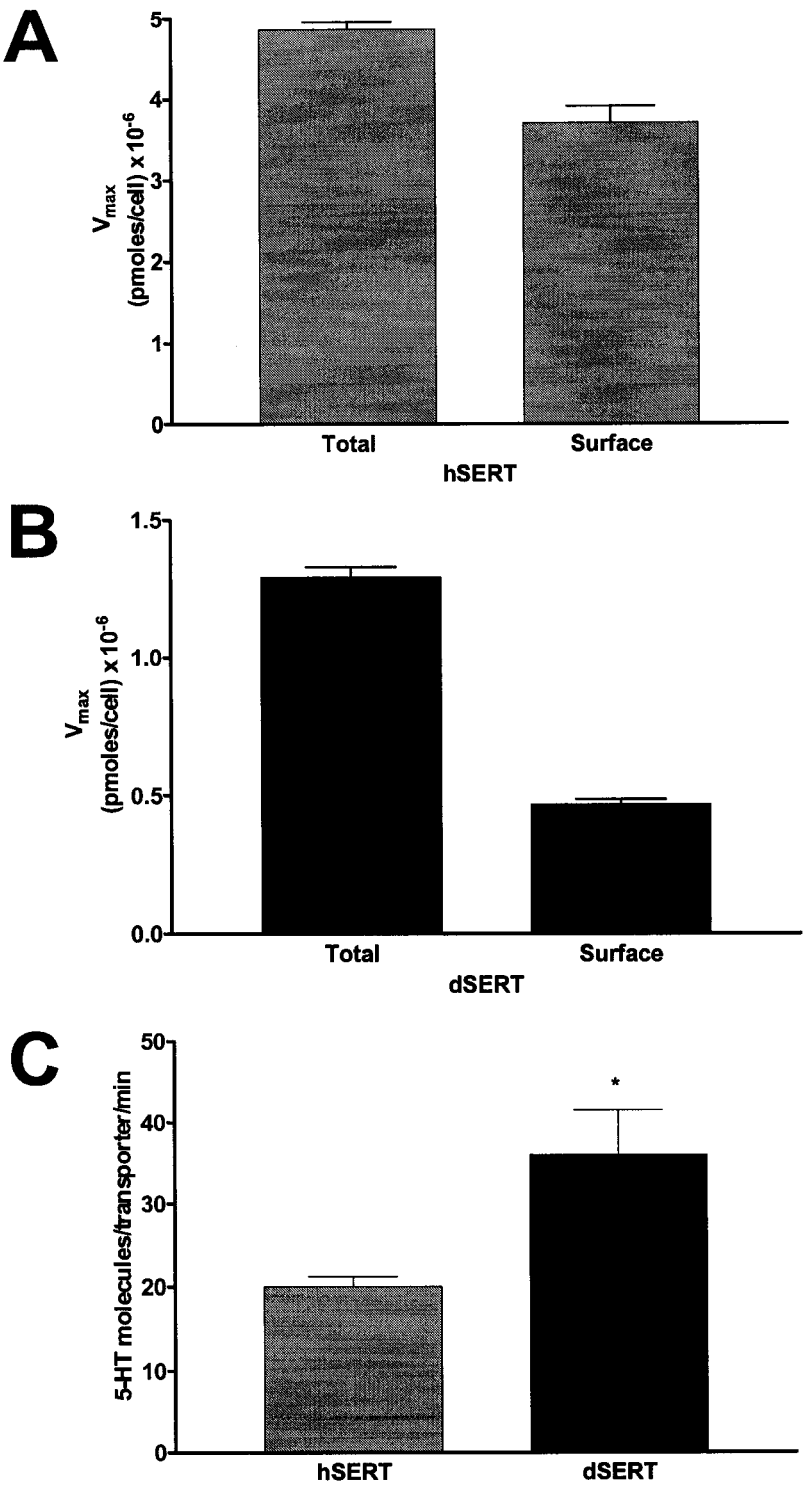
A
5
4
3
2
1
0
V_{max} (pmoles/cell) x 10^{-6}
Total
Surface
hSERT
B
1.5
1.0
0.5
0.0
V_{max} (pmoles/cell) x 10^{-6}
Total
Surface
dSERT
C
50
40
30
20
10
0
5-HT molecules/transporter/min
*
hSERT
dSERT

Figure 2.3

MPP^+ Transport Differences Between Human and *Drosophila* SERTs.

Although 5-HT appeared to be recognized similarly by hSERT and dSERT, I tested the hypothesis that other SERT substrates such as MPP^+ and substituted amphetamines would demonstrate species selectivity. Saturation studies in parental and chimeric SERTs were performed using the low-affinity substrate MPP^+. This compound has been used extensively to study SERT function (Sitte et al., 2000;Scholze et al., 2000;Sitte et al., 2001) as well as other monoamine transporters (Sitte et al., 1998). MPP^+ uptake at hSERT exhibited a K_m value of 24 μM and a V_{max} value of 5.7 x 10^{-17} mol/min/cell (Table 2.1). In contrast, neither dSERT nor the cross-species chimeras showed significant capacity to transport MPP^+ under my experimental conditions. These findings suggest that despite similar recognition properties for 5-HT, hSERT and dSERT possess distinctions for molecular recognition and translocation of other substrates.

There are two possible explanations for the lack of inward MPP^+ transport by dSERT and the cross-species chimeras: 1) dSERT and the cross-species chimeras lack the conformation or the binding site necessary to interact with MPP^+, or 2) MPP^+ binds but cannot be translocated through the transporter, acting like an antagonist instead of a substrate. To address this question, [^{3}H]5-HT uptake inhibition assays were performed in hSERT, dSERT, and the cross-species chimeras, revealing that MPP^+ can bind to all SERTs (Fig 2.4). The lack of transport for MPP^+ at dSERT and the chimeras suggests that MPP^+ may have distinct interactions with the two SERT species homologs. For example, MPP^+ binding to hSERT triggers transport, but residues involved in promoting MPP^+ transport are absent or inaccessible in dSERT.

Differences in Amphetamine Properties at the Human and *Drosophila* SERTs.

To explore species-specific differences in amphetamine recognition and translocation at hSERT and dSERT, the capability of six amphetamine analogs to

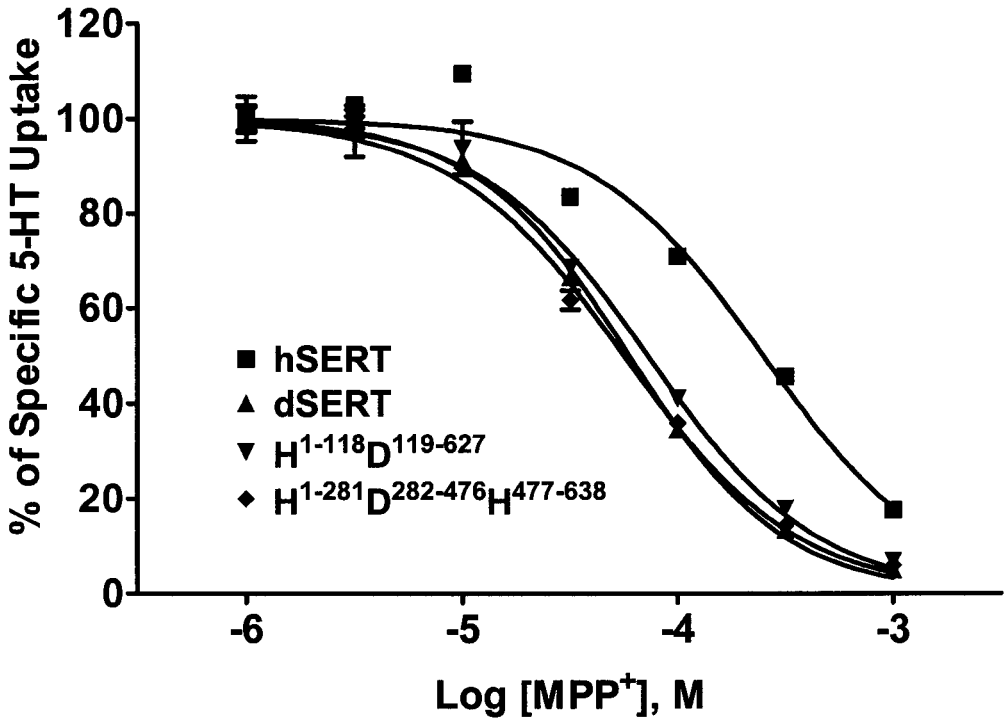

Figure 2.4: MPP^+ inhibition of 5-HT uptake at wild type and chimeric SERTs. [^{3}H]5-HT uptake assays were performed as described in Material and Methods. Nonspecific uptake was determined with 10 μM fluoxetine. Evaluation of MPP^+ potency at (■) hSERT (K_i=250 ± 50 μM), (▲) dSERT (K_i=59 ± 6.0 μM), (▼) $H^{1-118}D^{119-627}$ (K_i=73 ± 8.0 μM), and (◆) $H^{1-281}D^{282-476}H^{477-638}$ (K_i=56 ± 9.0 μM). Data were plotted as percentage of specific 5-HT uptake. Results shown represent mean ± standard errors of triplicate determination and are representative of three independent experiments.

evoke 5-HT efflux was assessed (Fig 2.1B and Table 2.2). The ability to induce efflux has been used as evidence that a compound is a substrate for transporters (Rudnick and Wall, 1992a,b). Efflux data revealed higher potency and efficacy of amphetamine-induced release through hSERT as compared with dSERT or the cross-species chimeras (Table 2.2 and Fig 2.5A). For example, the amphetamine analog MMAI was 6-fold more potent at hSERT (EC_{50} = 530 ± 80 nM) compared with dSERT (3050 ± 280 nM) and at least 24-fold more potent than at the cross-species chimeras (Table 2.2 and Fig 2.5A). Moreover, MMAI induced release of approximately 70% of the cytoplasmic 5-HT concentration in hSERT-expressing cells, but this amphetamine analog only released approximately 30% and 10% of internal 5-HT in the chimeras and dSERT, respectively (Fig 2.5A). Despite the lack of potency and efficacy for inducing 5-HT efflux at dSERT, MMAI and the other amphetamines (data not shown) were capable of inhibiting 5-HT transport at dSERT and the chimeras as assessed by [^{3}H]5-HT uptake inhibition assays (Fig 2.5B). The 5-HT transport inhibition studies further confirmed the fact that MMAI exhibited higher potency for hSERT than for dSERT. The amphetamine derivative 3,4-dichloroamphetamine was the most potent compound tested at all SERTs. The EC_{50} value for hSERT (70 ± 10 nM) was approximately 22-fold lower than that for dSERT (1340 ± 680 nM) or the cross-species chimeras (Table 2.2). The analog 3,4-difluoroamphetamine, which contains fluorines at the same positions as the chlorines in 3,4-dichloroamphetamine, did not evoke 5-HT efflux through dSERT or the chimeras. The two *para*-substituted analogs 4-trifluoromethamphetamine (EC_{50} = 270 ± 80 nM) and 4-methylthioamphetamine (EC_{50} = 210 ± 80 nM) were nearly 12-fold more potent at hSERT than was the *meta*-substituted derivative 3-methylthioamphetamine.

The data suggest that MMAI and the other amphetamines may not be effectively transported by dSERT and, thus, lack efficacy for inducing efflux. However, dSERT could have an impaired ability to outwardly transport substrates; therefore, I tested the ability of the known substrate 5-HT to induce

Table 2.2: Estimated EC_{50} values for [^{3}H]5-HT efflux in stably transfected HEK-293 cells.

Amphetamine derivative EC_{50} values (nM) for [^{3}H]5-HT efflux in HEK-293 cells stably expressing hSERT, dSERT, or cross-species chimeras. EC_{50} values represent mean ± S.E of three independent assays performed in triplicate. ND: Not determined due to lack of efficacy.

Table 2.2

Compound	hSERT (nM)	dSERT (nM)	$H^{1-118}D^{119-627}$ (nM)	$H^{1-281}D^{282-476}H^{477-638}$ (nM)
5-methoxy-6-methyl-2-aminoindan	530 ±80	3050 ± 280	35800 ± 2300	12600 ± 1060
3,4-dichloroamphetamine	70 ± 10	1340 ± 680	1560 ± 320	1560 ± 270
3,4-difluoroamphetamine	1560 ± 60	ND	ND	ND
4-trifluoromethylamphetamine	270 ± 80	6030 ± 2190	2150 ± 1100	6480 ± 1110
4-methylthioamphetamine	210 ± 80	19400 ± 5600	16600 ± 7300	23900 ± 2300
3-methylthioamphetamine	2780 ± 680	16700 ± 6200	9600 ± 1570	11890 ± 1700

Figure 2.5: Effects of MMAI on the efflux of [^{3}H]5-HT release at hSERT and dSERT (A), uptake inhibition (B), or cold 5-HT-induced [^{3}H]5-HT efflux (C) in HEK-293 cells stably transfected with hSERT, dSERT, or cross-species chimeras. HEK-293 cells stably transfected with (■) hSERT, (▲) dSERT, (▼)$H^{1-118}D^{119-627}$, and (◆) $H^{1-281}D^{282-476}H^{477-638}$ were loaded with [^{3}H]5-HT (50 nM) for five minutes (hSERT) or thirty minutes (dSERT and cross-species chimeras) and efflux induced by increasing concentration of unlabeled substrate as described in Materials and Methods. EC_{50} values for MMAI and the other amphetamine derivatives are in Table 2. Stimulation of [^{3}H]5-HT efflux assay (C) by unlabeled 5-HT was performed at hSERT (EC_{50}= 7.7 ± 0.8 μM) and dSERT (6.1± 0.4 μM) as described in Materials and Methods. Results shown represent mean ± standard errors of triplicate determination and are representative of three independent experiments.

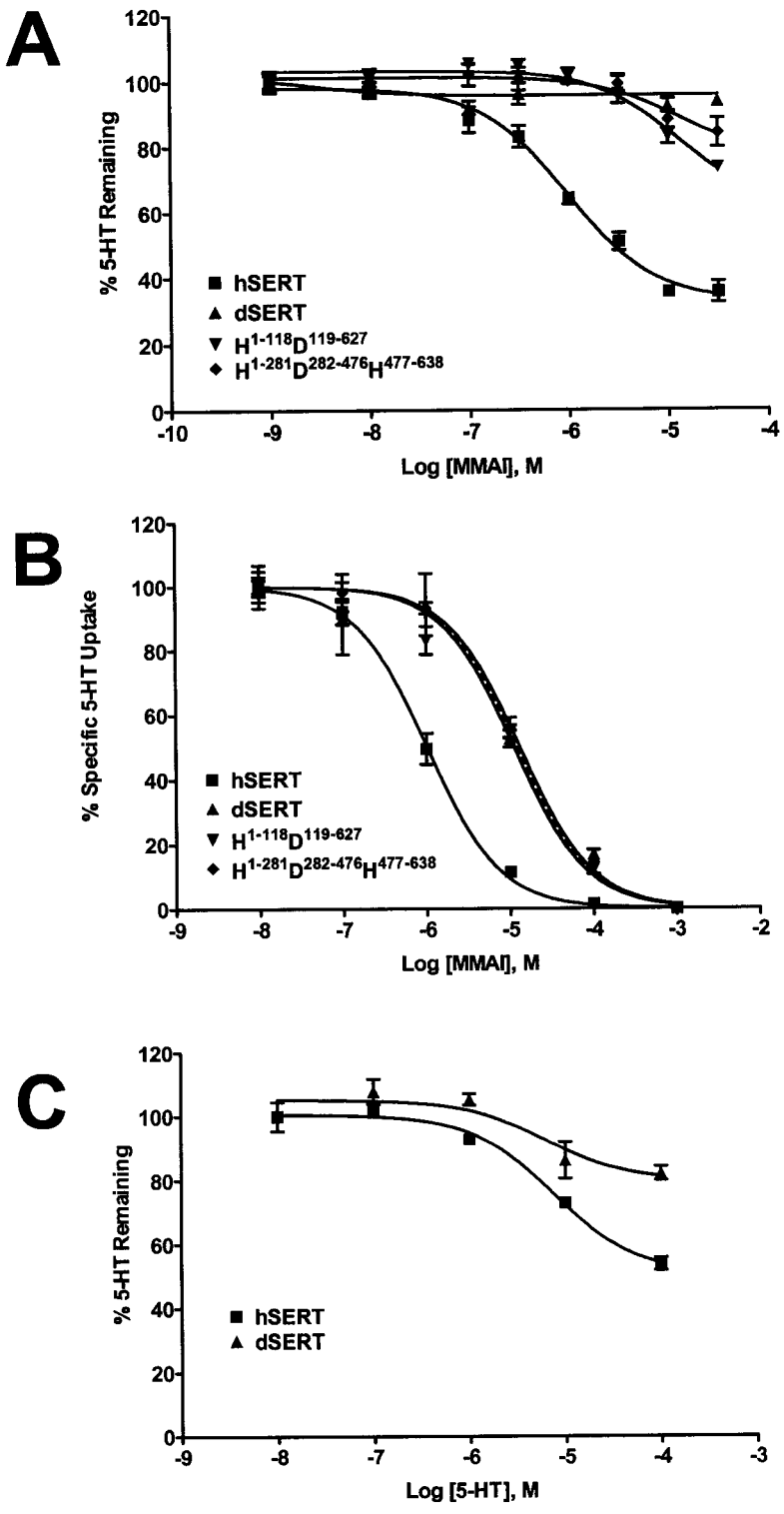
A
% 5-HT Remaining
Log [MMAI], M
hSERT
dSERT
H1-118D119-627
H1-281D282-476H477-638
B
% Specific 5-HT Uptake
Log [MMAI], M
hSERT
dSERT
H1-118D119-627
H1-281D282-476H477-638
C
% 5-HT Remaining
Log [5-HT], M
hSERT
dSERT

Figure 2.5

efflux at hSERT and dSERT. Similar to my findings with the amphetamine analogs, unlabeled 5-HT induced less release of internal substrate from dSERT compared with hSERT, suggesting that dSERT may have reduced capacity for reverse substrate transport (Fig 2.5C).

To characterize further the differences in 5-HT release between hSERT and dSERT, I examined the rates and the turnover number for 5-HT release. First, I determined the initial rate of [^{3}H]5-HT release stimulated by unlabeled 5-HT (10 μM). hSERT demonstrated a faster rate of release (13.0 ± 3.0 x 10^{-19} mol/min/cell) compared with dSERT (2.0 ± 0.6 x 10^{-19} mol/min/cell, Fig 2.6A). Release rates were normalized to the number of transporters at the cell surface to estimate the turnover number for efflux. Similar to inward 5-HT transport, the estimated turnover for efflux rate was statistically greater for dSERT. The estimated turnover rate for efflux was 0.32 ± 0.02 and 0.43 ± 0.01 molecules/min/transporter for hSERT and dSERT, respectively (Fig 2.6B). Although 5-HT-induced release studies suggest a reduced efflux capacity at dSERT, the estimated turnover number for efflux suggests that the apparent reduction in efflux capacity at dSERT is the result of lower cell surface expression.

Galli and coworkers (Saunders et al., 2000) demonstrated the regulation of human dopamine transporter (hDAT) surface expression by amphetamine. Amphetamine promoted a loss of hDAT expression from the cell surface by redistribution of the transporter. 5-HT could induce a loss of dSERT surface expression during my preloading step. Loss of dSERT from the cell surface would lead to fewer transporters to participate in efflux and could explain in part the differences of substrate release between hSERT and dSERT. Preincubation with 5-HT at a concentration equivalent to that used for loading in the efflux experiments did not change cell surface expression of hSERT or dSERT as determined by cell surface binding experiments (data not shown). This result indicates that the differences between hSERT and dSERT for substrate release are not the result of changing cell surface expression.

Figure 2.6: Time-course of [^{3}H]5-HT efflux (A) and efflux transport turnover rates (B) at hSERT and dSERT. HEK-293 cells stably transfected with hSERT or dSERT were preloaded with [^{3}H]5-HT at 37°C for 5 minutes (hSERT) or 30 minutes (dSERT) to provide equivalent loading. (A) Efflux was induced with unlabelled 5-HT (10 μM) and stopped with three washes of ice-cold KRH. Data was analyzed and efflux rate (5-HT moles/cell) calculated using linear regression analysis (GraphPad Software, San Diego, CA). (B) Turnover cycle for efflux was calculated using the rate of efflux divided by the number of transporters at the cell surface. Results represent the mean ± SEM of three independent experiments, *$p < 0.05$ using a two-tailed Student's t-test.

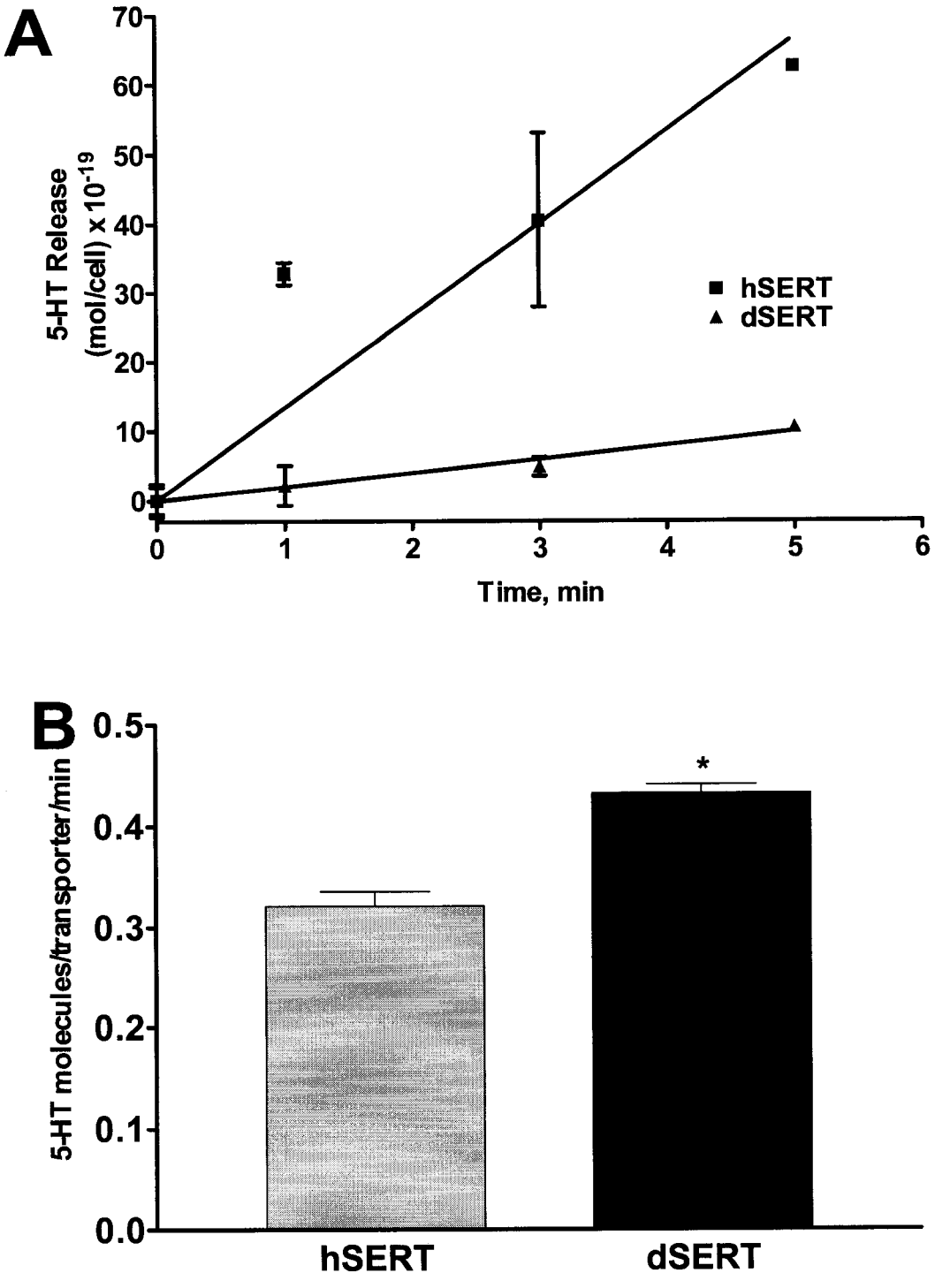
A
5-HT Release
(mol/cell) x 10-19
70
60
50
40
30
20
10
0
0
1
2
3
4
5
6
Time, min
hSERT
dSERT
B
5-HT molecules/transporter/min
0.5
0.4
0.3
0.2
0.1
0.0
*
hSERT
dSERT

Figure 2.6

Discussion

Although several studies have explored the inward (Barker et al., 1999;Adkins et al., 2001;Sitte et al., 2001) and outward (Rudnick and Wall, 1992 a,b,1993;Scholze et al., 2000;Sitte et al., 2000;Sitte et al., 2001) transport process in SERT as well as other monoamine transporters (Pifl and Singer, 1999), the molecular mechanisms of both processes remain poorly understood. Previous studies have exploited species-specific properties of SERTs to identify domains involved with transporter substrate and inhibitor recognition (Barker et al., 1994;Barker et al., 1998). For substrates, the SERT species variants approach was used to explore the interaction of tryptamine analogs with the human and *Drosophila* SERTs (Adkins et al., 2001). Species-scanning mutagenesis implicated a single amino acid at position 95 for tryptamine recognition, supporting the role of TMD I in the inward transport mechanism. Similarly, I used species variants and cross-species chimeras to explore regions in the SERT involved in the inward and outward transport mechanism.

Although both hSERT and dSERT were able to translocate 5-HT, dSERT did not readily transport other SERT substrates such as MPP^+ or amphetamines. K_m values for 5-HT revealed similar relative affinities for both transporters. In contrast, the greater V_{max} value for hSERT than for dSERT may suggest differences in inward transport capacity or cell surface expression levels. Moreover, whole-cell binding studies confirmed higher hSERT expression on the cell surface than dSERT expression, indicating that more human transporters are able to participate in uptake. I recognize that the whole-cell binding experiments require several assumptions and that the method has potential caveats. For example, the ability of the ligands used (both labeled and unlabeled) to permeate the membrane will vary depending upon the hydrophobicity of the specific compound. My experiments were performed under assumed equilibrium (one hour incubation) and, thus, the hydrophobic ligands should sufficiently distribute to fully bind intracellular transporters. In addition, separation of bound and free

radioligand can be problematic in whole-cell binding approaches. My washes were completed within 10 s, which should minimize any loss of bound radioligand for the high-affinity radioligands used (K_d values ≈ 3 nM).

Studies were performed using MPP^+ to further explore species selectivity for inward transport. As in previous reports, hSERT was able to transport MPP^+ (Sitte et al., 2000, 2001). Interestingly, neither dSERT nor the cross-species chimeras transported MPP^+, suggesting species distinction for substrate recognition and/or transport capacity between hSERT and dSERT. In additional studies, MPP^+ inhibited 5-HT uptake in both parental and chimeric SERTs with similar potencies, demonstrating the ability of all SERT constructs to recognize MPP^+. These findings suggest species distinction for MPP^+ interactions between hSERT and dSERT. This molecule has substrate properties at hSERT (i.e., 5-HT), but interacts with dSERT like a transport blocker. Furthermore, my results from cross-species chimeras implicate TMDs V to IX of SERT in the inward transport mechanism but not necessarily in substrate recognition. Previously, a study in rat DAT has suggested the importance of two serine residues localized in TMDs VII and XI for the inward transport of MPP^+ (Kitayama et al., 1993). Alanine substitutions for Ser^{350} and Ser^{353} at rat DAT preferentially increased V_{max} for MPP^+ transport. Interestingly, Ser^{350} is conserved among the monoamine transporters. Whereas hSERT has shared identity with rat DAT at position 353, dSERT has an alanine residue at the corresponding position. My results suggest the presence of specific residues in this region of SERT that are involved in the molecular mechanism of MPP^+ uptake. Residues divergent between hSERT and dSERT in the region flanked by TMDs V to IX will be explored in the next chapter.

Another characteristic of SERT and other GAT/NET transporter gene family members is the ability to outwardly transport substrate from the cytoplasm. A transporter-dependent release process has been demonstrated by changing transmembrane ion gradients (Pifl et al., 1997) or by the facilitated efflux model (Wall et al., 1995;Johnson et al., 1998;Sitte et al., 1998). My experiments

focused on studying facilitated exchange or efflux by SERT species variants as a method to identify whether the substituted amphetamines were transported. My data revealed that the amphetamines were not effectively transported by dSERT and, hence, failed to induce substrate efflux. Amphetamine analogs blocked the uptake of 5-HT at dSERT but were unable to induce substrate efflux. In addition, I observed that the substituted amphetamines were less potent at dSERT as compared with hSERT, suggesting that species-specific differences in the recognition of the amphetamines exist that may or may not influence actual translocation. Results from the cross-species chimeras suggest that TMDs V to IX of SERT may be responsible for amphetamine recognition and transport.

Previous studies have demonstrated a channel mode of behavior for dSERT and suggested that this mode may modulate substrate permeation at high extracellular substrate concentration (Galli et al., 1997;Petersen and DeFelice, 1999). If such a channel mode existed for dSERT, I would not expect efflux to occur because one major distinction between transporters and channels is the inability of channels to carry out substrate-induced efflux (Stein, 1986). Even in the case that dSERT may behave as a channel, 5-HT efflux has been shown at high extracellular substrate concentration (Petersen and DeFelice, 1999). dSERT may alternate between transport and channel modes and is influenced by the environment (i.e., high sodium concentration in the cytoplasm). Our laboratory has used two-electrode voltage clamp studies in oocytes injected with wild-type SERT and dSERT. MMAI only induced 7% of the 5-HT-induced current in oocytes expressing dSERT, whereas this amphetamine analog induced an inward current in oocytes expressing hSERT comparable to that observed for 5-HT (Rodriguez et al., 2003). The electrophysiological data support my findings that amphetamine analogs are poor substrates for dSERT. The complex behavior of dSERT in this regard warrants further study, since it may have some contributory influence on potential distinction in substrate recognition that modifies inward and outward transport properties.

I also explored whether differences exist in the turnover numbers for the inward and outward transport processes between hSERT and dSERT. Whole-cell binding experiments demonstrated higher surface expression for hSERT than for dSERT. This finding explains the greater V_{max} values for 5-HT uptake at hSERT than at dSERT. Calculation of the inward turnover number for dSERT revealed a 2-fold greater value than for hSERT. Interestingly, the turnover numbers for efflux demonstrated a much smaller difference between the species variants. These results suggest unequal flux between extracellular and intracellular substrates. hSERT and dSERT most likely differ in the rate of inward transport relative to the reorientation of the transporter. The net inward transport rate for the two SERTs is influenced by many factors, including the reorientation of the "empty" SERT to the outside. This reorientation rate could be altered by outwardly moving substrate during efflux, thus, possibly explaining the differences in inward and outward transport rates for hSERT and dSERT. A study performed in hDAT demonstrated that flux between an external substrate and internal dopamine is unequal (Chen and Justice, 2000). Simultaneous monitoring of tyramine uptake and induced dopamine efflux revealed that the initial efflux rate of internal dopamine is only 6% of the initial entry rate of external tyramine. These results confirm differences in the conformational requirements for inward and outward transport mechanisms that may be partially responsible for the asymmetric flux between internal and external substrates.

In summary, my studies revealed major differences between hSERT and dSERT for substrate recognition and translocation. My data demonstrated similar 5-HT kinetics for hSERT and dSERT, but major differences for other substrates might suggest that dSERT and hSERT possess fundamental differences for recognition of MPP^+ and amphetamines that do not allow for translocation. Alternatively, hSERT and dSERT could possess differences affecting how all substrates are recognized and translocated. For 5-HT, these differences are not apparent based on my transport kinetic measures but are revealed by other substrates. My studies implicate the middle region of the SERT in substrate

translocation through the membrane. Previously, a role of TMD I in the substrate permeation pathway has been defined (Barker et al., 1999). Recently, Ravna and Edvardsen (Ravna and Edvardsen, 2001) constructed a hypothetical three-dimensional model of the hSERT. Their arrangement of the TMDs places TMDs I and VII in the 5-HT permeation pathway. My results lead to several questions about SERT structure and the molecular mechanism involved in substrate permeation. For example, identification of residues within TMDs V to IX involved in the species-specific properties may in part clarify the molecular mechanism of substrate transport. Moreover, this region may also interact with other TMDs to stabilize a specific conformation that is favorable for inward and outward transport. Contribution of specific TMD important for substrate mechanism will be explored in subsequent chapters.

Chapter III

Potential contribution of TMD VII to the substrate permeation pathway.

Introduction

In the previous chapter, I demonstrated that differences in substrate translocation in hSERT, dSERT, and cross-species chimeras, implicated the middle portion of SERT for these differences. Among the TMDs that encompass this region, TMD VII has been the focus of several studies primarily due to its amphipathic nature. TMD VII in DAT was previously implicated in substrate recognition (Kitayama et al., 1993). In SERT, random mutagenesis in TMD VII identified critical residues for the sodium dependence of substrate transport (Penado *et al.*, 1998a). Recently, these residues were suggested to interact with other α-helices in SERT (Kamdar *et al.*, 2001a).

Several regions in SERT have been implicated in substrate and antagonist recognition, ion conductance, and substrate permeation. Studies using cross-species chimeras of the human and rat SERTs identified a region distal to TMD XI that dictates the increased sensitivity of hSERT to the tricyclic antidepressant imipramine (Barker et al., 1994). Mutagenesis studies in DAT and SERT revealed critical residues in TMD I for substrate transport and antagonist recognition (Kitayama *et al.*, 1992a;Barker *et al.*, 1999b;Barker *et al.*, 1998b). Mutation of D98 in hSERT abolished substrate transport without reducing surface density of the transporter (Barker *et al.*, 1999a). D98, a conserved residue among SERT, DAT, and NET, but divergent in the GABA transporter, is predicted to interact with the amine group of 5-HT, a critical event for the translocation of substrates. Y95, also in TMD I, has been shown to interact with antagonists and

tyramine analogs (Barker *et al.*, 1998a). More recently, SCAM studies in TMD I provided insights into the role of this α-helix in the permeation pathway (Henry et al., 2003). Mutagenesis studies also revealed residues in TMD III important for substrate translocation, cocaine binding, and ion conductance (Lin et al., 1996;Chen et al., 1997b;Chen and Rudnick, 2000). Mutation of TMD III residue N177 affected ion currents in SERT suggesting that this residue may be localized to a water-filled pore used in the permeation pathway (Lin et al., 1996). Rudnick and coworkers identified three residues, Ile-172, Tyr-176, and Ile-179, which are localized on the same face of the α-helix (Chen *et al.*, 1997). Moreover, I172 and Y176 are predicted to be in proximity to the binding site for 5-HT and cocaine. Recently, I179 was determined to be in a conformation sensitive position in TMD III and may be part of an external gate (Chen and Rudnick, 2000).

Cross-species chimeras from hSERT and dSERT identified the region from TMD V to IX as important for the differences in substrate transport (Rodriguez *et al.*, 2003a) and antagonist binding (Roman et al., 2003a,b) between these species. To further isolate specific residues involved in substrate transport, I identified residues in TMDs V to VIII divergent between hSERT and dSERT. These positions at hSERT were mutated to the residue at the equivalent position in dSERT. TMD VII mutants, V366S, M370L, S375A and T381S, showed a reduction in 5-HT and MPP^+ transport. Cysteine mutants at these positions in TMD VII were also generated, and MTS reagents were used to determine their accessibility from the extracellular environment. Only V366C and M370C reacted with MTSET in a way that disrupted 5-HT transport suggesting that these residues may be part of the permeation pathway for substrate translocation. Furthermore, residues S375 and T381, while seemingly insensitive to MTSET, may be involved in intra-protein interactions between TMD VII and other TMDs supporting previous studies on TMD VII (Penado *et al.*, 1998c).

Materials and Methods

Materials

The cDNA encoding the hSERT/C109A mutant in pBluescript KSII was a generous gift from Dr. Randy Blakely (Vanderbilt University). [^{3}H]5-hydroxytryptamine ([^{3}H]5-HT; 122 Ci/mmol) and [^{3}H]citalopram (85 Ci/mmol) were purchased from Amersham Biosciences Inc. (Piscataway, NJ). [^{3}H]MPP$^+$ (83.5 Ci/mmol) was obtained from PerkinElmer Life Sciences (Boston, MA). Fluoxetine, MPP$^+$, MDMA and pargyline were purchased from Sigma/RBI (Natick, MA). MTSET and MTSES ([2-(trimethylammonium)ethyl]methanethiosulfonate], were purchased from Toronto Research Chemical (Toronto, Canada). Unlabeled 5-HT was obtained from Sigma-Aldrich (St. Louis, MO). All other reagents were purchased from commercial sources.

Cell culture

HEK-293 wild-type and transiently transfected cells were maintained in Dulbecco's Modified Eagle's Medium (DMEM) with 10% dialyzed fetal bovine serum supplemented with penicillin, streptomycin, and L-glutamine. Cells were grown in a 37°C humidified environment with 5% CO_2. Transient transfection was performed in 24-well poly-D-lysine coated plates using Lipofectamine 2000 per manufacturer's instructions (Life Technologies, Gaithersburg, MD).

Site-directed mutagenesis

Residues in the TMD V to VIII region divergent between hSERT and dSERT were identified and mutated. Two criteria were used to select residues for mutagenesis: (1) localized between TMDs V to VIII region, and (2) divergent between hSERT and dSERT, where identity is similar to hDAT and dSERT

because dSERT has similar pharmacology for amphetamines interaction with DAT/NET. TMD IX was excluded from these studies because an hSERT/dSERT chimera constructed from hSERT with dSERT TMD IX inserted produced an inactive transporter. I generated seven mutants in this region where the residue at hSERT was mutated to the residue at the corresponding position in dSERT. The mutants A300V, V366S, V367I, M370L, S375A, T381S, and P418S were generated using the QuikChange® site-directed mutagenesis kit (Stratagene, La Jolla, CA). Oligos were designed to introduce the mutation at the corresponding positions (Table 3.1, Integrated DNA Technologies, Coralville, IA).

For the substituted-cysteine accessibility method (SCAM) I generated several cysteine mutants in TMD VII. The C109A/hSERT cDNA in pBluescript was digested with NotI and AgeI enzymes. The resulting fragment was inserted in hSERT/pcDNA 3.1+ and digested with NdeI to confirm the C109A mutation. This cDNA was used as the background to generate all of the cysteine mutants in hSERT to reduce background MTS reactivity. Residues S365, V366, V367, M370, F380, and T381 were selected for mutation. Site-directed mutagenesis was performed using the QuikChange® mutagenesis kit as described above with the corresponding oligos (Table 3.2). Mutations were confirmed by enzyme digestion and DNA sequencing (University of Michigan DNA sequencing core facility).

[^{3}H]Substrate uptake assays

Saturation transport assays and uptake inhibition experiments were performed in 24-well culture plates precoated with poly-D-lysine as described in Chapter II.

Table 3.1: Oligos used to generate mutants in TMD VII in hSERT to the corresponding position in dSERT.

Mutant	Oligos	
A300V	5′GGTGAGGGGTGTCACCCTCCCGGGAGCCTGGAG3′	(sense)
	3′ TCCAGGCTCCCGGGAGGGTGACACCCCTCACC5′	(antisense)
V366S	5′CCCTGGTGACCAGCTCGGTCAACTGCATGACGAG3′	(sense)
	3′CTCGTCATGCAGTTGACCGAGCTGGTCACCAGGG5′	(antisense)
V367I	5′GACCAGCGTGATCAACTGCATGACAAGCTTCGTTTC3′	(sense)
	3′GAAACGAAGCTTGTCATGCAGTTGATCACGCTGGTC5′	(antisense)
M370L	5′GGTGAACTGCTTGACAAGCTTCGTTTCG3′	(sense)
	3′CGAAACGAAGCTTGTCAAGCAGTTCACC5′	(antisense)
S375A	5′GGTGAACTGCATGACAAGCTTCGTTGCGGGATTTGTC3′	(sense)
	3′GACAAATCCCGCAACGAAGCTTGTCATGCAGTTCACC5′	(antisense)
T381S	5′GTCATCTTCTCAGTGCTCGGGTACATGGCTGAG3′	(sense)
	3′CTCAGCCATGTACCCGAGCACTGAGAAGATGAC5′	(antisense)
P418S	5′GCGATAGCCAACATGTCAGCGTCAACTTTCTTTGCC3′	(sense)
	3′GGCAAAGAAAGTTGACGCTGACATGTTGGCTATCGC5′	(antisense)

Table 3.2: Oligos used to generate cysteine mutants in TMD VII in hSERT.

Mutant	Oligos	
S365C	5′GCCCTGGTGACCTGCGTGGTCAACTGCATGACG3′	(sense)
	3′CGTCATGCAGTTGACCACGCAGGTCACCAGGGC5′	(antisense)
V366C	5′GCCCTGGTGACCAGCTGCGTCAACTGCATGACGAGC3′	(sense)
	3′GCTCGTCATGCAGTTGACGCAGCTGGTCACCAGGGC5′	(antisense)
V367C	5′GTGACCAGCGTGTGCAACTGCATGACAAGCTTCGTTTCG3′	(sense)
	3′CGAAACGAAGCTTGTCATGCAGTTGCACACGCTGGTCAC5′	(antisense)
M370C	5′CGTGGTGAACTGCTGCACAAGCTTCGTTTCG3′	(sense)
	3′CGAAACGAAGCTTGTGCAGCAGTTCACCACG5′	(antisense)
S375C	5′CGAGCTTCGTTTGCGGATTTGTAATATTCACAGTGC3′	(sense)
	3′GCACTGTGAATATTACAAATCCGCAAACGAAGCTCG5′	(antisense)
F380C	5′GATTTGTCATCTGCACAGTGCTCGGGTACATGGCTG3′	(sense)
	3′CAGCCATGTACCCGAGCACTGTGCAGATGACAAATC5′	(antisense)
T381C	5′GGATTTGTCATCTTCTGCGTGCTCGGGTACATGGCTGA3′	(sense)
	3′TCAGCCATGTACCCGAGCACGCAGAAGATGACAAATCC5′	(antisense)

Whole-cell radioligand binding assay

Whole-cell binding experiments were performed in 24-well plates ($1x10^5$ cells per well) precoated with poly-D-lysine as described previously in Chapter II.

MTS experiments

HEK-293 wild-type cells in 24-well tissue culture plates were transiently transfected with the cysteine mutant cDNAs of interest as described above. Following a 48-hour incubation, cells were washed once with PBS/CM buffer (137 mM NaCl, 2.7 mM KCl, 1.5 mM KH_2PO_4, 8.1 mM Na_2HPO_4, 0.1 mM $CaCl_2$, and 1.0 mM $MgCl_2$), and then incubated for 10 min at room temperature in the presence of an MTS reagent in PBS/CM buffer or buffer alone (total uptake). The concentration of MTS reagents for investigating accessibility of cysteine mutants were as follows: 1 mM MTSET and 2 mM MTSES (Toronto Research Chemicals). Following MTS treatment, cells were washed twice with PBS/CM and subjected to transport assays using 20 nM [^{3}H]5-HT or 50 nM [^{3}H]MPP^+. Nonspecific uptake was determined using 10 µM fluoxetine. Statistical evaluation of MTS sensitivity for different mutants were performed using one-way ANOVA with a post hoc Dunnett multiple comparison test, where $p < 0.05$ was determined to be significant. Results were plotted using normalized data for each mutant, where the untreated activity levels are normalized to 100% to permit visualization of MTS sensitivity across different activity levels of the individual mutants. Protection assays were performed in a similar manner to the MTS treatments described above with the following changes: hSERT/C109A or TMD VII Cys mutants were incubated for 5 min at 25°C with buffer, 50 µM cocaine, 100 nM fluoxetine, 20 µM MDMA, 20 µM 5-HT, or 200 µM MPP^+ followed by incubation in the presence or absence of MTSET for 10 min. Saturating concentrations of the substrates or antagonist were used to ensure full occupancy of transporters during MTS incubations. The cells were washed three

times with PBS/CM buffer to remove ligands and MTSET, and then assayed for uptake activity as described above. A one-way ANOVA with a post hoc Dunnett multiple comparison test of significance was used to identify residues showing ligand modulation, where $p < 0.05$ was determined to be significant.

Data analysis

V_{max} and K_m values in saturation experiments were calculated and exchange EC_{50} values were estimated using nonlinear curve-fitting analysis (Prism 3.0; GraphPad Software Inc., San Diego, CA). All results were expressed as mean ± S.E.M. for at least three experiments performed in triplicate.

Results

Mutations in TMD VII of hSERT affect substrate transport and surface density.

Residues in the TMD V to VIII region divergent between hSERT and dSERT were identified and mutated. Previously, the TMD V to VIII region of SERT and other monoamine transporters has been implicated in substrate translocation and antagonist binding (Kitayama *et al.*, 1992b;Penado *et al.*, 1998b;Kamdar *et al.*, 2001b;Rodriguez *et al.*, 2003b);Roman et al. 2003 a,b). I generated seven mutants in this region where the residue at hSERT was mutated to the residue at the equivalent position in dSERT (Fig 3.1). 5-HT and MPP^+ transport assays were performed on wild-type hSERT and mutants using saturating concentrations of substrate to ensure measurement of full capacity of these transporters (Fig 3.2A and B). Mutants V366S, M370L, S375A, and T381S showed a decrease in transport activity for both substrates in comparison with wild-type. V_{max} values for V366S, M370L, and T381S mutants were lower in comparison to hSERT (Table 3.3). Interestingly, K_m values for 5-HT at these mutants were also lower than wild-type hSERT (Table 3.3). The MPP^+/5-HT transport ratio was calculated for wild-type and mutants to determine if particular mutations specifically affected one substrate over another (Fig 3.2C). This ratio for dSERT is zero because dSERT is incapable of transporting MPP^+ (Chapter II). If a particular mutation in hSERT affects a specific substrate transport process, the MPP^+/5-HT ratio would deviate from wild-type values. The ratio for hSERT was approximately 0.25 ± 0.04 molecules of MPP^+ transported per molecule of 5-HT. The four mutations with reduced transport capacity also showed lower MPP^+/5-HT ratios (V366S = 0.11 ± 0.06; M370L = 0.06 ± 0.09; S375A = 0.01 ± 0.05; T381S = 0.08 ± 0.01) in comparison to wild-type (Fig 3.2C). Lower MPP^+/5-HT ratios for V366S, M370L, S375A, and T381S suggest that the mutations at these positions to the equivalent residue at dSERT alter MPP^+

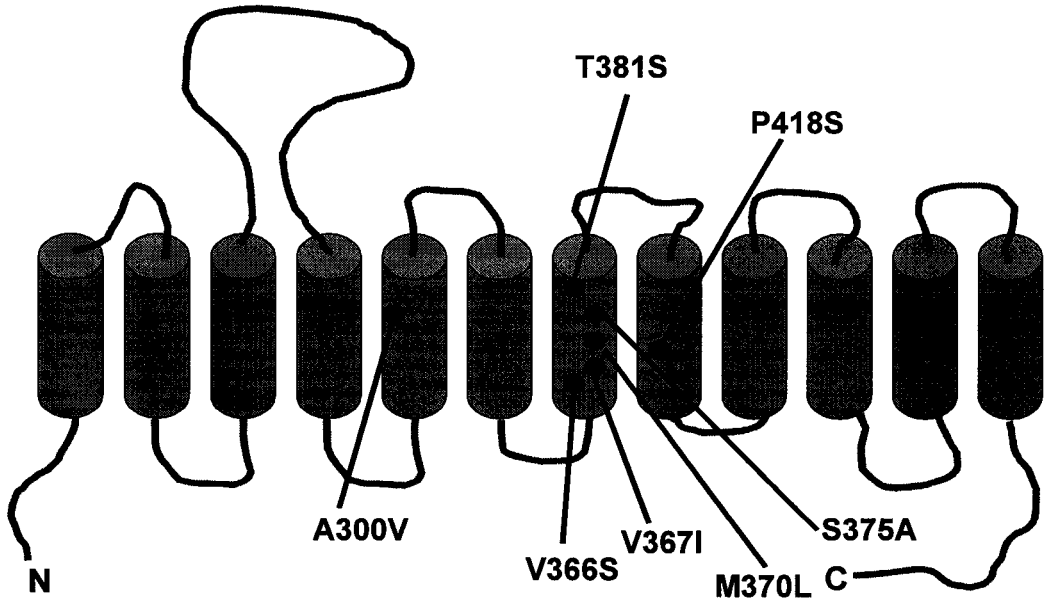

Figure 3.1: Topology and mutations in the TMD V to VIII region of hSERT. Residues in the TMD V to VIII region divergent between hSERT and dSERT were identified and mutated as described in the Materials and Methods.

Table 3.3: Kinetic parameters for wild-type and TMD VII hSERT mutants transiently transfected in HEK-293 cells.

	K_m (μM)	V_{max} (moles/min/cell) x 10^{-18}
hSERT	**4.9 ± 0.5**	**22.9 ± 1.0**
V366S	**1.2 ± 0.2***	**5.5 ± 0.2***
V367I	**5.5 ± 0.2**	**33.3 ± 0.4**
M370L	**1.4 ± 0.4***	**10.0 ± 1.0***
S375A	**2.0 ± 0.5***	**29.0 ± 2.0**
T381S	**1.2 ± 0.1***	**1.5 ± 0.1***

Kinetic values of 5-HT uptake in HEK-293 cells transiently transfected with wild-type hSERT or TMD VII hSERT mutants. Values represent mean ± standard errors for at least three independent experiments. *$p < 0.05$ using a one-way ANOVA test with a post hoc Dunnett test.

Figure 3.2: Uptake of (A) 5-HT, (B) MPP^+, and (C) MPP^+/5-HT ratios in HEK-293 cells transiently transfected with hSERT or hSERT mutants. Cells were plated and transfected as described in Materials and Methods. Specific uptake was determined using fluoxetine (10 μM) as nonspecific. Data represent mean ± SEM for at least two independent experiments performed in triplicate. MPP^+/5-HT ratios were calculated using the specific uptake for 5-HT and MPP^+ (Fig 3.2A and B). Bars represent the mean of three independent experiments ± SEM, $^*p < 0.05$ using a one-way ANOVA test with a post hoc Dunnett test.

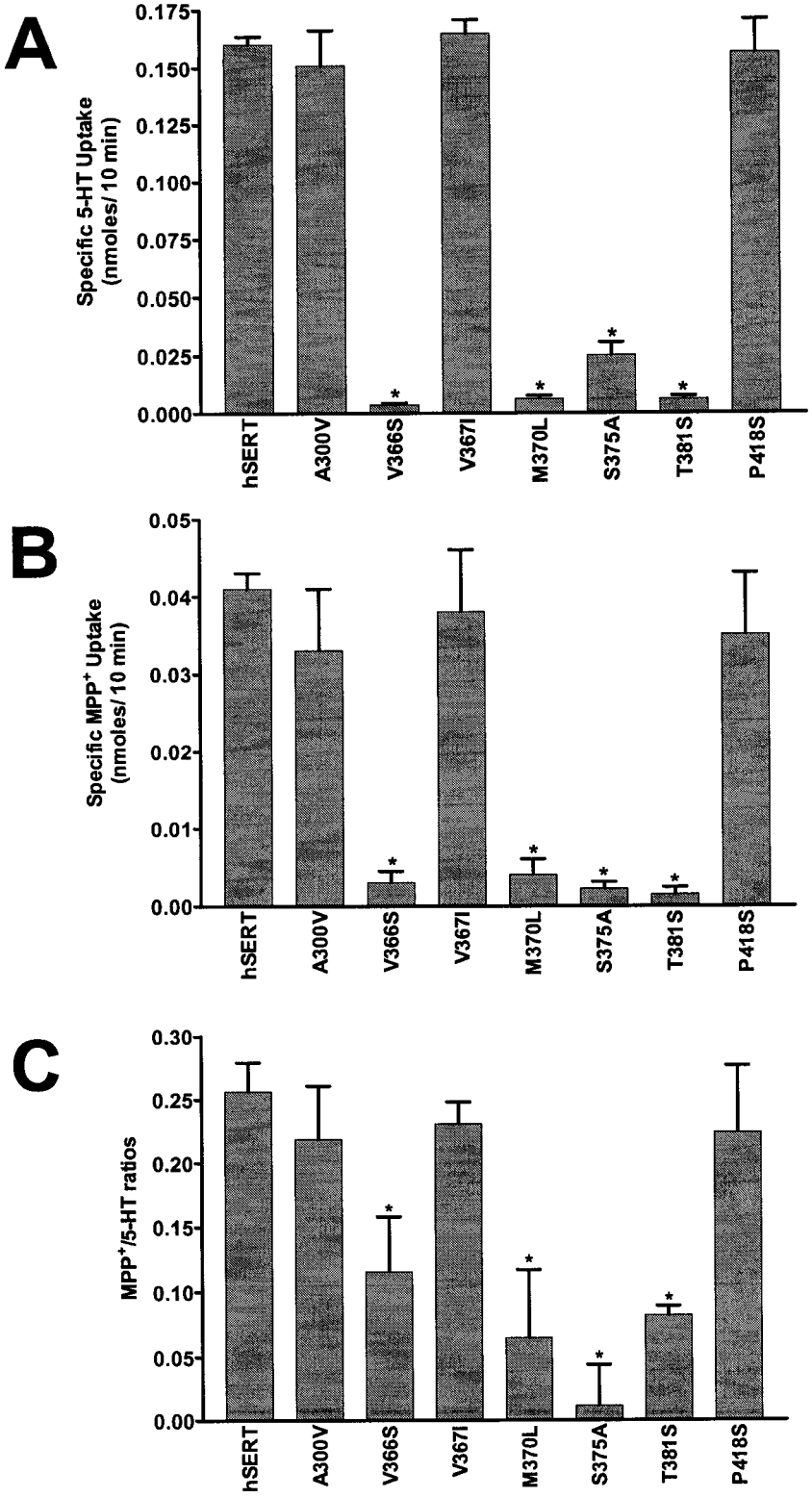
A
Specific 5-HT Uptake (nmoles/ 10 min)
0.175
0.150
0.125
0.100
0.075
0.050
0.025
0.000
hSERT
A300V
V366S
V367I
M370L
S375A
T381S
P418S
B
Specific MPP+ Uptake (nmoles/ 10 min)
0.05
0.04
0.03
0.02
0.01
0.00
hSERT
A300V
V366S
V367I
M370L
S375A
T381S
P418S
C
MPP+/5-HT ratios
0.30
0.25
0.20
0.15
0.10
0.05
0.00
hSERT
A300V
V366S
V367I
M370L
S375A
T381S
P418S

Figure 3.2

transport to a greater extent than 5-HT transport. All four mutants with reduced transport activity and lower MPP^+/5-HT ratios are localized within TMD VII.

To determine if the decrease of transport capacity in these mutants was due to lower surface expression, we performed whole-cell binding experiments. Surface expression of mutants V366S, M370L, S375A, and T381S were lower than wild-type (Fig 3.3), partially explaining the reduction in V_{max} values for these mutants (Table 3.3).

V366C and M370C mutants are accessible to MTSET and partially protected by substrates.

My mutagenesis studies suggest that at least a portion of TMD VII may be part of the permeation pathway for substrates at SERT. Based upon a helical wheel, residues V366, M370, and T381 are predicted to face the same side of the α-helix on TMD VII, whereas S375 is predicted to be localized on the other side of TMD VII. To further explore the role of these residues in the transport process, I generated cysteine mutants at positions S365, V366, V367, M370, S375, F380, and T381. These residues were selected to study different regions of TMD VII. Previously, cysteine substitutions have been used in SERT and other membrane proteins to map externally accessible regions that may be important for substrate translocation. Studies at wild-type hSERT using MTS reagents have demonstrated that the native cysteine at position 109, localized in the first extracellular loop, is sensitive to MTS reagents for 5-HT uptake (Chen et al., 1997a). Upon MTS modification, 5-HT transport is reduced in hSERT, but the C109A mutant reestablished full transport capacity. For my studies, I used the C109A/hSERT as a background to generate all the cysteine mutants. [^{3}H]5-HT transport assays revealed similar uptake capacity for S365C, V367C, and S375C in comparison with C109A/hSERT (Fig 3.4A). Two mutants, F380C and T381C, showed approximately 50% reduction in 5-HT transport. Mutants V366C

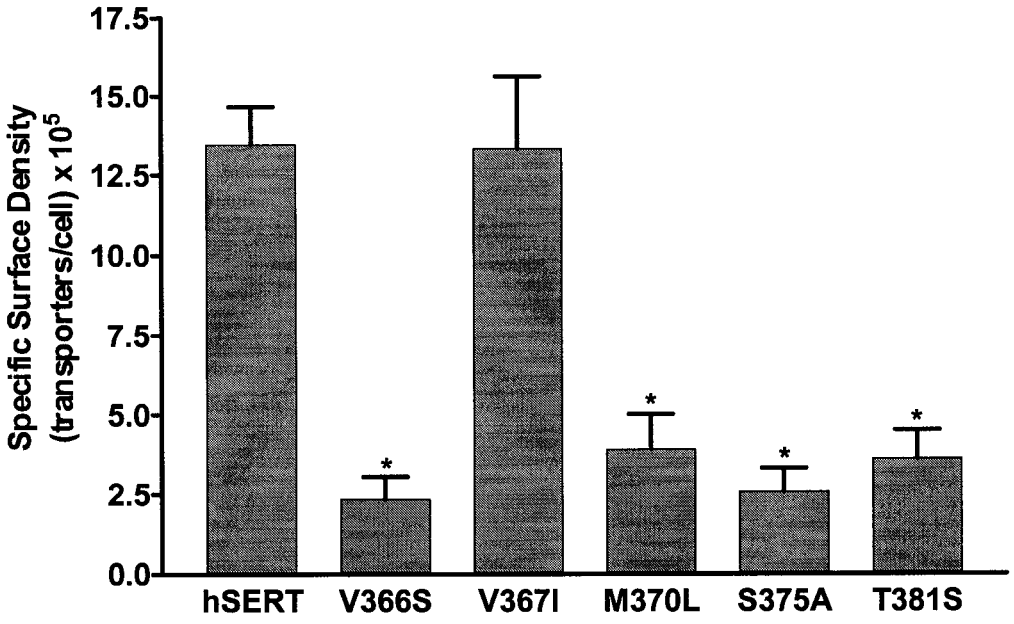

Figure 3.3: Whole-cell radioligand binding in HEK-293 cells transiently transfected with wild-type or hSERT mutants. Assays were performed in 24-well plates coated with poly-D-lysine as described under Materials and Methods. A saturating concentration of [^{3}H]citalopram (20 nM) was used for hSERT and mutants. Nonspecific binding was defined as the binding of radiolabeled ligand in the presence of 10 µM fluoxetine. Internal binding was determined as the binding of [^{3}H]citalopram in the presence of 200 µM MPP^+. Specific surface binding was calculated as (total binding – binding in the presence fluoxetine) – (binding in the presence of MPP^+ – binding in the presence of fluoxetine). Bars represent the mean of three independent experiments ± SEM. *, $p < 0.05$ using a one way ANOVA with post hoc Dunnett test.

Figure 3.4: Transport activity of cysteine mutants in TMD VII. C109A/hSERT and TMDVII mutants were transiently transfected in HEK-293 cells as described in Material and Methods. (A) Transport activity in the presence of [^{3}H]5-HT (20 nM) for 10 min. (B) Transport activity in the presence of [^{3}H]MPP$^+$ (50 nM) for 10 min. Bars represent mean ± SEM from three experiments performed in triplicate. *, $p < 0.05$ using a one way ANOVA with a post hoc Dunnett test.

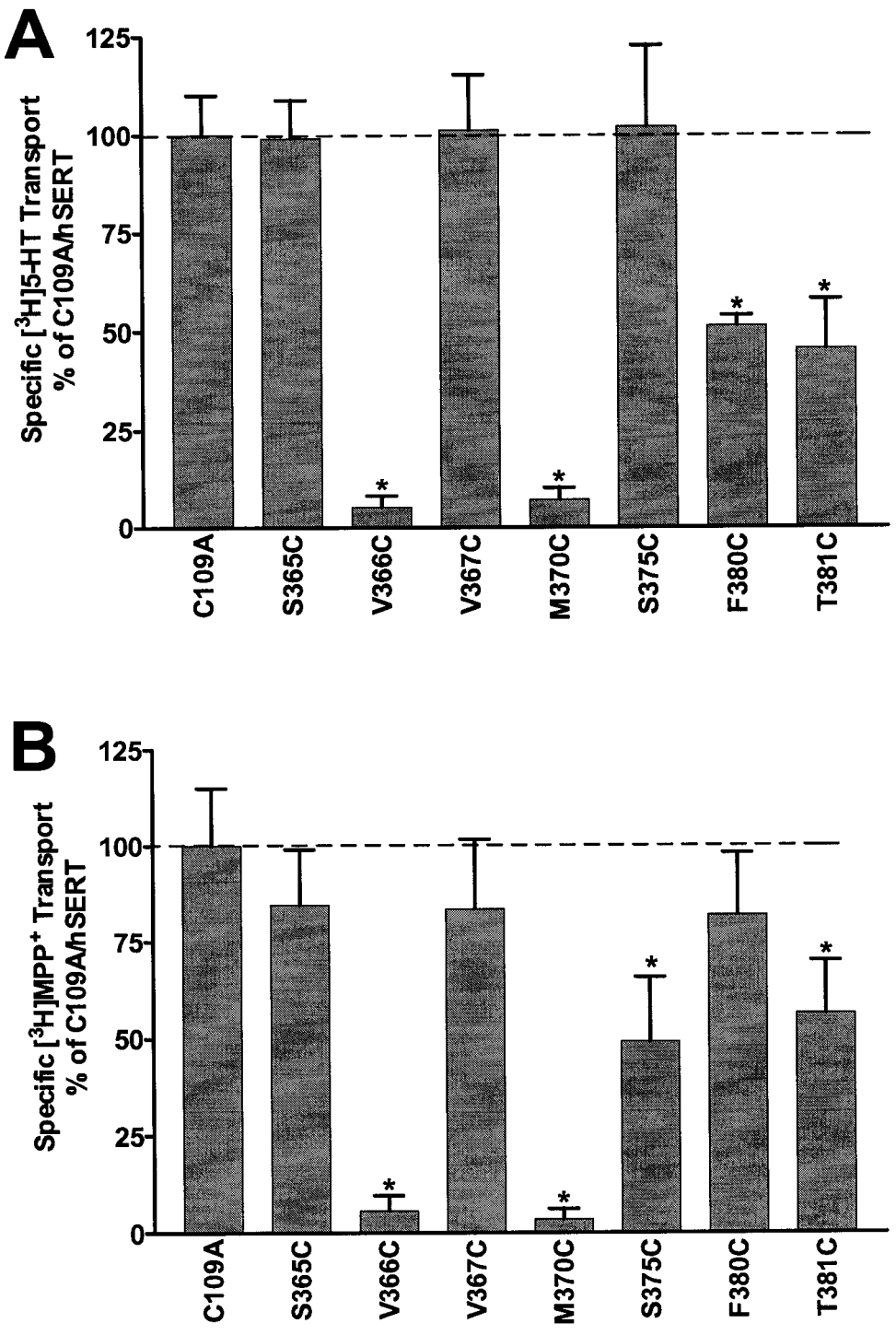
A
Specific [3H]5-HT Transport
% of C109A/hSERT
125
100
75
50
25
0
C109A
S365C
V366C
V367C
M370C
S375C
F380C
T381C
B
Specific [3H]MPP+ Transport
% of C109A/hSERT
125
100
75
50
25
0
C109A
S365C
V366C
V367C
M370C
S375C
F380C
T381C

Figure 3.4

and M370C showed the greatest loss of transport capacity with approximately 5% of C109A/hSERT transport. Likewise, I performed transport assays in these mutants using [^{3}H]MPP$^+$. V366C and M370C showed the greatest reduction in MPP$^+$ transport (less than 3%) in comparison to C109A/hSERT (Fig 3.4B). S365C, V367C, or F380C did not exhibit statistically different MPP$^+$ transport with respect to C109A/hSERT. Interestingly, the S375C mutant showed a 50% reduction in MPP$^+$ transport. This mutation did not affect 5-HT transport, supporting in part our previous results that suggested that mutation at this position affects MPP$^+$ transport to a greater extent than 5-HT uptake (Fig 3.2).

I used membrane-impermeable MTS reagents to determine the accessibility of the cysteine mutants to the hydrophilic environment and to address the possibility that these residues may be part of the pore-forming region in SERT. Pretreatment with MTSET (Fig 3.5A and B) or MTSES (data not shown) caused a decrease in [^{3}H]5-HT transport capacity for V366C (approximately 25% reduction) and M370C (approximately 55% reduction). Furthermore, MTS accessibility was prevented by incubation with unlabeled 5-HT (20 μM) or MPP$^+$ (200 μM) only in V366C (Fig 3.5A). These results suggest that both V366C and M370C are accessible to the external environment in a region that may be involved in substrate translocation. Although my data do not provide evidence that these residues are part of the substrate binding site or interacting directly with the substrate, it may suggest that these residues are part of the pore used by both substrates.

Assays similar to those outlined above were performed in sodium-free buffer (Fig 3.5C and D). Previous SCAM experiments with cysteine mutants show an increase in MTS reactivity in the absence of Na^+ (Ni et al., 2001). Sodium is a key component for substrate transport by SERT. Upon sodium binding, changes in conformation of SERT may alter accessibility of cysteine residues. To determine if sodium alters the accessibility of V366C or M370C, I replaced sodium with lithium, thus, maintaining the buffer's ionic strength. Sodium-free buffer was used only during the pretreatment with MTS reagents.

Figure 3.5: Effects of MTSET in the inactivation of [^{3}H]5-HT transport in HEK-293 transiently transfected cells with C109A or Cys-mutants. 48-hours after transfection, cells were preincubated with MTSET (1 mM) for 10 minutes at room temperature, followed by [^{3}H]5-HT (20 nM) uptake as described under the Material and Methods section. Preincubation with MTSET was performed in the presence of: (A) PBS/CM buffer ± 20 µM unlabeled 5-HT, (B) PBS/CM buffer ± 200 µM unlabeled MPP^+, (C) KRH/sodium-free buffer ± 20 µM unlabeled 5-HT, or (D) KRH/sodium-free buffer ± 200 µM unlabeled MPP^+. Sodium was replaced with equimolar concentration of LiCl to maintain the buffer's ionic strength. Unlabeled substrate was used to determine the ability to protect the mutants from MTS-inactivation. Bars represent mean ± SEM from three experiments performed in triplicate. *, $p < 0.05$ as significant from control using a one way ANOVA with a post hoc Dunnett test. # symbol is statistically different from MTSET treatmen

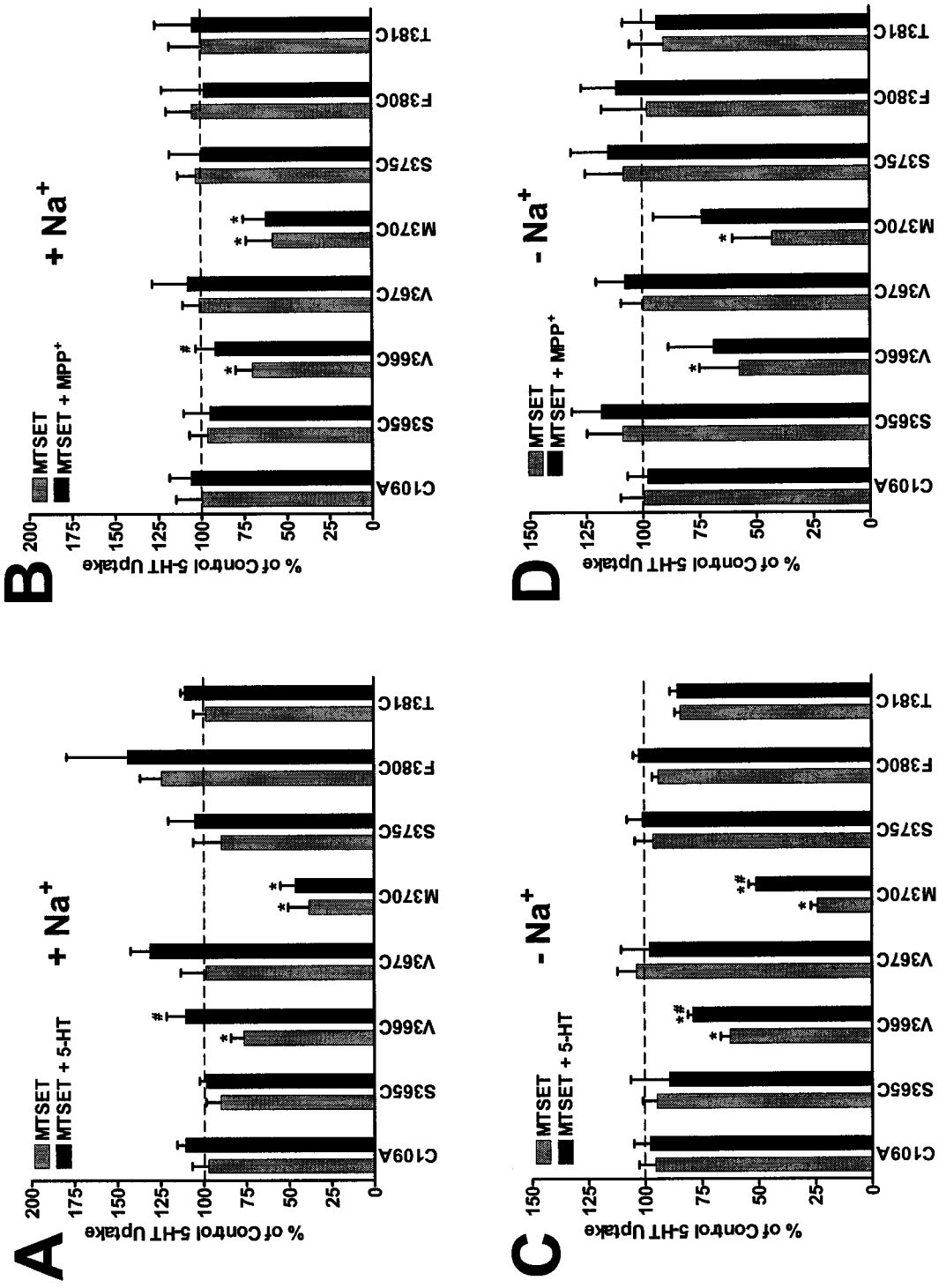
A
+ Na+
MTSET
MTSET + 5-HT
% of Control 5-HT Uptake
200
175
150
125
100
75
50
25
0
C109A
S365C
V366C
V367C
M370C
S375C
F380C
T381C
B
+ Na+
MTSET
MTSET + MPP+
C
- Na+
MTSET
MTSET + 5-HT
D
- Na+
MTSET
MTSET + MPP+

Figure 3.5

Lithium-containing buffer did not alter accessibility of V366C, M370C, or other TMD VII cysteine mutant to MTSET (Fig 3.5C and D), similar to what we observed using sodium-containing buffer (Fig 3.5A and B). These studies also support that these residues are localized in the pore-forming region and the interaction with MTS reagents is not due to conformational changes of the protein upon sodium binding. One difference found when sodium was replaced by lithium was the ability of 5-HT to partially protect M370C from MTS interaction, whereas this substrate partially lose the ability to protect the V366C mutant. I attempted uptake studies using [^{3}H]MPP$^+$ as a substrate in the V366C and M370C mutants, but due to the low transport capacity of MPP$^+$ by these SERT mutants (Fig 3.4B), the effects of MTSET on MPP$^+$ transport were not detected. Other mutants did not show statistically significant differences in MPP$^+$ transport capacity upon MTSET treatment in comparison to C109A/hSERT (data not shown).

I also explored the ability of various SERT ligands including fluoxetine, cocaine, and MDMA to protect the V366C and M370C mutants from MTSET accessibility. The cysteine mutations at positions V366 and M370 did not alter the K_i values for these drugs in comparison with C109A/hSERT (data not shown). Coincubation of saturating concentrations of these drugs completely protected both mutants from MTSET inactivation (Fig 3.6). The SERT antagonists fluoxetine and cocaine as well as the substrate MDMA were able to protect V366C from MTSET interaction, similar to 5-HT and MPP$^+$. Interestingly, these drugs also protected M370C, whereas 5-HT and MPP$^+$ did not protected M370C from MTSET inactivation when assayed in Na^+-containing buffer. Another observation from these studies was that unlike the other substrates, 5-HT and MPP$^+$, MDMA not only prevented MTSET inactivation in V366C, but also induced an increase in transport capacity for 5-HT uptake in comparison to C109A/hSERT.

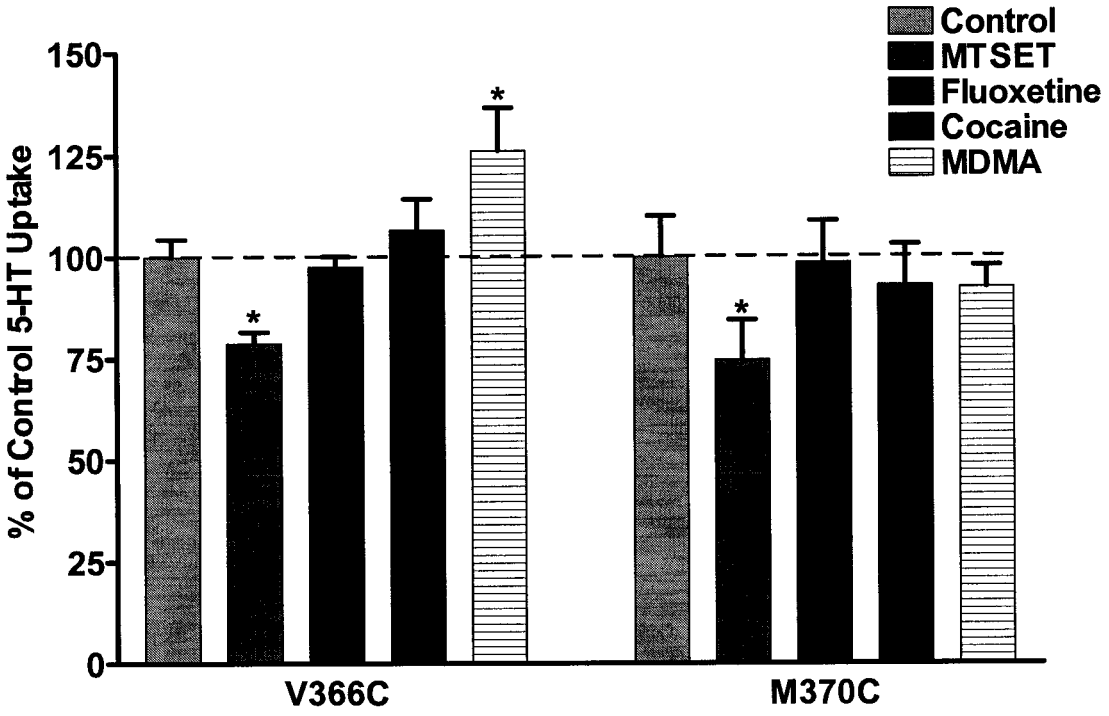

Figure 3.6: MTS accessibility and protection assays using fluoxetine, cocaine, and MDMA in HEK-293 cells transiently transfected V366C or M370 mutant. Saturating concentration of fluoxetine (100 nM), cocaine (200 μM), or MDMA (200 μM) were coincubated with MTSET (1 mM) for 10 minutes at room temperature. Nonspecific transport was determined in the presence of fluoxetine (10 μM). After MTSET/antagonist pretreatment, cells were washed three times with KRH buffer to remove the drugs previous to the substrate transport assay. Cysteine mutants at positions V366 and M370 did not altered these drugs K_i values for 5-HT transport inhibition (data not shown). Bars represent mean ± SEM for three independent experiments performed in triplicate. *, $p < 0.05$ using a one way ANOVA with a post hoc Dunnett test.

Discussion

Different TMDs and extracellular loops of SERT have been implicated for substrate recognition and transport. Among them, TMD VII has been the focus of several studies. Early studies identified three serine residues in hDAT at positions S351, S356, and S359 that were implicated in substrate recognition and translocation (Kitayama et al., 1992, 1993). These residues were suggested to interact with the hydroxyl groups in the catecholamine ring of dopamine, similar to the interaction of this neurotransmitter with adrenergic receptors (Strader et al., 1989). To date, none of the mutagenesis studies in hSERT have identified any of the three serines in TMD VII to either be important for substrate recognition or the translocation process. However, structural studies identified an endogenous Zn^{2+} binding site in DAT that positions TMD VII close to TMD III. TMD III has been demonstrated to have determinants for substrate recognition and transport process as well as transport-associated ion conductance, thus, TMD VII may also be part of the substrate permeation pathway.

Guided by studies using cross-species chimeric SERTs (Chapter II; Rodriguez et al. 2003), I mutated several residues between TMD V to VIII to further explore the role of this region in substrate recognition and the translocation process. Residues divergent between hSERT and dSERT were identified and those positions in hSERT were mutated to the corresponding identity in dSERT. My rationale was that neither dSERT nor the SERT chimeras were able to transport MPP^+, thus, changing the residue from the hSERT to the dSERT identity would allow for identification of determinants in the TMD V to VIII region that may specifically alter MPP^+ recognition or translocation. These studies could also provide more evidence to support differences between the 5-HT and MPP^+ translocation mechanisms at the molecular level.

Functional assays performed on the mutants identified four mutants (V366S, M370L, S375A, and T381S) that decreased transport capacity for the two substrates tested, 5-HT and MPP^+. Interestingly, all of these residues are

predicted to be localized in TMD VII. Although all four mutants identified exhibited lower substrate transport, the MPP^+/5-HT uptake ratios imply that these mutations affected MPP^+ transport to a greater extent than 5-HT transport. My results suggest the possibility that these residues may be part of the substrate permeation pathway. Analysis of the predicted sequence of TMD VII using a helical wheel model localized residues V366, M370, and T381 to the same face of the α-helix whereas S375 is predicted to be on the opposite side. These mutants also exhibited lower cell surface expression in comparison to wild-type hSERT explaining the lower V_{max} for 5-HT transport and suggesting that these mutations may also affect SERT trafficking to the plasma membrane.

To address the possibility that TMD VII may form part of the pore used for substrate translocation, I generated cysteine mutants at position S365, V366, V367, M370, S375, F380, and T381. These mutations were selected to explore different regions in the helix that could be exposed to the hydrophilic environment. SCAM studies using the membrane-impermeable MTSET revealed reactivity with mutants V366C and M370C. These results suggest that V366 and M370 residues are exposed to the hydrophilic environment and possibly part of the permeation pathway. In the presence of Na^+, coincubation of unlabeled 5-HT or MPP^+ was able to protect V366C but not the M370C mutant from MTSET interaction. Interestingly, when Na^+ was replaced with Li^+, unlabeled 5-HT was able to partially protect the M370C mutant from MTSET interaction. The topology of SERT predicts that V366 is localized deeper in the pore than M370, thus reflecting the ability of 5-HT to protect only V366C mutant. One possibility is that the 5-HT binding site is deeper in the pore making V366 closer to the contact site than M370, although there is no evidence that V366 has direct contact with the substrate. The localization of V366 in the pore makes this residue more vulnerable to inactivation by MTSET during 5-HT translocation whereas M370 could remain accessible to MTS inactivation. This model is supported by the observation that in the presence of Li^+, a condition where 5-HT still can bind to the transporter but not trigger translocation, V366C and M370C mutants are

partially protected by 5-HT. However, in the presence of Na^+ and 5-HT, only the residue deeper in the pore (V366) is protected from MTSET inactivation (Fig 3.7).

The other cysteine mutants did not show sensitivity to MTSET. Although in the first set of experiments mutation of residues S375 and T381 to the counterpart in dSERT suggested the possibility that these residues may be part of the pore, SCAM on the cysteine mutants at these positions did not show MTSET inactivation. One possible explanation is that S375 and T381 form interactions with other TMDs necessary for the conformational changes required for substrate translocation. From my studies I cannot rule out the possibility that MTSET was inaccessible to S375C or T381C mutants due to a steric constraint in this region or unfavorable interaction with the positively-charged MTSET. Interestingly, the SERT antagonists fluoxetine, cocaine, and MDMA were able to protect V366 and M370 from MTSET inactivation. My findings suggest that M370 and V366 residues are in close proximity to the binding site for these drugs, thus, upon antagonist binding these sites are protected from interacting with MTSET. Although from my studies, I must consider the possibility that these drugs could induce conformational changes that prevent the accessibility of these residues from interacting with MTSET. This possibility is supported by a recent study in DAT that identified determinants in TMDs VII to VIII for cocaine-dependent conformational changes (Norregaard et al., 2003).

Previously, random mutagenesis studies in TMD VII identified five residues (N368, F373, F377, F380, and Y385) that form a stripe suggested to be important for the translocation of 5-HT and ions (Penado et al., 1998). The stripe of residues down TMD VII was the subject of further analysis to determine their role in SERT function. SCAM provided evidence that these residues are necessary for the propagation of conformational changes occurring after ion binding to the transporter (Kamdar et al., 2001). Perhaps, this domain is an essential part of the translocation mechanism as the stripe region is likely to represent a close contact site for TMD VII and one or more other TMDs.

There are some discrepancies between my results and the data obtained from the random mutagenesis study. Among the SERT mutants generated in this previous study, S375A and F380C showed different activity than what I observed in my studies. In the case of S375A, they observed a high transport capacity for this mutant whereas in my studies this mutation drastically reduced the transport capacity. They also observed approximately 22% reduction in 5-HT transport for F380C. I observed approximately 50% transport reduction for this mutant. These discrepancies may be the result of using different methodologies to perform the experiments. First, different cell lines were used to perform the experiments. For my studies, I utilized HEK-293 cells while HeLa cells were used in the other study. This could be a factor because, previously, our laboratory has observed different pharmacological profiles for hSERT between these two cell lines (Saldana and Barker, 2003). Moreover, MPP^+ uptake in HeLa cells transiently expressing hSERT showed higher nonspecific transport making it impossible to accurately study this process in HeLa cells (Rodriguez and Barker, unpublished observations). For this reason, my studies were performed in HEK-293 cells. Furthermore, surface expression of S375A or F380C was not calculated in HeLa cells making it impossible to determine if cell surface expression is another factor for the discrepancy. Another possibility is the method used to transfect the cells. In my studies, I used Lipofectamine 2000 whereas the other study used the T7 vaccinia virus method. Differences in transfection efficiency between these two methods could also contribute to the discrepancies found in these two experiments. A third factor that could influence the results obtained was the methodology used to measured 5-HT uptake. Although the methods in both studies were similar, the concentration of [^{3}H]5-HT used was different. Penado et al. used 14.6 nM of radiolabeled 5-HT. In my studies, 5-HT uptake assays were performed with a saturating concentration of substrate (20 μM) to ensure measurement of full transport capacity for these mutants.

Significant analysis of TMD VII has been performed and the consensus appears that this domain does provide a major contribution for conformational changes associated with substrate uptake (Kamdar et al., 2001;Norregaard et al., 2003). My results from the mutants at S375 and T381 are consistent with this conclusion, although my studies also suggest that the side of the helix where V366 and M370 residues (S351 and L355 in hDAT, respectively) may actually form part of the permeation pathway. Interestingly S351 in hDAT was implicated in MPP^+ transport (Kitayama et al., 1993). Based upon proximity studies that place TMD VII near TMD III, my results suggest that this domain does form part the permeation path and play an important role in overall conformation changes that support substrate translocation. Moreover, the ion composition in the media influences the interaction of substrates with positions V366 and M370 as well as the ability of substrates to protect from MTSET consistent with the potential role of this region in the permeation pathway (Fig 3.7).

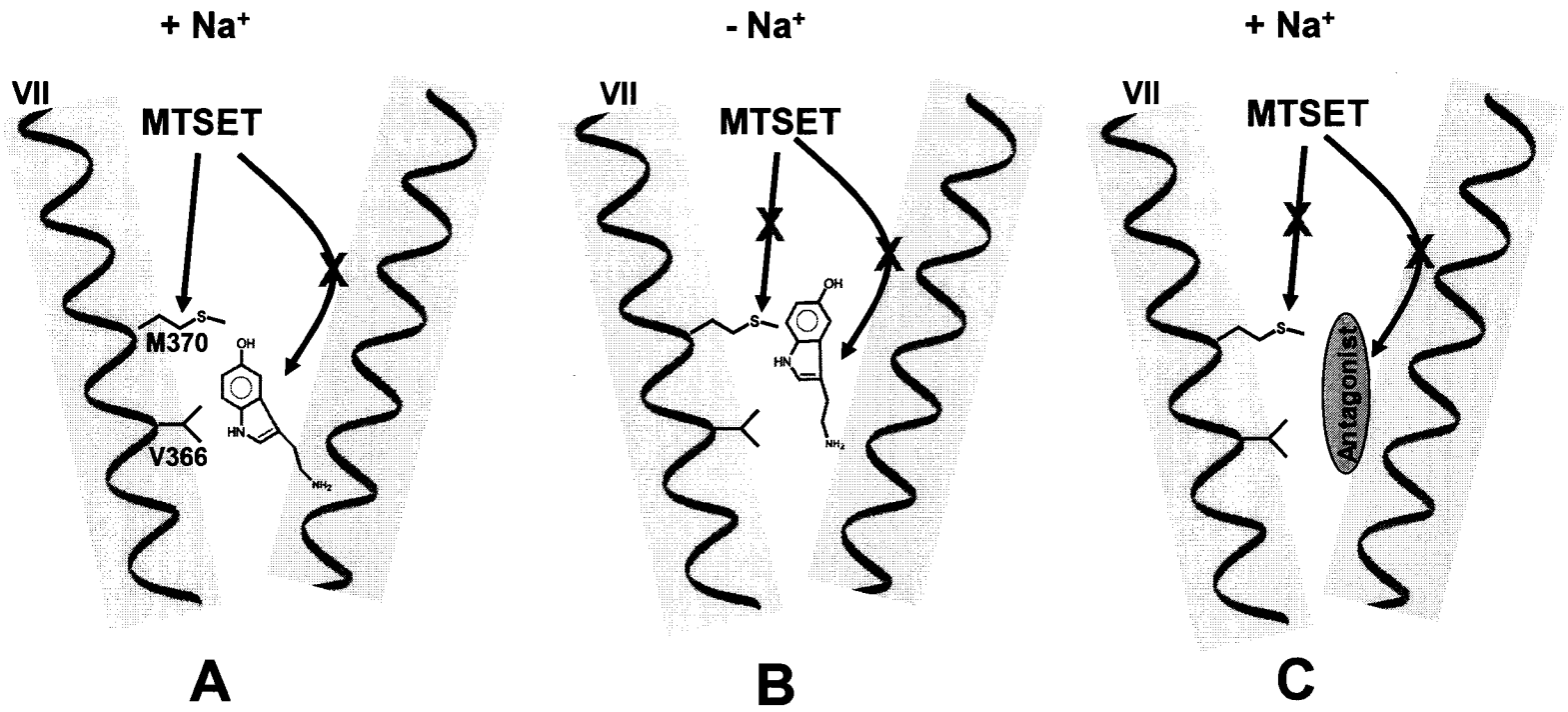

Figure 3.7: Hypothetical model for ion influence of 5-HT or antagonist protection of M370C from MTSET inactivation. (A) In the presence of Na^+, V366 is protected by 5-HT from MTSET reagent whereas still accessible. (B) When Na^+ is replaced by Li^+, both residues are protected by 5-HT. (C) Fluoxetine, cocaine, and MDMA also protected both residues from MTSET interaction. The gray oval represents either antagonist used in these studies.

Chapter IV

The role of TMD XI of SERT in the substrate transport mechanism.

Introduction

In the previous chapter I used mutagenesis and SCAM approaches to study the role of TMD VII in the substrate permeation pathway of SERT. Mutation of residues V366S, M370L, S375A, and T381S in TMD VII reduced transport capacity. SCAM studies in this region identified mutants V366C and M370C as accessible to MTS reagents suggesting exposure to the extracellular environment and a possible role in the permeation pathway. In this chapter, I will extend my studies to explore two residues in TMD XI, F551 and F556 (Fig 4.1) that have specifically been implicated in MPP^+ transport (Kitayama et al., 1993, Ravna and Edvardsen 2001). Mutation in rDAT at the corresponding position of F551 and F556 of hSERT increased MPP^+ affinity (Kitayama et al., 1993). These mutations exerted modest effects on dopamine uptake and had little impact on cocaine analogs affinity. Although the study suggests determinants in TMD XI of rDAT important for MPP^+ transport, the specific role of these residues in DAT function remains unclear. In my studies, mutation of F556S but not F551T reduced the uptake for 5-HT and MPP^+ by hSERT. Cysteine mutants were generated to further explore the possibility that these residues are localized in the pore-forming region in SERT. F556C was accessible to MTSET and upon reaction, reduced transport capacity of the substrate. No effect of MTSET was observed for F551C. The accessibility of MTSET was partially protected by coincubation with unlabeled 5-HT. Fluoxetine, cocaine, and MDMA were unable to protect this residue from MTSET. Replacement of sodium with lithium did not

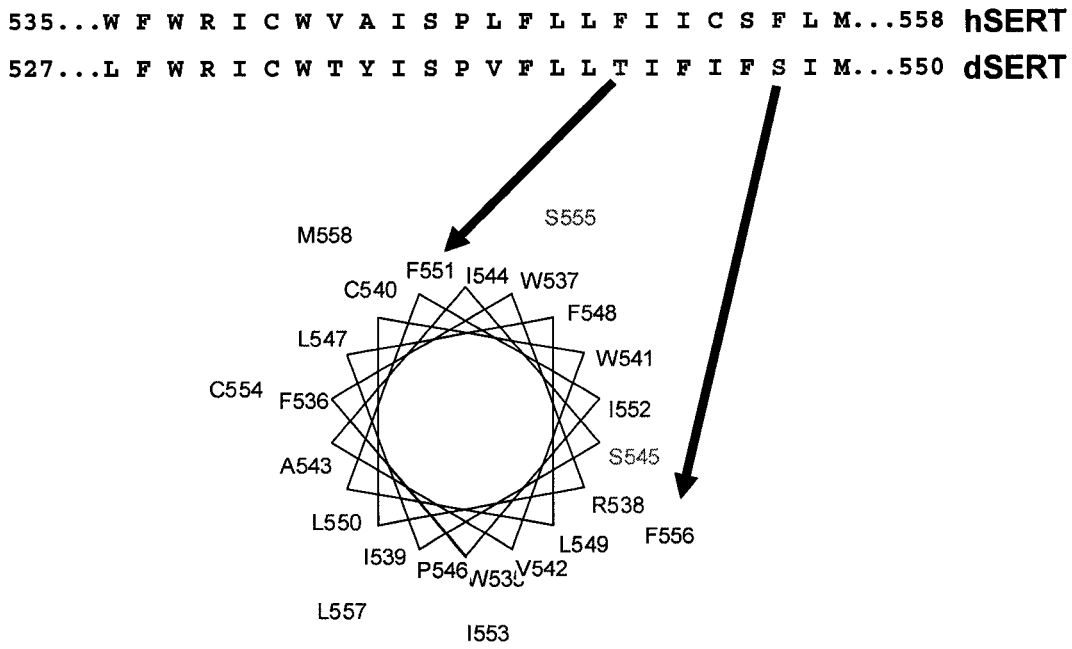

Figure 4.1: Comparison of TMD XI sequences between the human and *Drosophila* SERTs and TMD XI helical wheel of hSERT. F551 and F556 were mutated to the corresponding residues in dSERT. The hSERT sequence for TMD XI was selected to generate a helical wheel using WinPep 3.01 (Lars Hennig, 2002).

affect the ability of 5-HT to partially protect F556C from MTSET interaction. My studies demonstrate that F556 is exposed to the extracellular environment and may be localized in a conformational-sensitive region that is close to the 5-HT binding site. Furthermore, my studies are consistent with TMD XI forming part of the permeation pathway for substrate translocation in SERT.

Materials and Methods

Materials

The cDNA encoding the C109A/ hSERT mutant in pBluescript KSII was a generous gift from Dr. Randy Blakely (Vanderbilt University). [^{3}H]5-hydroxytryptamine ([^{3}H]5-HT; 122 Ci/mmol) and [^{3}H]citalopram (85 Ci/mmol) were purchased from Amersham Biosciences Inc. (Piscataway, NJ). [^{3}H]MPP$^+$ (83.5 Ci/mmol) was obtained from PerkinElmer Life Sciences (Boston, MA). Fluoxetine, MPP$^+$, MDMA, cocaine and pargyline were purchased from Sigma/RBI (Natick, MA). MTSET and MTSES were purchased from Toronto Research Chemicals (Toronto, Canada). Unlabeled 5-HT was obtained from Sigma-Aldrich (St. Louis, MO). All other reagents were purchased from commercial sources.

Cell culture

HEK-293 wild-type and transiently transfected cells were maintained as described in Chapter II. Transient transfection was performed in 24-well poly-D-lysine coated plates using Lipofectamine 2000 as described above (Chapter III).

Site-directed mutagenesis

Residues F551 and F556 in TMD XI of hSERT were mutated to the residue at the equivalent position in dSERT. The mutants F551T and F556S were generated using the QuikChange® site-directed mutagenesis kit (Stratagene, La Jolla, CA). Oligos were designed to introduce the mutation at the corresponding positions (Table 4.1, Integrated DNA Technologies, Coralville, IA).

Table 4.1: Oligos used to generate mutants in TMD XI in hSERT.

Mutant	Oligos	
F551T	5′TCTCCTGACCATCATTTGCAGTTTTCTCATGAGCCC3′	(sense)
	3′GGGCTCATGAGAAAACTGCAAATGATGGTCAGGAGA5′	(antisense)
F556S	5′CATCATTTGCAGTTCTCTCATGAGCCC3′	(sense)
	3′GGGCTCATGAGAGAACTGCAAATGATG5′	(antisense)
F551C	5′CCTGTGCATCATATGCAGTTTTCTGATGAGCC3′	(sense)
	3′GGCTCATCAGAAAACTGCATATGATGCACAGG5′	(antisense)
F556C	5′CCTGTTCATCATATGCAGTTGTCTGATGAGCCC3′	(sense)
	3′GGGCTCATCAGACAACTGCATATGATGAACAGG5′	(antisense)

For the substituted-cysteine accessibility method (SCAM), I generated the F551C and F556C mutants in TMD XI. Cysteine mutants were generated using the C109A/hSERT cDNA as a template to reduce background MTS reactivity as described in Chapter III. C109A/hSERT cDNA in pBluescript was digested with NotI and AgeI enzymes. The resulting fragment was inserted in hSERT/pcDNA 3.1+ and digested with NdeI to confirm the C109A mutation. Site-directed mutagenesis was performed using the QuikChange® mutagenesis kit as described above. Mutations were confirmed by enzyme digestion and DNA sequencing (University of Michigan DNA sequencing core facility).

[^{3}H]Substrate uptake assays

Saturation transport assays were performed as described in Chapter II.

Whole-cell radioligand binding assay

Whole-cell binding experiments were performed in 24-well plates ($1x10^5$ cells per well) precoated with poly-D-lysine as described previously (Chapter II).

MTS experiments

HEK-293 wild-type cells in 24-well tissue culture plates were transiently transfected with the cysteine mutant cDNAs of interest as described above (Chapter III).

Results

Substitution of phenylalanine at position 556 with serine reduced hSERT transport capacity and cell surface expression.

Previous studies in the dopamine transporter suggest a role for two serines (phenylalanines at position 551 and 556 in hSERT) for MPP^+ transport. Sequence comparison between hSERT and dSERT revealed threonine and serine in the *Drosophila* clone at the corresponding positions of hSERT F551 and F556. Because dSERT is unable to transport MPP^+ (Chapter II; Rodriguez et al. 2003), phenylalanines at these positions in TMD XI of hSERT may implicate these residues in the translocation of MPP^+ by SERT. I mutated both positions at hSERT to the equivalent residue at dSERT. 5-HT transport assays showed a decrease in 5-HT transport capacity for the F556S mutant (0.06 ± 0.01 5-HT molecules/10 min) in comparison to wild-type (0.16 ± 0.01 5-HT molecules/10 min), whereas F551T (0.15 ± 0.01 5-HT molecules/10 min) did not show any difference in transport capacity from hSERT (Fig 4.2A). Similar results were obtained when I examined MPP^+ transport (0.006 ± 0.001 MPP^+ molecules/10 min and 0.040 ± 0.002 MPP^+ molecules/10 min for F556S and hSERT, respectively, Fig 4.2B). In both cases, saturating concentrations of substrates were used in the experiments to ensure measurement of full transport capacity. The MPP^+/5-HT ratio was calculated for wild-type, F551T, and F556S to determine if either mutation affected uptake of a particular substrate to a greater extent than another (Fig 4.2C). The MPP^+/5-HT ratio for dSERT is zero because this SERT clone is unable to transport MPP^+. If a particular mutation maintains a ratio similar to hSERT, I may conclude that recognition of a particular substrate is unaltered. Conversely, a reduction in the ratio may suggest that the mutation affects MPP^+ transport preferentially over 5-HT transport. The MPP^+/5-HT ratio for F551T was unchanged compared to hSERT (approximately 0.25 nmoles of MPP^+ per nmole of 5-HT, Fig 4.2). However, the ratio for the F556S mutant

Figure 4.2: Uptake of [^{3}H]5-HT (A), [^{3}H]MPP^+ (B), and MPP^+/5-HT ratios (C) in HEK-293 cells transiently transfected with hSERT or hSERT mutants in TMD XI. Cells were plated and transfected as described in Materials and Methods. Specific uptake was determined using fluoxetine (10 μM) to define nonspecific uptake. MPP^+/5-HT ratios were calculated using the specific uptake (Fig 4.2A and 4.2B). Bars represent the mean of three independent experiments ± SEM, $^*p < 0.05$ using a one-way ANOVA test with a post hoc Dunnett test.

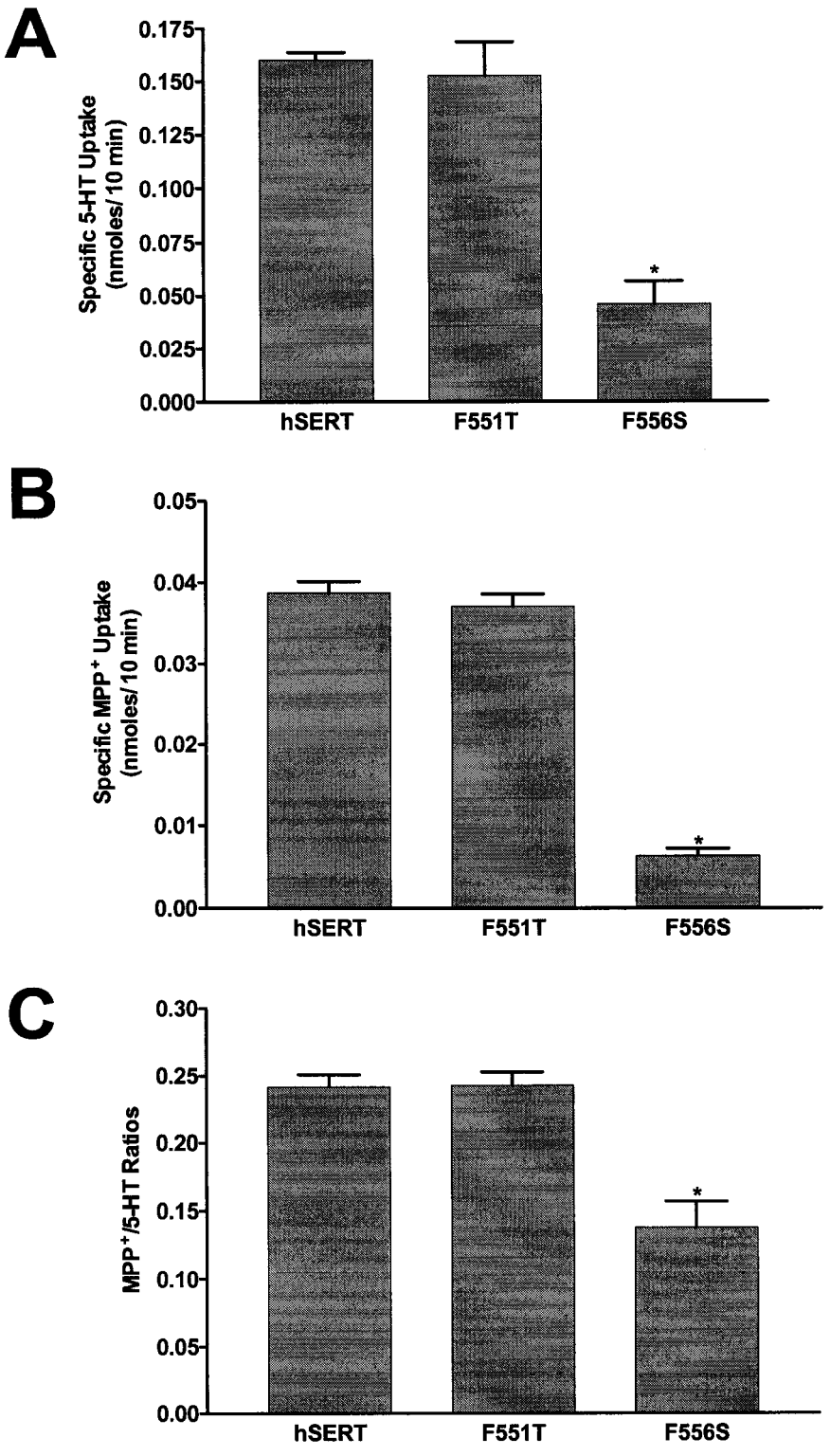
A
Specific 5-HT Uptake (nmoles/10 min)
0.175
0.150
0.125
0.100
0.075
0.050
0.025
0.000
*
hSERT
F551T
F556S
B
Specific MPP+ Uptake (nmoles/10 min)
0.05
0.04
0.03
0.02
0.01
0.00
*
hSERT
F551T
F556S
C
MPP+/5-HT Ratios
0.30
0.25
0.20
0.15
0.10
0.05
0.00
*
hSERT
F551T
F556S

Figure 4.2

showed a 40% decrease in comparison to wild-type (approximately 0.15 nmoles of MPP^+ per nmole of 5-HT).

Whole-cell binding experiments were performed to determine the ability of these mutants to reach the plasma membrane. This approach has been used previously to determine the surface density of wild-type and mutant SERTs (Rodriguez et. al. 2003). For hSERT, cell surface expression was calculated as approximately 1.6×10^6 transporters per cell. Of the two mutants generated in TMD XI, only F556S showed a statistically significant reduction in surface expression (approximately 0.5×10^6 transporters per cell surface) in comparison to wild-type hSERT (Fig 4.3). The decrease in surface expression of F556S may explain in part the reduction of transport capacity of this mutant for 5-HT and MPP^+ uptake.

F556C is accessible to MTSET.

The SCAM is a powerful technique that allows analysis of the pore-lining residues in membrane proteins. This technique has been used to explore the topology of SERT as well as the accessibility of TMDs I, III, and VII to the extracellular environment (Chapter III;Chen et al., 1997b, 1998; Cheng and Rudnick, 2000;Kamdar et al., 2001;Androutsellis-Theotokis and Rudnick, 2002;Henry et al. 2003). The MTS reagents used in these studies are membrane-impermeable and specific for the cysteine sulfhydryl group. To further explore the role of these residues in the function of SERT, I generated cysteine mutants at positions F551 and F556. These mutants were generated using MTS-insensitive C109A/hSERT previously described (Chapter III). The cysteine mutants generated in TMD XI were functional for both 5-HT and MPP^+ uptake (Fig 4.4A and B). The hSERT F551C mutant did not show any difference in uptake of either substrate in comparison with hSERT/C109A. Conversely, the F556C showed a reduction in transport capacity for both substrates. This

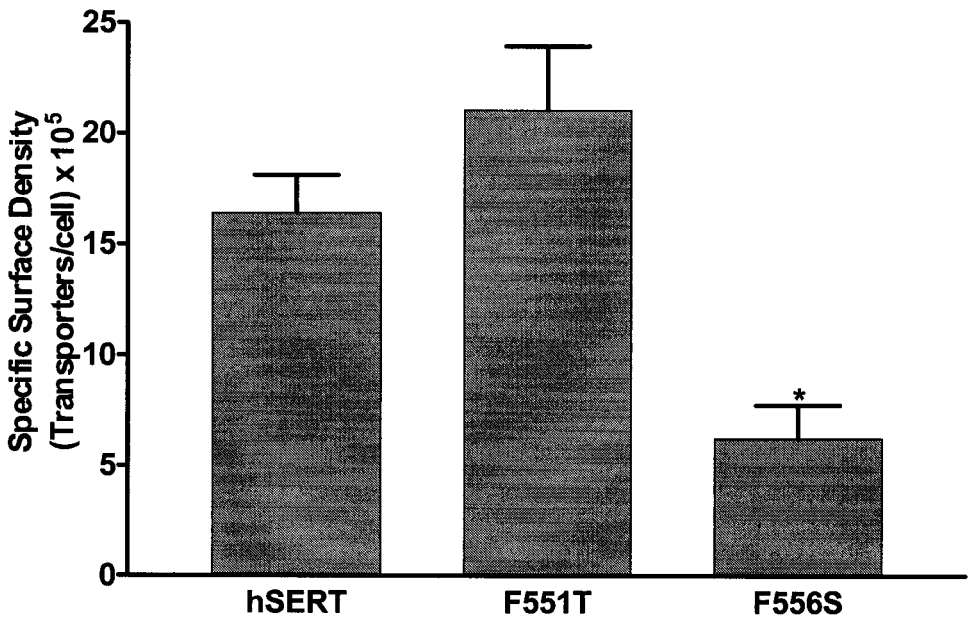

Figure 4.3: Whole-cell radioligand binding in HEK-293 cells transiently transfected with wild-type or hSERT mutants. Assays were performed in 24-well plates coated with poly-D-lysine as described under Materials and Methods. A saturating concentration of [^{3}H]citalopram (20 nM) was used for hSERT and mutants. Nonspecific binding was defined as the binding of radiolabeled ligand in the presence of 10 µM fluoxetine. Internal binding was determined as the binding of ^{3}Hcitalopram in the presence of 200 µM MPP^+. Specific surface binding was calculated as (total binding – binding in the presence fluoxetine) – (binding in the presence of MPP^+ – binding in the presence of fluoxetine). Bars represent the mean of three independent experiments ± SEM. * $p < 0.05$ using a one-way ANOVA with post hoc Dunnett test.

Figure 4.4: Transport activity of cysteine mutants in TMD XI. C109A/hSERT and TMD XI mutants were transiently transfected in HEK-293 cells as described in Material and Methods. Transport activity in the presence of [^{3}H]5-HT (20 nM) for 10 min (A). Transport activity in the presence of [^{3}H]MPP$^+$ (50 nM) for 10 min(B). Bars represent mean ± SEM from three experiments performed in triplicate. *, $p < 0.05$ using a one-way ANOVA with a post hoc Dunnett test.

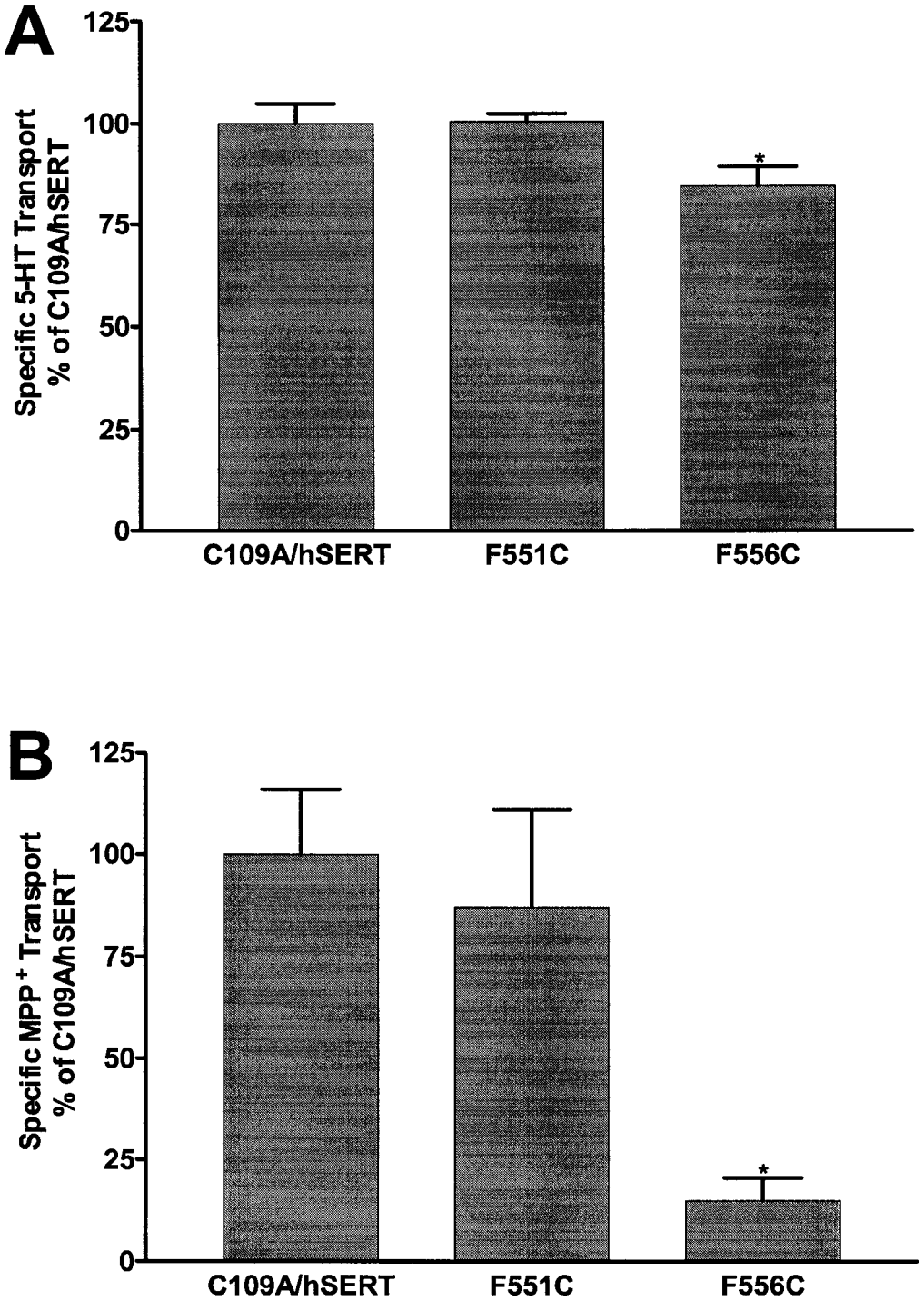
A
Specific 5-HT Transport
% of C109A/hSERT
125
100
75
50
25
0
*
C109A/hSERT
F551C
F556C
B
Specific MPP+ Transport
% of C109A/hSERT
125
100
75
50
25
0
*
C109A/hSERT
F551C
F556C

Figure 4.4

residue appears to be important for the proper substrate translocation mechanism and may form part of the pore used for substrate uptake.

Cysteine mutants were pretreated with MTSET to determine if these residues are exposed to the extracellular environment and possibly part of the substrate permeation pathway. For F556C, ten minute treatment with 1 mM MTSET in PBS/CM buffer effectively inhibited 5-HT transport (approximately 65%, Fig 4.5A). Coincubation with unlabeled 5-HT partially prevented the reactivity of MTSET with the F556C mutant. No effect of MTSET was observed for the C109A/hSERT or the F551C mutant. Uptake assays using MPP^+ as a substrate also showed a decrease in transport capacity for the F556C mutant after MTSET treatment (Fig 4.5B). One difference noted was that the magnitude of the inhibition was statistically greater for MPP^+ in comparison to 5-HT uptake (approximately 45% vs. 60%, respectively, Fig 4.5). Interestingly, C109A/hSERT and the F551C mutant showed an increase in MPP^+ uptake after pretreatment of MTSET (Fig 4.5B). This effect was not observed for 5-HT transport (Fig 4.5 A).

I also performed similar studies in the absence of sodium to determine if this cation may induce a conformational change that alters accessibility of F556C to MTSET. Sodium is essential for substrate uptake in SERT. Replacement of sodium with lithium does not alter 5-HT binding to SERT, but will prevent 5-HT translocation (Humphreys et al., 1994). If the presence of lithium affects the accessibility of F556C to MTSET, it will indicate that sodium induces a conformational change necessary to trigger substrate translocation, and subsequently, expose this residue to the extracellular environment. For my studies, the pretreatment with MTSET was performed in KRH buffer where sodium chloride was replaced with an equimolar amount of lithium chloride to maintain the ionic strength, whereas the substrate uptake was performed in sodium-containing KRH buffer. In the presence of lithium, MTSET reduced 5-HT and MPP^+ uptake in F556C with no effect at the C109A/hSERT or the F551C mutant similar to the effects observed in the presence of Na^+ (Fig 4.6A and B).

Figure 4.5: Effects of MTSET in the inactivation of [^{3}H]5-HT (A) and [^{3}H]MPP$^+$ transport in HEK-293 transiently transfected cells with C109A/hSERT or Cys-mutants. 48-hours after transfection, cells were preincubated with MTSET (1 mM) for 10 minutes at room temperature, followed by [^{3}H]5-HT (20 nM) or [^{3}H]MPP$^+$ (50 nM) uptake as described in Material and Methods. Preincubation with MTSET was performed in the presence of PBS/CM buffer ± 20 μM unlabeled 5-HT. Unlabeled 5-HT was used to determine the ability to protect the mutants from MTS inactivation. Bars represent mean ± SEM from three experiments performed in triplicate. * ($p < 0.05$) represent statistically difference from control cells using a one-way ANOVA with a post hoc Dunnett test. # symbol is statistically different from MTSET treatment.

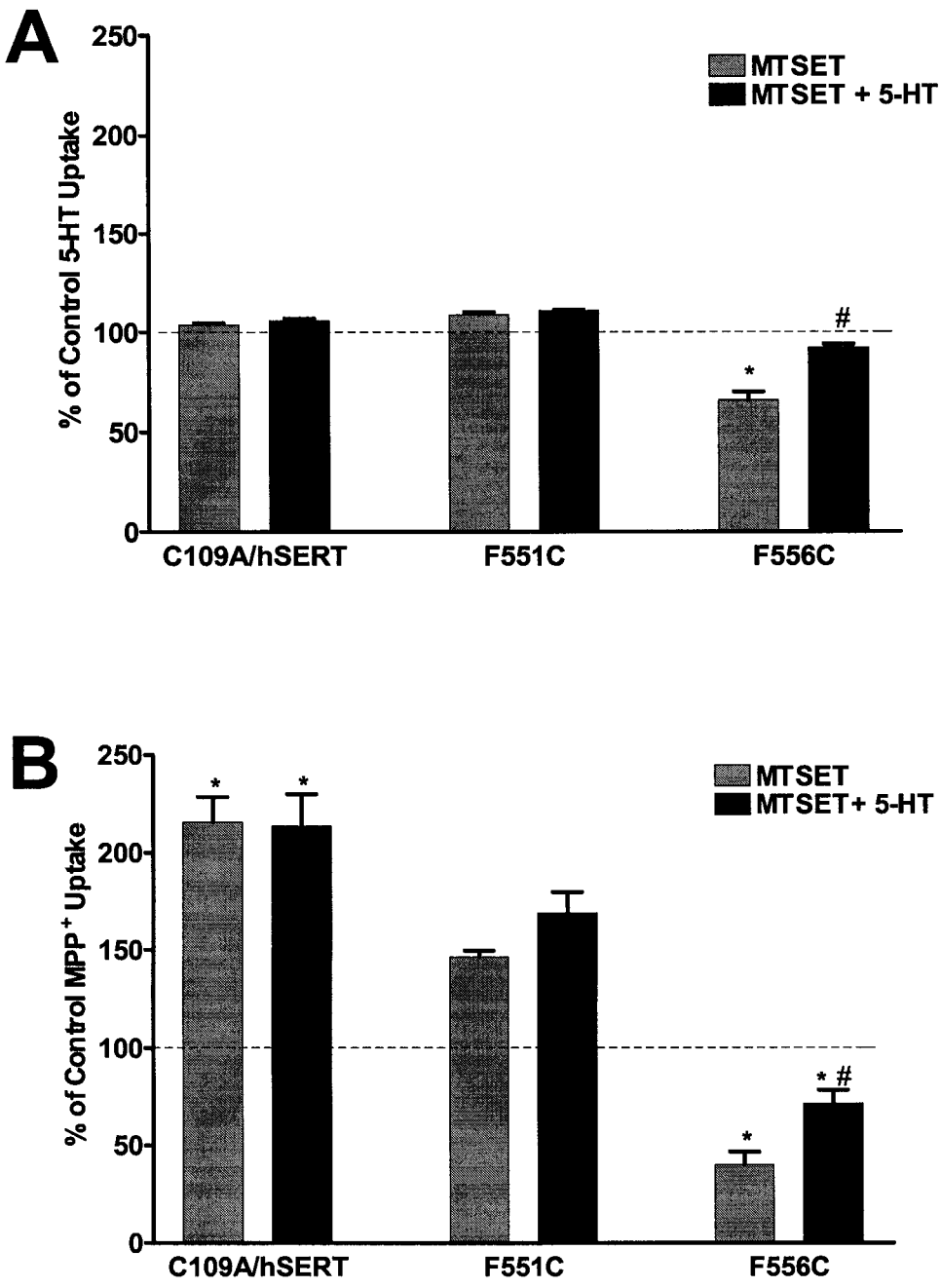
A
250
200
150
100
50
0
% of Control 5-HT Uptake
MTSET
MTSET + 5-HT
*
#
C109A/hSERT
F551C
F556C
B
250
200
150
100
50
0
% of Control MPP+ Uptake
MTSET
MTSET+ 5-HT
*
*
*
*#
C109A/hSERT
F551C
F556C

Figure 4.5

Figure 4.6: Effects of MTSET in the inactivation of [^{3}H]5-HT (A) and [^{3}H]MPP$^+$ (B) transport in HEK-293 transiently transfected cells with C109A/hSERT or Cys-mutants in the absence of Na^+. 48-hours after transfection, cells were preincubated with MTSET (1 mM) for 10 minutes at room temperature, followed by [^{3}H]5-HT (20 nM) or [^{3}H]MPP$^+$ (50 nM) uptake as described in Material and Methods. Preincubation with MTSET was performed in the presence of KRH-Li buffer ± 20 μM unlabeled 5-HT. Sodium chloride was replaced with an equimolar concentration of lithium chloride to maintain the buffer's ionic strength. Unlabeled 5-HT was used to determine the ability to protect the mutants from MTS-inactivation. Bars represent mean ± SEM from three experiments performed in triplicate. * ($p < 0.05$) represent statistically difference from control cells using a one-way ANOVA with a post hoc Dunnett test.

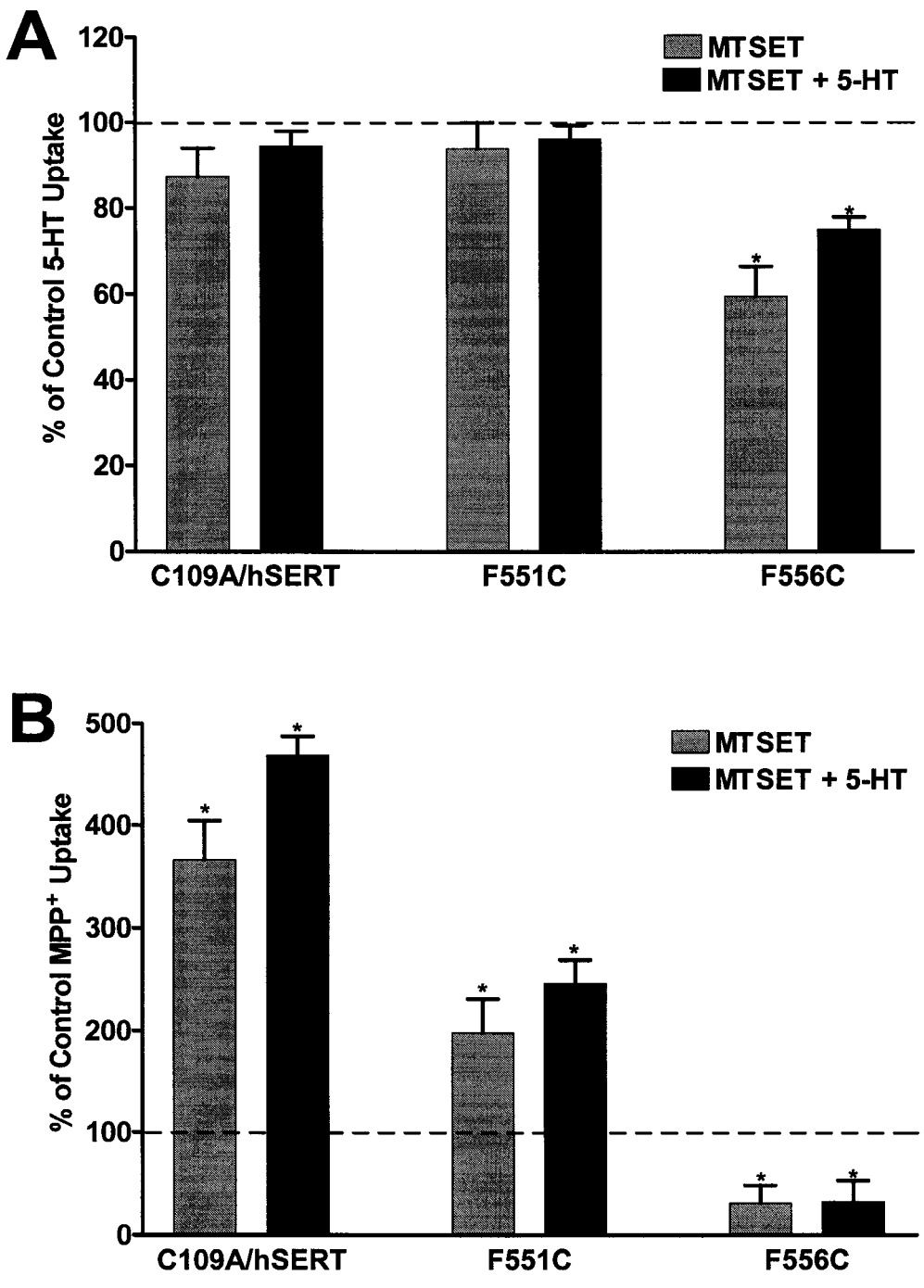
A
120
100
80
60
40
20
0
% of Control 5-HT Uptake
MTSET
MTSET + 5-HT
C109A/hSERT
F551C
F556C
B
500
400
300
200
100
0
% of Control MPP+ Uptake
MTSET
MTSET + 5-HT
C109A/hSERT
F551C
F556C

Figure 4.6

Unlabeled 5-HT was able to partially protect the F556C site when [^{3}H]5-HT uptake was measured (Fig 4.6A). In contrast to the assays performed using sodium in the buffer, unlabeled 5-HT did not protect this residue during [^{3}H]MPP^+ uptake (Fig 4.6B) although the magnitude of MTSET inhibition was similar for both cations (Fig 4.5B and 4.6B). Lithium did not make F551C reactive with MTSET as measured by [^{3}H]5-HT and [^{3}H]MPP^+ transport. Similar to the studies performed in the presence of Na^+, I observed enhanced MPP^+ transport in the C109A/hSERT (366%) and the F551C mutant (198%) when lithium was present (Fig 4.6B), although the magnitude of the effect was greater than that detected in the presence of sodium (215% and 146% for C109A/hSERT and F556C, respectively; Fig 4.5B). Regardless of cation present, MTSET induced an increase in MPP^+ uptake at C109A/hSERT. My results may imply that another endogenous cysteine other than C109A in hSERT is exposed to the extracellular environment and, may react with MTSET. Reaction of this additional endogenous cysteine promotes MPP^+ transport suggesting that this site is near or strongly influences the MPP^+ transport pathway without altering 5-HT transport.

I further explored the ability of fluoxetine, cocaine, and MDMA to protect F556C from MTSET interaction. The F556C mutation increased the K_i value for fluoxetine and MDMA without altering the ability of cocaine to inhibit [^{3}H]5-HT transport drugs in comparison with C109A/hSERT (Table 4.2). Coincubation of inhibiting concentrations of these drugs with MTSET did not protect the F556C site (Fig 4.7). Fluoxetine and cocaine are antagonists that bind to SERT and prevent substrate transport. My results suggest that binding of these drugs does not influence accessibility of F556C to MTSET.

Table 4.2: K_i values for fluoxetine, cocaine, and MDMA in HEK-293 cells transiently transfected with C109A and C109A/F556C mutants.

	K_i		
	Fluoxetine	**Cocaine**	**MDMA**
C109A/hSERT	**21 ± 4**	**3800 ± 380**	**1600 ± 360**
C109A/F556C	**80 ± 3***	**3600 ± 270**	**9500 ± 250***

* ($p < 0.05$) represent statistically difference from C109A/hSERT using a Student's *t* test.

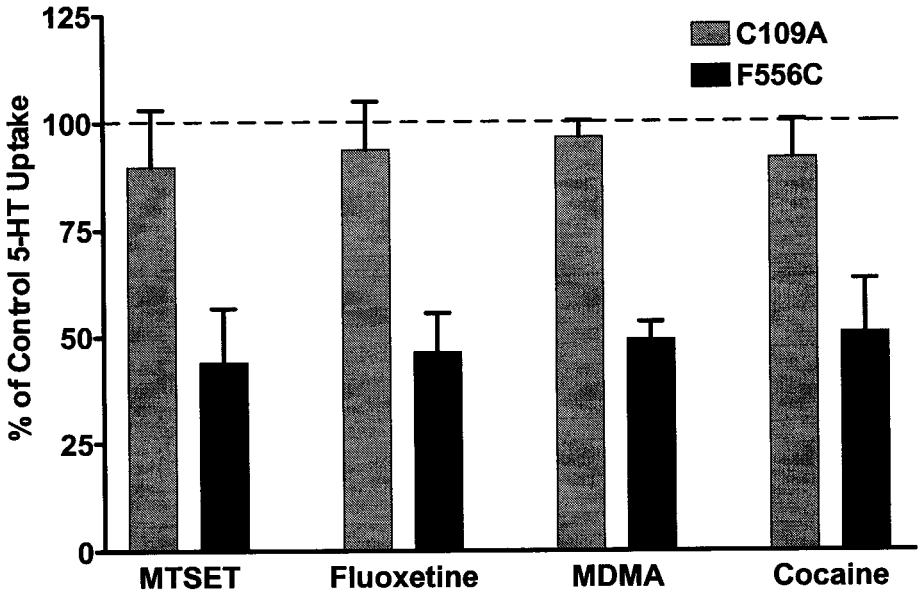

Figure 4.7: MTS accessibility and protection assays using fluoxetine, cocaine, and MDMA in HEK-293 cells transiently transfected with C109A/hSERT or F556C mutant. Inhibiting concentration of fluoxetine (100 nM), cocaine (200 μM), or MDMA (200 μM) were coincubated with MTSET (1 mM) for 10 minutes at room temperature. Nonspecific transport was determined in the presence of fluoxetine (10 μM). After MTSET/antagonist pretreatment, cells were washed three times with KRH buffer to remove the drugs prior to the substrate transport assay. Bars represent mean ± SEM for three independent experiments performed in triplicate.

SERT chimeras implicate a region involved with MTSET-induced increase in MPP^+ transport.

It is well documented that C109, a conserved cysteine in the first extracellular loop of SERT, is exposed to extracellular environment. In a mutagenesis study where all the cysteines in the membrane-spanning region of SERT were systematically mutated and replaced one at the time, none were suggested to be in the pore of SERT as interaction with MTS reagents did not inhibit [^{3}H]5-HT transport (Chen et al., 1997b). Is important to note that these studies relied solely of inhibition of [^{3}H]5-HT uptake to determine reactivity of cysteine mutants. Preincubation of the C109A/hSERT and the F551C mutant with MTSET showed an increase in MPP^+ uptake (Fig 4.5B and 4.6B). Interestingly, this phenomenon was specific for MPP^+ because MTSET did not alter the transport capacity of these mutants for 5-HT. My results suggest that another cysteine in hSERT is accessible to MTSET and may specifically influence MPP^+ transport.

From my previous studies I have shown that dSERT does not transport MPP^+. Preincubation of wild-type dSERT with MTSET did not increase MPP^+ uptake above baseline (data not shown). I also performed activity studies for MPP^+ transport in HEK-293 cells transiently transfected with the $H^{1-281}D^{282-476}H^{477-638}$ (TMD V to IX from dSERT) and $H^{1-118}D^{119-627}$ (TMDs II to XII from dSERT) SERT chimeras (Fig 4.8A). Only the $H^{1-281}D^{282-476}H^{477-638}$ chimera showed an increase in MPP^+ suggesting that an cysteine residue found in the hSERT sequence reacts with MTSET to produce the potentiation of MPP^+ uptake (Fig 4.8 B).

Figure 4.8: Diagram of wild-type hSERT, dSERT, and cross-species chimeras (A) and MTSET effects on MPP^+ transport at the cross-species SERT chimeras (B). Generation of cross-species chimeras has been described previously (Barker et. al. 1998, Rodriguez et. al. 2003). Cross-species chimeras were transiently transfected in HEK-293 cells. MTSET (1 mM) treatment and the MPP^+ (50 nM) transport assay were performed as described in Materials and Methods. Nonspecific transport was determined in the presence of fluoxetine (10 μM). Bars represent mean ± SEM for three experiments performed in triplicate.

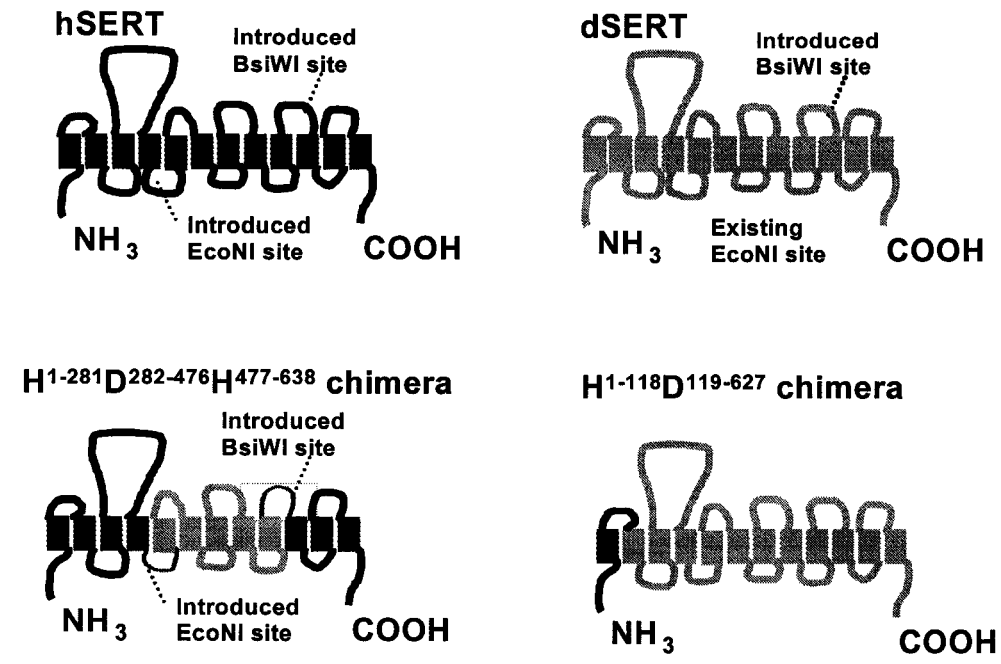
hSERT
Introduced
BsiWI site
NH 3
Introduced
EcoNI site
COOH
dSERT
Introduced
BsiWI site
NH 3
Existing
EcoNI site
COOH
H1-281D282-476H477-638 chimera
Introduced
BsiWI site
NH 3
Introduced
EcoNI site
COOH
H1-118D119-627 chimera
NH 3
COOH

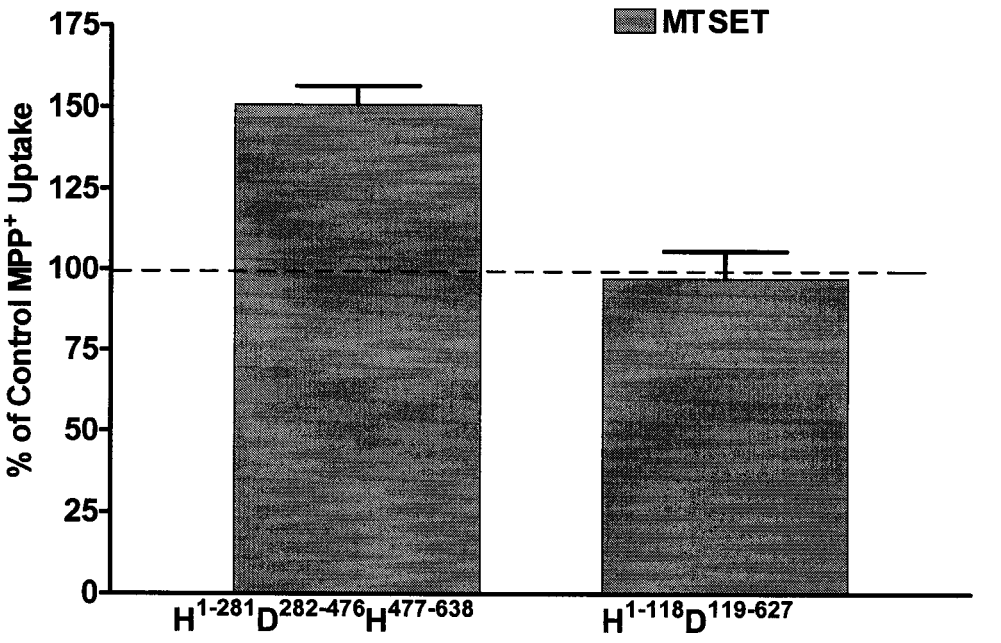
MTSET
% of Control MPP+ Uptake
175
150
125
100
75
50
25
0
H1-281D282-476H477-638
H1-118D119-627

Figure 4.8

Discussion

Studies of DAT have suggested that TMD XI may contain residues critical for MPP^+ translocation (Kitayama et al., 1993). Based upon these reports I anticipated that phenylalanines at position 551 and 556 localized in TMD XI of hSERT could be essential for MPP^+ uptake. These residues are divergent between hSERT and dSERT, and thus, I speculated that they could contribute to the species differences observed for MPP^+ transport (Rodriguez et. al. 2003). Sequence comparison between hSERT and dSERT revealed that dSERT contains Thr and Ser at the corresponding position of hSERT F551 and F556, respectively. I mutated both positions at hSERT to the equivalent residue at dSERT. Of the two mutants in hSERT, only the F556S mutant exhibited a decrease in transport capacity for 5-HT and MPP^+. Whole-cell binding assays confirmed lower surface expression for F556S partially explaining the reduction in transport capacity for this mutant. The mutants generated in dSERT, where phenylalanines were introduced in the corresponding position in hSERT, did not show MPP^+ uptake or affect 5-HT translocation (data not shown). My results suggest that only F556S affects substrate translocation consistent with DAT studies that suggested effects on MPP^+ uptake (Kitayama et al., 1993). Furthermore, this mutation altered MPP^+ uptake to a greater extent than 5-HT.

Recently, Ravna and Edvardsen proposed a SERT model for an MPP^+ permeation pathway (Ravna and Edvardsen, 2001). In this model, Phe 551 and 556 are key components for MPP^+ translocation. If these residues are exposed to the hydrophilic environment present through the permeation pathway, they may interact with MPP^+, for example through π-π interactions. To explore the possibility that these residues are localized in the permeation pathway for substrate translocation, I generated cysteine mutants at position F551 and F556 of hSERT. Only the F556C mutant showed lower transport capacity for both substrates in comparison to C109A/hSERT. These results support my earlier observations with F556S suggesting that this position may be close to the

substrate translocation pathway. Pretreatment with MTSET decreased the transport activity of F556C for 5-HT and MPP^+. Coincubation of 5-HT with MTSET partially protected F556C. These results support the model where F556C is exposed to the hydrophilic environment of the permeation pathway and may suggest that F556C is localized close to the binding site for substrate or in a conformationally sensitive site that upon substrate binding, makes F556C less accessible to MTSET. I also used fluoxetine, cocaine, and MDMA to prevent the accessibility of MTSET to F556C, but none of these drugs were able to protect this residue from reaction with MTS reagent. Although the binding site for fluoxetine and cocaine are unknown, these studies imply that F556 is localized distal to the site of interaction of these antagonists. The SERT substrate MDMA was also unable to protect F556C mutants from MTSET inactivation. Several possibilities could be drawn from these findings. One possibility is that MDMA binds to the 5-HT binding site, but is not bulky enough to prevent accessibility of F556C to MTSET. Another possibility is that MDMA binds to a region in SERT other than the 5-HT binding site and keeps F556C exposed to the hydrophilic environment, but is too distant to protect this site from MTSET interaction. It is also possible that 5-HT and MDMA bind to different sites, thus, demonstrating different properties for protection of F556C from MTSET inactivation. I cannot rule out the possibility that the protection of F556 observed in the presence of 5-HT is a consequence of conformational changes related to the substrate transport rather than substrate recognition. Further studies are necessary to determine the cause for the differences for F556C protection between 5-HT and MDMA.

MTSET did not affect substrate transport in the F551C mutant. My results suggest that this residue is not in the permeation pathway for either substrate. Although my data do not prove that residue is inaccessible, pretreatment with MTSET confirms my previous observation that F551 is not required for the proper function of hSERT. These studies are consistent with F551 and F556 residing on

opposite sides of TMD XI and challenge the model proposed by Ravna and colleagues.

I also performed studies in sodium-free buffer. Sodium is a key component for substrate transport by SERT. Upon sodium binding, changes in SERT conformation may alter accessibility of F556 from the permeation pore. To further explore this possibility, I replaced sodium with lithium, thus, maintaining the buffer's ionic strength. In the presence of lithium, 5-HT is able to bind to SERT but cannot be translocated inside the cell (Humphreys et al., 1994), thus, I can explore whether sodium-induced conformational changes affect the accessibility of F556C to MTSET. Sodium-free buffer was used only during the pretreatment with MTSET. Lithium-containing buffer did not alter MTSET reactivity with the F556C mutant. Similar observations were obtained when sodium was replaced by choline (data not shown). In sodium-containing buffer, 5-HT was able to partially protect F556C from interaction with MTSET. Interestingly, in the presence of lithium, unlabeled 5-HT is unable to protect this site from MTSET inactivation. These results may imply a sodium-induced conformational change that moves F556C closer to the substrate site or cause F556C to be more exposed to the hydrophilic environment. Because sodium and not lithium triggers substrate translocation, the conformational changes associated with sodium binding that appear to affect F556C localization within the pore may also be important for substrate translocation.

It is well documented that C109, a conserved cysteine in the first extracellular loop of SERT, is accessible from the extracellular environment (Chen et al., 1997a). Among the cysteines in the membrane-spanning region of SERT, none have been suggested to be in the pore of SERT as interaction with MTS reagents does not disrupt [^{3}H]5-HT transport (Chen et al., 1997a). For my SCAM studies I used the C109A/hSERT as a template, thus, preventing the inhibition of transport by MTS reagents at the C109 position. Pretreatment of HEK-293 cells transiently expressing C109A/hSERT or F551C with MTSET did not alter [^{3}H]5-HT transport. However, experiments performed on C109A/hSERT

and F551C showed an increase in MPP^+ transport after pretreatment with MTSET. This MTSET-induced increase in MPP^+ transport was also noted in experiments examining MPP^+ uptake by cysteine mutants in TMD VII (data not shown) supporting the observation with TMD XI mutants. MTSET increased [^{3}H]MPP^+ transport in C109A/hSERT without affecting [^{3}H]5-HT translocation. My results may suggest that MTSET interacts with a cysteine in hSERT other than C109 that specifically alters MPP^+ transport.

From my previous studies I have shown that dSERT does not transport MPP^+. I performed activity studies for MPP^+ transport in HEK-293 cells transiently transfected with the $H^{1-281}D^{282-476}H^{477-638}$ (TMD V to IX from dSERT) and $H^{1-118}D^{119-627}$ (TMD II to XII from dSERT) SERT chimeras. Only the $H^{1-281}D^{282-476}H^{477-638}$ chimera exhibited an increase in MPP^+ transport after pretreatment with MTSET suggesting that a residue between TMD III and IV or X and XII may interact with MTSET to produce the potentiation of MPP^+ transport. Moreover, similar experiments in dSERT did not trigger MPP^+ transport. I propose that a cysteine other than C109, and only present in hSERT, may be important for MPP^+ transport. There are two candidate cysteines in hSERT, one in TMD XI at position 554 and another in TMD XII at position 580, that are absent in the equivalent position of dSERT.

In summary, my studies demonstrate that F556 in SERT is important for substrate translocation. F556 is predicted to be close to the extracellular surface. SCAM studies suggest that F556C is exposed to the hydrophilic environment and may be close to the substrate binding site, or conformational changes that occur upon substrate binding make F556C less accessible to MTS interaction. Another possibility is that a steric effect produced by the binding of substrates prevents the interaction of MTSET with F556C. From the model proposed for MPP^+ uptake through SERT, my results support the role of F556 for not only MPP^+, but also for 5-HT transport. SCAM studies also demonstrate that at least a portion of TMD XI is exposed to the extracellular environment and may be part of the pore-forming region for substrate translocation. Previous studies have shown that

TMDs I, III, and VII are also exposed to the extracellular environment suggesting that these three TMDs form part of the pore for substrate translocation. A full cysteine-scanning study of TMD XI is necessary to further delineate the role of TMD XI in SERT function. These studies will provide insight into the structure of SERT and further explore where substrates and antagonists interact with this protein. Because of sequence and topological similarity among the GABA/NET transporter family, the results from these experiments can be extrapolated to understand the structure and function of this gene family.

CHAPTER V

Proposed SERT translocation mechanism model

The study of substrate translocation processes across the membrane is a fundamental area in the biological sciences. Several research groups have focused on understanding the transport mechanism of the sodium- and chloride-dependent transporter protein family (Nelson, 1998;Torres et al., 2003b). The cloning of several members of this transporter family provided the tools necessary to investigate the substrate translocation process at the molecular level although, to date, no high resolution structure of any member of the monoamine transporter family is available. Similarities in the primary structure and topology of these membrane transporters suggest comparative mechanisms for substrate translocation.

Mutagenesis studies from different laboratories have provided preliminary data regarding the role of amino acids in SERT and other monoamine transporters for substrate translocation, protein stability, and antagonist binding domains. For example, residues in TMD I, III, VII, and XI in SERT and other monoamine transporters have been implicated for substrate translocation. Barker and coworkers identified residues D98 and Y95, which are one rotation away from each other on the first putative α-helix in hSERT, as contributing to the recognition of transporter antagonist and substrates (Barker et al. 1998, 1999). Mutagenesis studies in DAT and GAT also implicated the conserved aspartate at the corresponding position of hSERT D98 to be essential for substrate transport (Kitayama et al., 1993; Pantanowitz et al. 1993). Although evidence from GABA and glycine transporters has challenged the topology of TMD I (Bennett and

Kanner, 1997, Olivares et al., 1997), several structural studies of SERT support the twelve putative TMD secondary structure predicted from the SERT sequence (Chen et al., 1998; Androutsellis-Theotokis and Rudnick 2002). Recently, Blakely and coworkers systematically mutated each residue of TMD I to cysteine and confirmed the exposure of D98 and Y95 to the hydrophilic environment using SCAM (Henry et al., 2003). These results support the role of D98 in the permeation pathway where the carboxyl group of this residue is proposed to interact with the positively-charged amine group of 5-HT and other substrates. Recently, Ravna et al. proposed a model suggesting Y95 is involved in the selectivity of the binding of the SERT antagonist citalopram (Ravna et al., 2003a). In DAT and NET, the corresponding position for Y95 is a phenylalanine. Ravna's model suggests that the hydroxyl group of Y95 interacts with the nitril group of S-citalopram. Furthermore, the model also hypothesized that cocaine non-selectively binds to monoamine transporters by π-π interactions with the aromatic ring of Y95. This model remains to be confirmed by functional studies where the phenylalanine in DAT is mutated to the corresponding tyrosine of SERT. SCAM of TMD I also found that mutation of residues L99 and P106 to cysteine are intolerable. These residues face the same region in TMD I and could be a contact region with other TMDs or important for protein stability. Another residue, G94, is inaccessible to MTSET reagents. This glycine is highly conserved among the monoamine transporters and was previously implicated in ion interaction and may be part of the cytoplasmic gate in the GABA transporter (Kanner, 2003). Together, these studies demonstrate that a portion of the TMD I α-helix forms part of the permeation pathway for substrate translocation and antagonist binding.

Other regions of SERT beside TMD I have been implicated in substrate transport. Two research groups independently identified several residues in TMD III that are implicated in recognition and transport of 5-HT as well as transporter-associated ion conductance (Chen et al., 1997b;Lin et al., 1996). I179 influenced substrate translocation, I172 and Y176 appear to be involved

with substrate recognition (Chen et al., 1997b;Chen and Rudnick, 2000), and N177 may lie within or near the permeation pathway for ions (Lin et al., 1996). Studies using random mutagenesis in TMD VII identified a stripe of residues that may be important for substrate recognition and translocation (Penado et al., 1998), but further studies implied that these residues are involved in either TMD-TMD interactions or conformational changes essential for substrate transport rather than a direct contact site during the translocation mechanism (Kamdar et al., 2001). Based on the contribution of serines to the binding of catecholamines to adrenergic receptors (Strader et al. 1989), serine residues in TMD VII and XI have been suggested to influence recognition of substrate at DAT (Kitayama et al. 1992, 1993). Additionally, several studies in DAT support that TMD VII may be part of the pore-forming region in SERT (Norregaard et al., 1998;Norregaard et al., 2000;Norregaard et al., 2003). Recently, Gether and colleagues identified a cysteine mutant (M371C) in the extracellular end of TMD VII in hDAT that is accessible to MTSET inactivation (Norregaard et al., 2003). MTSET inactivation at this position was prevented by dopamine suggesting that this residue is localized in the substrate pathway of DAT.

Studies performed with hSERT and dSERT cross-species chimeras suggest the region containing TMDs V to IX are important for substrate transport and for antagonist recognition (Chapter II;Rodriguez et al. 2003;Roman et al. 2003a,b). To further explore the role of this region, I performed site-directed mutagenesis studies where residues in hSERT were mutated to the corresponding residue in dSERT. My studies identified four mutants in TMD VII that decreased substrate translocation (Chapter III). Cysteine mutants at these and another three positions in TMD VII were generated to determine if this predicted α-helix is part of the permeation pathway. SCAM in TMD VII demonstrated that V366 and M370 residues are exposed to the hydrophilic environment and could be part of the permeation pathway, establishing that a section of TMD VII does indeed form part of the pore for substrate translocation.

TMD XI is another region in SERT and other monoamine transporters implicated in the substrate translocation mechanism. Uhl and coworkers generated mutants in TMD XI and identified two residues, Y533 and S538 (corresponding to positions F551 and F556 in hSERT, respectively), that selectively alter MPP^+ transport in rDAT (Kitayama et al., 1993;Mitsuhata et al., 1998). Additionally, mutation of S545 in the rat SERT to alanine was found to alter the cation dependence of 5-HT uptake, thus, S545 in TMD XI could be a crucial determinant for substrate translocation (Sur et al., 1997). My site-directed mutagenesis and SCAM studies showed that residue F556, but not F551, is inactivated by MTSET and suggested that this residue is, at minimum, near the substrate permeation pathway (Chapter VI). Interestingly, F556 is predicted to be localized on the same face as S545 (Fig 4.1) thus, this face of TMD XI may form part of the pore for substrate translocation.

The limited mutagenesis data available for SERT and other monoamine transporters has been used to propose several arrangements of TMDs for substrate translocation and antagonist binding, but these models remain to be confirmed (Ravna and Edvardsen, 2001;Ravna et al., 2003a,b). Ravna and colleagues proposed a hypothetical model for MPP^+ translocation where TMDs I, IV, VII, and XI form the permeation pathway. This model predicts that F551 and F556 are key determinant in MPP^+ permeation. My data challenge the role of F551 because SCAM studies did not determine that this residue is accessible to the hydrophilic environment. I cannot reject the possibility that steric factors prevented MTSET interaction at this position, although a helical wheel model predicts F551 and F556 to be located on opposite faces of TMD XI. Future studies focused on a complete SCAM analysis of TMD XI are necessary to determine other regions of the TMD exposed to the hydrophilic environment and to confirm the aforementioned model.

The twelve TMD arrangement for SERT and DAT proposed by Ravna and coworkers has also been challenged by structural data from DAT. Endogenous Zn^{2+} binding sites in DAT determined that TMDs III, VII, and VIII are close in

proximity (Norregaard et al., 1998;Norregaard et al., 2000; Fig 5.1). Information from Zn^{2+} binding proteins suggests that the distance from the Zn^{2+} ion to the coordinating residues is 2.0-2.3 Å. The ability of Zn^{2+} to inhibit the translocation process by binding to residues situated spatially around the external ends of TMD VII and VIII of hDAT supports the role of this region in the substrate mechanism. Similar results were obtained using engineered Zn^{2+} sites in the GABA transporters to suggest a conserved structure among the monoamine transporters (MacAulay et al., 2001). The proposed arrangement of the putative TMDs in SERT (Ravna and Edvardsen, 2001) and the recent hypothetical model for hDAT (Ravna et al., 2003b), did not account for the proximity of TMDs III, VII, and VIII casting doubt on part of this hypothetical model.

A new model of SERT for substrate permeation and partial TMD arrangement can be constructed using the available data and my studies. In the model for substrate translocation, TMDs I, III, VII, and XI form the permeation pathway (Fig 5.2). Among the residues implicated in substrate translocation, F556 is the closest to the extracellular side. This could be localized close to the first point of contact between substrate and the transporter. Other residues in the extracellular end of TMDs may contribute to the recognition of substrates. Possible candidates are F105 in TMD I which mutation to cysteine abolished substrate transport (Henry et al., 2003) or Y175 in TMD III which mutation of the corresponding residue in DAT (F155) reduced dopamine affinity (Lin et al., 1999).

5-HT interaction with residues close to F556 may induce conformational changes in the transporter that increase the exposure of D98 in TMD I, thus, making the substrate binding site more accessible (Fig 5.2). Within the binding site, the amine group of 5-HT may interact with the carboxylic group of D98 making an electrostatic interaction. The bound 5-HT could also form hydrophobic interactions with I172 or hydrogen bonding with Y176, which have been proposed to be close to the 5-HT binding site and are separated by one turn in the α-helix (Chen and Rudnick, 2000). V366 in TMD VII may also help

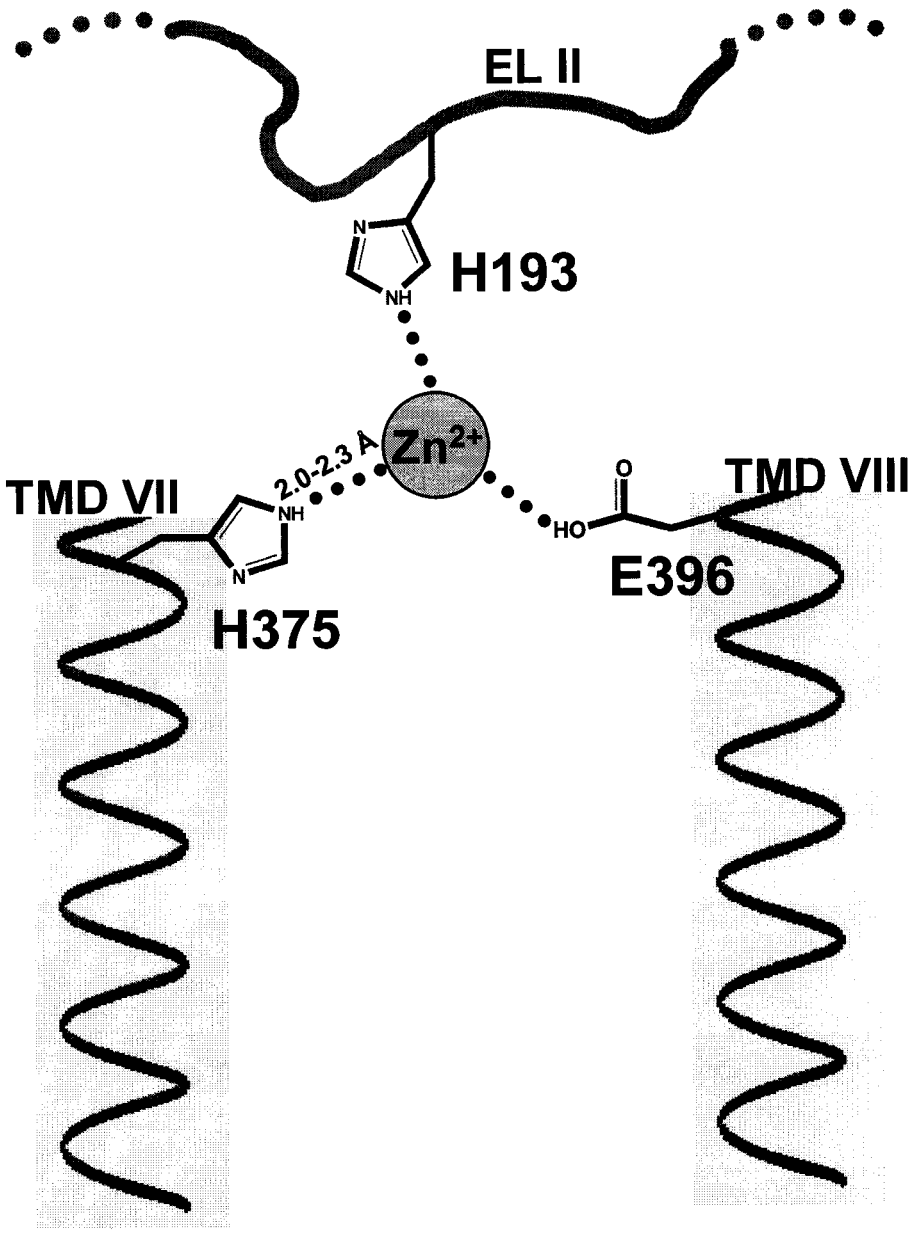

Figure 5.1: Two-dimensional representation of the endogenous Zn^{2+} binding site in hDAT. Residue H193 in the second extracellular loop coordinate Zn^{2+} with residues H375 (TMD VII) and E396 (TMD VIII). The three residues that were identified as coordinates in an endogenous Zn^{2+} binding site are shown in blue (Norregaard et al., 1998;Norregaard et al., 2000).

Figure 5.2: Model of SERT for 5-HT permeation. Mutagenesis and structural data suggest that TMDs I, III, VII, and XI form the permeation pathway for substrate translocation. The proposed model for 5-HT translocation by SERT consists of three steps: (1) 5-HT is recognized by SERT from the external medium; (2) 5-HT binds deep in the externally-accessible binding site where 5-HT may interact with D98, Y176, and I172; (3) the transporter changes to a conformation that faces the cytoplasm and 5-HT is released into the cytoplasm. Na^+ and Cl^- interactions with SERT were not included in this model for simplicity.

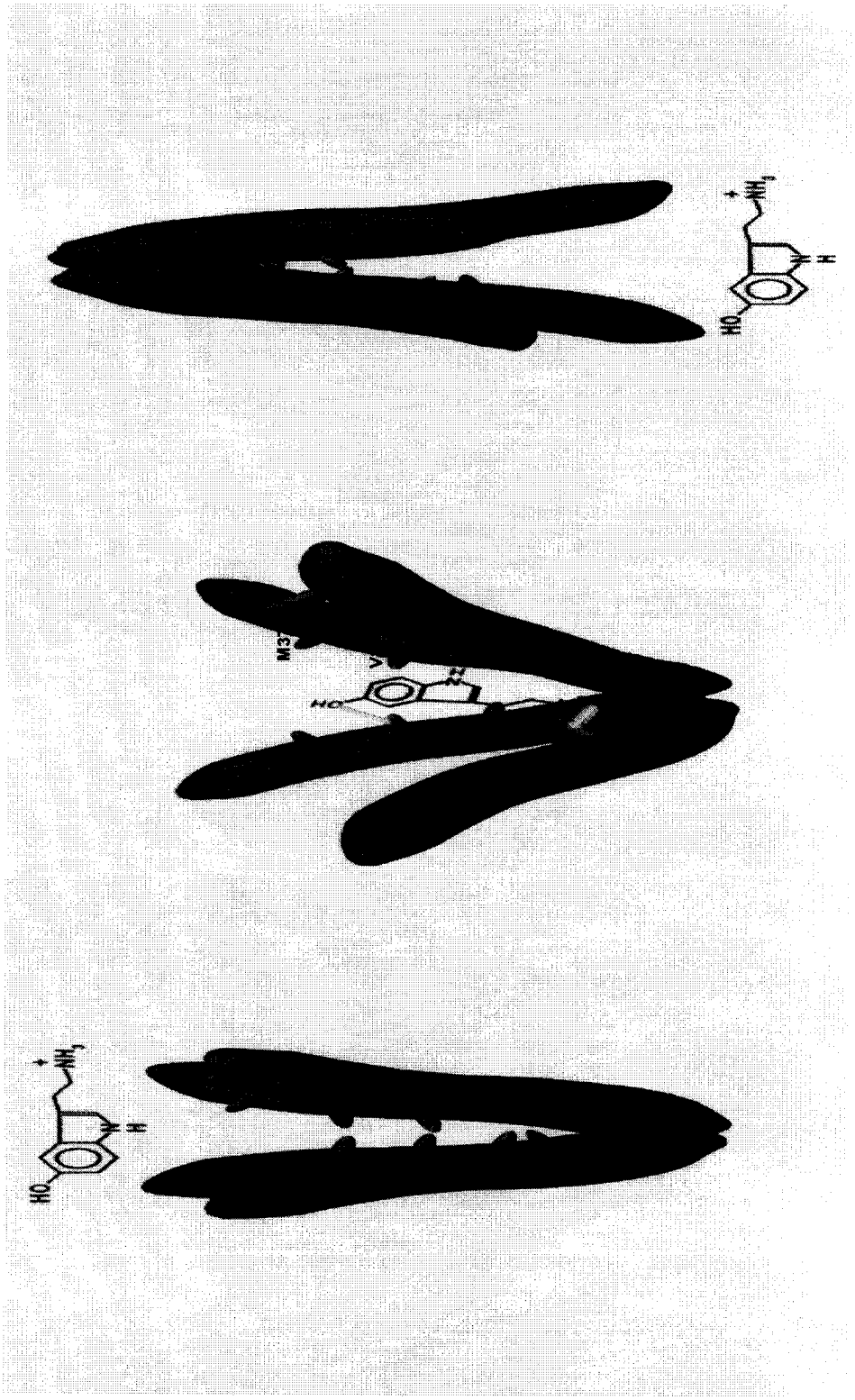

Figure 5.2

stabilize 5-HT interactions in the binding site, although, my mutagenesis data demonstrated that V366 is not essential for 5-HT translocation. M370 is not expected to be part of the binding site for 5-HT because substrates were unable to protect this position from MTSET in the presences of Na^+ (Fig 3.7). Nevertheless, M370 might form part of an external gate that was prevented from closing when the cysteine at that position was modified by MTSET. The SERT I179C mutant in TMD III showed similar properties to M370C and is also proposed to be part of an external gate (Chen and Rudnick, 2000). Furthermore, a glycine at position 63 in TMD I of GABA transporter (corresponding to G94 in hSERT) was implicated in controlling sodium-coupled GABA flux, cation leak current, and a cysteine mutant at this position is accessible to MTSET (Kanner, 2003). Cysteine mutation of G94 in hSERT was inaccessible to MTSET inactivation suggesting either differences in the transport mechanism between hSERT and hGAT or steric factors protecting this site in hSERT (Henry et al., 2003).

The stoichiometry proposed for the substrate cycle is that one Na^+ and one Cl^- are required to trigger substrate translocation (Gu et al.,1996). Presumably, Na^+ is already bound to SERT before 5-HT interacts with the transporter. 5-HT interaction with the substrate binding site may trigger conformational changes that allow Cl^- interaction and substrate translocation. Cl^- binding to the transporter increases the V_{max} value and decreases K_m value for 5-HT (Nelson and Rudnick, 1982), suggesting that Cl^- makes substrate transport more efficient (faster) and induces conformational changes that increase the affinity of 5-HT to the binding site. This could be a key step in the transport mechanism because these conformational changes would reduce the probability of 5-HT dissociation from the transporter before the cycle is completed. The full transporter then opens to the cytoplasm, releases the cargo, and binds one K^+ to return to a conformation that would allow another cycle similar to the model for the alternating-access mechanism (Fig 1.5). The translocation model proposed will need to be revised to accommodate the possible role of oligomerization in the

function of SERT. To date, it is known that oligomerization is important for trafficking of transporters to the cell membrane (Torres et al., 2003a;Sorkina et al., 2003), but there is no evidence for the functional impact of this quaternary structure.

A model for the arrangement of putative transmembrane α-helices is more challenging because not all TMDs have been studied to determine their role in SERT structure. Moreover, no empirical data is available for TMD-TMD or membrane-TMD interactions. Furthermore, the lengths of extracellular and intracellular loops need to be considered in order to accommodate the TMDs in the model. In an attempt to generated a hypothetical TMD arrangement for SERT, I considered the mutagenesis and structural data available (Fig 5.3). From the substrate translocation model (Fig 5.2), TMDs I, III, VII, and XI form part of the pore for substrate permeation. The short sequence between TMD I and II suggests that these TMDs are in close proximity. Incorporation of photoaffinity ligands and subsequent proteolysis and epitope-specific immunoprecipitation confirmed this assumption and indicated that the binding site for cocaine analogs in DAT is formed by the close association of TMDs I and II (Vaughan et al., 2001). Moreover, the accessibility of MTS reagents to C109 in the extracellular loop between TMD I and II suggest that at least a portion of this loop is close to the pore. Other studies identified a leucine zipper localized in TMD II that was suggested to be a contact site in the formation of oligomers, thus, this TMD is localized in the exterior of the protein (Norgaard-Nielsen et al., 2002;Torres et al., 2003a). TMDs IV and VI are also implicated in the formation of oligomers (Hastrup et al., 2003). On the other hand, TMD V is hypothesized to be close to the pore between TMDs XI and VII. Previously, mutations in TMD V were suggested to be important for conformational changes required for substrate translocation (Lin et al., 2000). Future SCAM studies are necessary to determine if TMD V actually forms part of the pore. Furthermore, the short length (only eight residues) of the intracellular loop between TMD IV and V suggests a close proximity between these two α-helices. On the other hand, endogenous

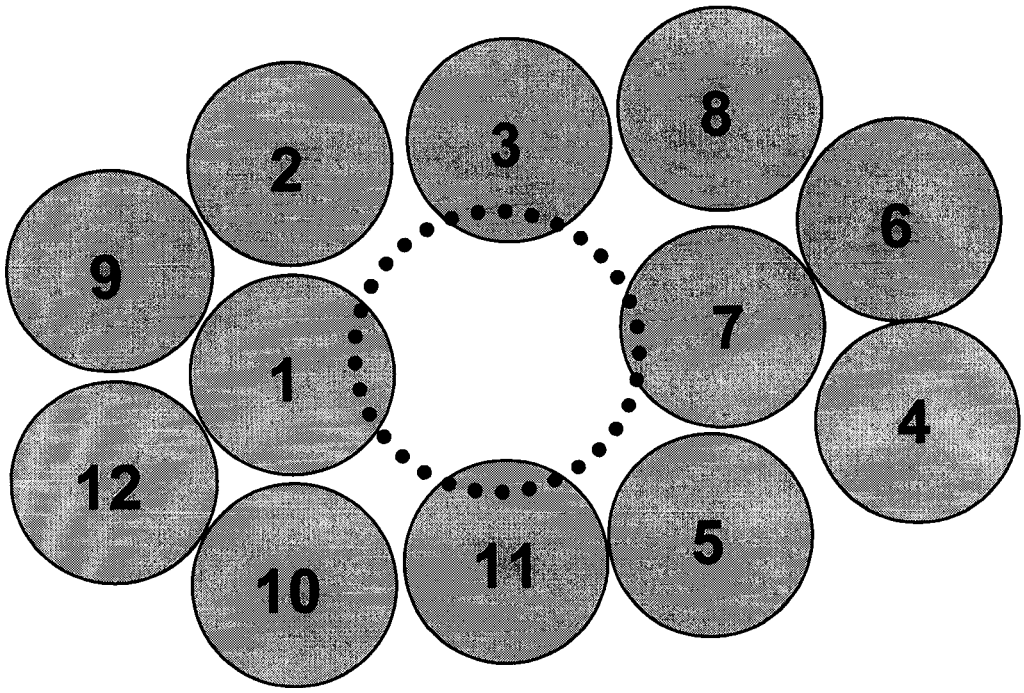

Figure 5.3: Hypothetical arrangement of putative transmembrane α-helices in hSERT. SCAM and structural studies implicated TMDs I, III, VII, and XI to form the substrate permeation pathway (dotted circle). Localization of other TMDs is supported by mutagenesis data from SERT and DAT. The length of extracellular and intracellular loops was also considered to hypothesize the arrangement of hSERT TMDs. The figure represents a cross-side view from the top.

and engineered Zn^{2+} binding sites in hDAT localized TMDs VII and VIII in proximity to TMD III. Although the model localized TMD III distal to TMD IV, the large extracellular loop between these TMDs would accommodate a greater separation. Moreover, mutagenesis studies on TMDs IX and XII implicated these regions in protein stability rather than providing direct contact sites for substrates (Golovanesky and Kanner, 1999; Hahn et al., 2003). A mutation in TMD IX (A457P) disrupted surface expression (Hahn et al., 2003). Furthermore, this mutant has a dominant negative effect when it is coexpressed with wild-type hNET suggesting that TMD IX has determinants that prevents oligomerization. Similarly, mutagenesis studies in TMD X identified two residues, Y495 and F513 important for citalopram binding and possibly protein structure stabilization (Mortensen et al. 2001). Finally, Barker and coworkers implicated F586 to be important for tricyclic antidepressants interaction (Barker and Blakely, 1994). Future SCAM studies are necessary to determine if this residue or part of TMD XII is exposed to the extracellular environment but the F586 data and the short extracellular loop between TMD XI and XII would suggest a location close to TMD XI.

Although the models proposed above are highly speculative, they are supported by the available mutagenesis and structural data. Future structural studies will provide insights that could refine or reject these models. For example, cross-linking and engineered Zn^{2+} binding site studies between the proposed TMDs involved in the permeation pathway could confirm the proposed model. Furthermore, the spatial limitation of Zn^{2+} binding sites and the use of variable length cross-linkers may provide insight into the size of the pore cavity. Identification of other TMDs or residues directly involved in the permeation pathway could also help in the development of novel antidepressant drugs. More structural data is also necessary to identify the binding sites for sodium and chloride. Although the stoichiometry of sodium and chloride for substrate translocation was determined in the late eighties prior to the cloning of SERT, where these ions interact in the transporter remains unclear. These data will

help to define a better model for substrate translocation of the Na^+- and Cl^--dependent transporters at the molecular level.

LIST OF REFERENCES

LIST OF REFERENCES

Abramson J, Smirnova I, Kasho V, Verner G, Kaback HR, and Iwata S (2003) Structure and mechanism of the lactose permease of *Escherichia coli*. *Science* **301**:610-615.

Adams SV and Defelice LJ (2002) Flux coupling in the human serotonin transporter. *Biophys.J.* **86**:3268-3282.

Adkins EM, Barker EL, and Blakely RD (2001) Interactions of tryptamine derivatives with serotonin transporter species variants implicate transmembrane domain I in substrate recognition. *Mol.Pharmacol* **59**:514-523.

Allikmets R, Singh N, Sun H, Shroyer NF, Hutnchinson A, Chidabaram A, Gerrard B, Baird L, Stauffer D, Peiffer A, Rattner A, Smallwood P, Li Y, Anderson KL, Lewis RA, Nathans J, Lepper M, Dean M, and Lupski JR (1997a) A photoreceptor cell-specific ATP-binding transporter gene (ABCR) is mutated in recessive Stargardt macular dystrophy. *Nat.Genet.* **17**:236-246.

Allikmets R, Shroyer NF, Singh N, Seddon JM, Lewis RA, Bernstein PS, Peiffer A, Zabriskie NA, Li Y, Hutchinson A, Dean M, Lupski JR, and Leppert M (1997b) Mutation of the Stargardt disease gene (ABCR) in age-related macular degeneration. *Science* **277**:1805-1807.

Alvarez J, Lee DC, Baldwin SA, and Chapman D (1987) Fourier transform infrared spectroscopic study of the structure and conformational changes of the human erythrocyte glucose transporter. *J.Biol.Chem.* **262**:3502-3509.

Ames GF, Mimura CS, Holbrook SR, and Shyamala V (1992) Traffic ATPases: a superfamily of transport proteins operating from *Escherichia coli* to humans. *Adv.Enzymol.Relat Areas Mol.Biol.* **65**:1-47.

Androutsellis-Theotokis A and Rudnick G (2002) Accessibility and conformational coupling in serotonin transporter predicted internal domains. *J.Neurosci.* **22**:8370-8378.

Arriza JL, Kavanaugh MP, Fairman WA, Wu YN, Murdoch GH, North RA, and Amara SG (1993) Cloning and expression of a human neutral amino acid transporter with structural similarity to the glutamate transporter gene family. *J.Biol.Chem.* **268**:15329-15332.

Arriza JL, Eliasof S, Kavanaugh MP, and Amara SG (1997) Excitatory amino acid transporter 5, a retinal glutamate transporter coupled to a chloride conductance. *Proc.Natl.Acad.Sci. USA* **94**:4155-4160.

Barker EL, Kimmel HL, and Blakely RD (1994) Chimeric human and rat serotonin transporters reveal domains involved in recognition of transporter ligands. *Mol.Pharmacol.* **46**:799-807.

Barker EL and Blakely RD (1995) Norepinephrine and serotonin transporters: molecular targets for antidepressant drugs,in Psychopharmacology: The Fourth Generation of Progress (Bloom F and Kupfer D eds) pp 321-333,Raven Press,New York., pp 321-333.

Barker EL and Blakely RD (1998) Structural determinants of neurotransmitter transport using cross-species chimeras: studies on serotonin transporter. *Methods Enzymol.* **296**:475-498.

Barker EL, Perlman MA, Adkins EM, Houlihan WJ, Pristupa ZB, Niznik HB, and Blakely RD (1998) High affinity recognition of serotonin transporter antagonists defined by species-scanning mutagenesis. An aromatic residue in transmembrane domain I dictates species-selective recognition of citalopram and mazindol. *J.Biol.Chem.* **273**:19459-19468.

Barker EL, Moore KR, Rakhshan F, and Blakely RD (1999) Transmembrane domain I contributes to the permeation pathway for serotonin and ions in the serotonin transporter. *J.Neurosci.* **19**:4705-4717.

Bendahan A, Armon A, Madani N, Kavanaugh MP, and Kanner BI (2000) Arginine 447 plays a pivotal role in substrate interactions in a neuronal glutamate transporter. *J.Biol.Chem.* **275**:37436-37442.

Bennett ER and Kanner BI (1997) The membrane topology of GAT-1, a (Na^+ + Cl^-)-coupled gamma-aminobutyric acid transporter from rat brain. *J.Biol.Chem.* **272**:1203-1210.

Biswas EE and Biswas SB (2000) The C-terminal nucleotide binding domain of the human retinal ABCR protein is an adenosine triphosphatase. *Biochemistry* **39**:15879-15886.

Blakely RD, Berson HE, Fremeau RT, Caron MG, Peek MM, Prince HK, and Bradley CC (1991) Cloning and expression of a functional serotonin transporter from rat brain. *Nature* **354**:66-70.

Brown GK (2000) Glucose transporters: structure, function and consequences of deficiency 4. *J.Inherit.Metab.Dis.* **23**:237-246.

Bruss M, Hammermann R, Brimijoin S, and Bonisch H (1995) Antipeptide antibodies confirm the topology of the human norepinephrine transporter. *J.Biol.Chem.* **270**:9197-9201.

Buck KJ and Amara SG (1994) Chimeric dopamine-norepinephrine transporters delineate structural domains influencing selectivity for catecholamines and 1-methyl-4-phenylpyridinium. *Proc.Natl.Acad.Sci. USA* **91**:12584-12588.

Buck KJ and Amara SG (1995) Structural domains of catecholamine transporter chimeras involved in selective inhibition by antidepressants and psychomotor stimulants. *Mol.Pharmacol.* **48**:1030-1037.

Burant CF, Takeda J, Brot-Laroche E, Bell GI, and Davidson NO (1992) Fructose transporter in human spermatozoa and small intestine is GLUT5. *J.Biol.Chem.* **267**:14523-14526.

Cao Y, Mager S, and Lester HA (1997) H^+ permeation and pH regulation at a mammalian serotonin transporter. *J.Neurosci.* **17**:2257-2266.

Chang G and Roth CB (2001) Structure of MsbA from E. coli: a homolog of the multidrug resistance ATP binding cassette (ABC) transporters. *Science* **293**:1793-1800.

Chapliin L, Cohen AH, Huettl P, Kennedy M, Njus D, and Temperley SJ (1985) Reserpine acid as an inhibitor of norepinephrine transport into chromaffin vesicle ghosts. *J.Biol.Chem.* **260**:10981-10985.

Chen JG, Liu-Chen S, and Rudnick G (1997a) External cysteine residues in the serotonin transporter. *Biochemistry* **36**:1479-1486.

Chen JG, Sachpatzidis A, and Rudnick G (1997b) The third transmembrane domain of the serotonin transporter contains residues associated with substrate and cocaine binding. *J.Biol.Chem.* **272**:28321-28327.

Chen JG, Liu-Chen S, and Rudnick G (1998) Determination of external loop topology in the serotonin transporter by site-directed chemical labeling. *J.Biol.Chem.* **273**:12675-12681.

Chen JG and Rudnick G (2000) Permeation and gating residues in serotonin transporter. *Proc.Natl.Acad.Sci. USA* **97**:1044-1049.

Chen, N and Justice, JB (2000) Differential effect of structural modification of human dopamine transporter on the inward and outward transport of dopamine. *Brain Res.Mol.Brain Res.* **75**, 208-215.

Chin JJ, Jung EK, Chen V, and Jung CY (1987) Structural basis of human erythrocyte glucose transporter function in proteoliposome vesicles: circular dichroism measurements. *Proc.Natl.Acad.Sci. USA* **84**:4113-4116.

Clark JA (1997) Analysis of the transmembrane topology and membrane assembly of the GAT-1 gamma-aminobutyric acid transporter. *J.Biol.Chem.* **272**:14695-14704.

Conradt M and Stoffel W (195) Functional analysis of the high affinity, Na(+)-dependent glutamate transport GLAST-1 by site-directed mutagenesis. *J.Biol.Chem.* **270**:25207-25212

Cooper GM (2000) *The Cell: A molecular approach*. Washington, DC.

Corey JL, Quick MW, Davidson N, Lester HA, and Guastella J (1994) A cocaine-sensitive *Drosophila* serotonin transporter: cloning, expression, and electrophysiological characterization. *Proc.Natl.Acad.Sci. USA* **91**:1188-1192.

Cushman SW and Wardzala LJ (1980) Potential mechanism of insulin action on glucose transport in the isolated rat adipose cell. Apparent translocation of intracellular transport systems to the plasma membrane. *J.Biol.Chem.* **255**:4758-4762.

Danbolt NC, Pines G, and Kanner BI (1990) Purification and reconstitution of the sodium- and potassium-coupled glutamate transport glycoprotein from rat brain. *Biochemistry* **29**:6734-6740.

Danbolt NC (2001) Glutamate uptake. *Prog.Neurobiol.* **78**:560-568

Danbolt NC, Storm-Mathisen J, and Kanner BI (1992) An [Na^+ + K^+]coupled L-glutamate transporter purified from rat brain is located in glial cell processes. *Neuroscience* **51**:295-310.

Dunlop J, Lou Z, Zhang Y, and McIlvain HB (1999) Inducible expression and pharmacology of the human excitatory amino acid transporter 2 subtype of L-glutamate tranporter. *Br.J.Pharmacol.* **128**:1485-1490.

Demchyshyn LL, Pristupa ZB, Sugamori KS, Barker EL, Blakely RD, Wolfgang WJ, Forte MA, and Niznik, HB (1994) Cloning, expression, and localization of a chloride-facilitated, cocaine-sensitive serotonin transporter from *Drosophila* melanogaster. *Proc.Natl.Acad.Sci. USA* **91**, 5158-5162.

Eiden LE (2000) The vesicular neurotransmitter transporters: current perspective and future prospects. *FASEB J.* **14**:2396-2400.

Eliasof S, Arriza JL, Leighton BH, Kavanaugh MP, and Amara SG (1998) Excitatory amino acid transporters of the salamander retina: identification, localization, and function. J.*Neurosci.* **18**:698-712.

Elmendorf JS (2002) Signals that regulate GLUT4 translocation1. *J.Membr.Biol.* **190**:167-174.

Eskandari S, Kreman M, Kavanaugh MP, Wright EM, and Zampighi GA (2000) Pentameric assembly of a neuronal glutamate transporter. *Proc.Natl.Acad.Sci. USA* **97**:8641-8646.

Fairman WA, Vandenberg RJ, Arriza JL, Kavanaugh MP, and Amara SG (1995) An excitatory amino-acid transporter with properties of a ligand-gated chloride channel. *Nature* **375**:599-603.

Furtado LM, Somwar R, Sweeney G, Niu W, and Klip A (2002) Activation of the glucose transporter GLUT4 by insulin1. *Biochem.Cell Biol.* **80**:569-578.

Galli A, DeFelice LJ, Duke BJ, Moore KR, and Blakely RD (1995) Sodium-dependent norepinephrine-induced currents in norepinephrine-transporter-transfected HEK-293 cells blocked by cocaine and antidepressants. *J.Exp.Biol.* **198**:2197-2212.

Galli A, Petersen CI, deBlaquiere M, Blakely RD, and DeFelice LJ (1997) *Drosophila* serotonin transporters have voltage-dependent uptake coupled to a serotonin-gated ion channel. *J.Neurosci.* **17**, 3401-3411.

Golovanevsky V and Kanner BI (1999) The reactivity of the gamma-aminobutyric acid transporter GAT-1 toward sulfhydryl reagents is conformationally sensitive. Identification of a major target residue. *J.Biol.Chem.* **274**:23020-23026.

Gould GW and Bell GI (1990) Facilitative glucose transporters: an expanding family. *Trends Biochem.Sci.* **15**:18-23.

Grunewald M, Bendahan A, and Kanner BI (1998) Biotinylation of single cysteine mutants of the glutamate transporter GLT-1 from rat brain reveals its unusual topology. *Neuron* **21**:623-632.

Grunewald M and Kanner BI (2000) The accessibility of a novel reentrant loop of the glutamate transporter GLT-1 is restricted by its substrate. *J.Biol.Chem.* **275**:9684-9689.

Guastella J, Nelson N, Nelson H, Czyzyk L, Keynan S, Miedel MC, Davidson N, Lester HA, and Kanner BI (1990) Cloning and expression of a rat brain GABA transporter. *Science* **249**:1303-1306.

Gu H, Wall SC, and Rudnick G (1994) Stable expression of biogenic amine transporters reveals differences in inhibitor sensitivity, kinetics, and ion dependence. *J.Biol.Chem.* **269**:7124-7130.

Gu HH, Wall S, Rudnick G (1996) ion coupling stoichiometry for the norepinephrine transporter in membrane vesicle from stably transfected cells. *J.Biol.Chem.* **271**:6911-6916.

Hahn MK, Robertson D, Blakely RD (2003) A mutation in the human norepinephrine transporter gene (SLC6A2) associated with orthostatic intolerance disrupts surface expression of mutant and wild-type transporters. *J.Neurosci.* **23**:4470-4478.

Hastrup H, Sen N, and Javitch JA (2003) The human dopamine transporter forms a tetramer in the plasma membrane: cross-linking of a cysteine in the fourth transmembrane segment is sensitive to cocaine analogs. *J.Biol.Chem.* **278**:45045-45048.

Hebert DN and Carruthers A (1992) Glucose transporter oligomeric structure determines transporter function. Reversible redox-dependent interconversions of tetrameric and dimeric GLUT1. *J.Biol.Chem.* **267**:23829-23838.

Henry LK, Adkins EM, Han Q, and Blakely RD (2003) Serotonin- and cocaine-sensitive inactivation of human serotonin transporters by methanethiosulfonates targeted to transmembrane domain I. *J.Biol.Chem.* **278**:37052-37063.

Hersch SM, Yi H, Heilman CJ, Edwards RH, and Levey AI (1997) Subcellular localization and molecular topology of the dopamine transporter in the striatum and substantia nigra. *J.Comp.Neurol.* **388**:211-227.

Higgins CF (1992) ABC transporters: from microorganisms to man. *Annu.Rev.Cell Biol.* **8**:67-113.

Higgins CF and Gottesman MM (1992) Is the multidrug transporter a flippase? *Trends Biochem.Sci.* **17**:18-21.

Hoffman BJ, Mezey E, and Brownstein MJ (1991) Cloning of a serotonin transporter affected by antidepressants. *Science* **254**:579-580.

Huang Y, Lemieux MJ, Song J, Auer M, and Wang DN (2003) Structure and mechanism of the glycerol-3-phosphate transporter from *Escherichia coli*. *Science* **301**:616-620.

Humphreys CJ, Wall SC, and Rudnick G (1994) Ligand binding to the serotonin transporter: equilibria, kinetics, and ion dependence. *Biochemistry* **33**:9118-9125.

Jacobs BL and Fornal CA (1995) Serotonin and behavior: A general hypothesis, in Psychopharmacology: The Fourth Generation of Progress (Bloom F and Kupfer D eds), pp 461-469, Raven Press, New York.

Javitch JA (1998) Probing structure of neurotransmitter transporters by substituted-cysteine accessibility method. *Methods Enzymol.* **296**:331-346.

Jess U, Betz H, and Schloss P (1996) The membrane-bound rat serotonin transporter, SERT1, is an oligomeric protein. *FEBS Lett.* **394**:44-46.

Johnson RA, Eshleman AJ, Meyers T, Neve KA, and Janowsky A (1998) [^{3}H]substrate- and cell-specific effects of uptake inhibitors on human dopamine and serotonin transporter-mediated efflux. *Synapse* **30**:97-106.

Jung EK, Chin JJ, and Jung CY (1986) Structural basis of human erythrocyte glucose transporter function in reconstituted system. Hydrogen exchange. *J.Biol.Chem.* **261**:9155-9160.

Kaback HR, Sahin-Toth M, and Weinglass (2001) The Kamikaze approach to membrane transport. *Nat.Rev.Mol.Cell Biol.* **2**:610-620.

Kamdar G, Penado KM, Rudnick G and Stephan MM (2001) Functional role of critical stripe residues in transmembrane span 7 of the serotonin transporter. Effects of Na^+, Li^+, and methanethiosulfonate reagents. *J.Biol.Chem.* **276**:4038-4045.

Kanai Y and Hediger MA (1992) Primary structure and functional characterization of a high-affinity glutamate transporter. *Nature* **360**:467-471.

Kanner BI (2003) The interaction of the gamma-aminobutyric acid transporter GAT-1 with the neurotransmitter is selectively impaired by sulfhydryl modification of a conformationally sensitive cysteine residue engineered intro extracellular loop VI. *J.Biol.Chem.* **278**:3705-3712.

Kavanaugh MP, Bendahan A, Zerangue N, Zhang Y, and Kanner BI (1997) Mutation of an amino acid residue influencing potassium coupling in the glutamate transporter GLT-1 induces obligate exchange. *J.Biol.Chem.* **272**:1703-1708.

Kayano T, Burant CF, Fukumoto H, Gould GW, Fan YS, Eddy RL, Byers MG, Shows TB, Seino S, and Bell GI (1990) Human facilitative glucose transporters. Isolation, functional characterization, and gene localization of cDNAs encoding an isoform (GLUT5) expressed in small intestine, kidney, muscle, and adipose tissue and an unusual glucose transporter pseudogene-like sequence (GLUT6). *J.Biol.Chem.* **265**:13276-13282.

Khan AH and Pessin JE (2002) Insulin regulation of glucose uptake: a complex interplay of intracellular signalling pathways. *Diabetologia* **45**:1475-1483.

Kilic F and Rudnick G (2000) Oligomerization of serotonin transporter and its functional consequences. *Proc.Natl.Acad.Sci. USA* **97**:3106-3111.

Kilty JE, Lorang D, and Amara SG (1991) Cloning and expression of a cocaine-sensitive rat dopamine transporter. *Science* **254**:578-579.

Kitayama S, Shimada S, Xu H, Markham L, Donovan DM, and Uhl GR (1992) Dopamine transporter site-directed mutations differentially alter substrate transport and cocaine binding. *Proc.Natl.Acad.Sci. USA* **89**:7782-7785.

Kitayama S, Wang JB, and Uhl GR (1993) Dopamine transporter mutants selectively enhance MPP^+ transport. *Synapse* **15**:58-62.

Knoth J, Zallakian M, and Njus D (1981) Stoichiometry of H+-linked dopamine transporter in chromaffin granule ghosts. *J.Biol.Chem.* **260**:10981-10985.

Kubar J and Van Obberghen E (1989) Oligomeric states of the insulin receptor: binding and autophosphorylation properties. *Biochemistry* **28**:1086-1093.

Lee SH, Kang SS, Son H, and Lee YS (1998) The region of dopamine transporter encompassing the 3rd transmembrane domain is crucial for function. *Biochem.Biophys.Res.Commun.* **246**:347-352.

Li D, Randhawa VK, Patel N, Hayashi M, and Klip A (2001) Hyperosmolarity reduces GLUT4 endocytosis and increases its exocytosis from a VAMP2-independent pool in l6 muscle cells. *J.Biol.Chem.* **276**:22883-22891.

Lieb WR (1982) A kinetic approach to transport studies, in Red Cell Membrane: A Methodological Approach (Ellory JC and Young JD eds), pp 135-164, Academic Press, London.

Lin F, Lester HA, and Mager S (1996) Single-channel currents produced by the serotonin transporter and analysis of a mutation affecting ion permeation. *Biophys.J.* **71**:3126-3135.

Lin Z, Wang W, Kopajtic T, Revay RS, and Uhl GR (1999) Dopamine transporter: transmembrane phenylalanine mutations can selectively influence dopamine uptake and cocaine analog recognition. *Mol.Pharmacol.* **56**:434-447.

Lin Z, Wang W, and Uhl GR (2000) Dopamine transporter truptophan highlight candidate dopamine- and cocaine-selective domains. *Mol.Pharmacol.* **58**:1581-1592.

Liu Y, Peter D, Roghani A, Schuldiner S, Prive GG, Eisenberg D, Brecha N, and Edwards RH (1992) A cDNA that suppress MPP+ toxicity encodes a vesicular amine transporter. *Cell* **70**:539-551.

Locher KP, Lee AT, and Rees DC (2002) The E. coli BtuCD structure: a framework for ABC transporter architecture and mechanism. *Science* **296**:1091-1098.

MacAulay N, Bendahan A, Loland CJ, Zeuthen T, Kanner BI, and Gether (2001) Engineered Zn(2+) switches in the gamma-aminobutyric acid (GABA) transporter-1. *J.Biol.Chem.* **276**:40476-40485.

Mager S, Min C, Henry DJ, Chavkin C, Hoffman BJ, Davidson N, and Lester HA (1994) Conducting states of a mammalian serotonin transporter. *Neuron* **12**:845-859.

Maragakis NJ and Rothstein JD (2001) Glutamate transporters in neurologic disease. *Arch.Neurol.* **58**:365-370.

Marette A, Richardson JM, Ramlal T, Balon TW, Vranic M, Pessin JE, and Klip A (1992) Abundance, localization, and insulin-induced translocation of glucose transporters in red and white muscle. *Am.J.Physiol.* **263**:C443-C452.

McCarty NA (2000) Permeation through the CFTR chloride channel 8. *J.Exp.Biol.* **203**:1947-1962.

McKeegan KS, Borges-Walmsley MI, and Walmsley AR (2003) The structure and function of drug pumps: an update2. *Trends Microbiol.* **11**:21-29.

Merickel A, Rosandich P, Peter D, and Edward RH (1995) Identification of residues involved in substrate recognition by a vesicular monoamine transporter. *J.Biol.Chem.* **270**:25798-25804.

Merickel A, Kaback HR, and Edwards RH (1997) Charged residues in transmembrane domains II and XI of a vesicular monoamine transporter form a charge pair that promotes high affinity substrate recognition. *J.Biol.Chem.* **272**:5403-5498.

Mitsihata C, Kitayama S, Morita K, Vandenbergh D, Uhl D, and Dohi T (1998) Tyrosine-533 of rat dopamine transporter: involvement in interactions with 1-methyl-4-phenylpyridinium and cocaine. *Brain Res.Mol. Brain Res.* **56**:84-88.

Moore KR and Blakely RD (1994) Restriction site-independent formation of chimeras from homologous neurotransmitter-transporter cDNAs. *Biotechniques* **17**:130-137.

Mortensen OV, Kristensen AS, and Wiborg O (2001) Species-scanning mutagenesis of the serotonin transporter reveals essential in selective, high-affinity recognition of antidepressants. *J.Neurochem.* **79**:237-247.

Murakami S, Nakashima R, Yamashita E, and Yamaguchi A (2002) Crystal structure of bacterial multidrug efflux transporter AcrB. *Nature* **419**:587-593.

Nelson N (1998) The family of Na+/Cl- neurotransmitter transporters. *J.Neurochem.* **71**:1785-1803.

Nelson PJ and Rudnick G (1982) The role of chloride ion in platelet serotonin transport. *J.Biol.Chem.* **257**:6151-6155.

Neyfakh AA (2002) Mystery of multidrug transporters: the answer can be simple. *Mol.Microbiol.* **44**:1123-1130.

Nguyen ML, Cox GD, and Parsons SM (1998) Kinetic parameters for the vesicular acetylcholine transporter: twp protons are exchange for one acetylcholine. *Biochemistry* **37**:13400-13410.

Ni YG, Chen JG, Androutsellis-Theotokis A, Huang CJ, Moczydlowski E, and Rudnick G (2001) A lithium-induced conformational change in serotonin transporter alters cocaine binding, ion conductance, and reactivity of Cys-109. *J.Biol.Chem.* **276**:30942-30947.

Norgaard-Nielsen K, Norregaard L, Hastrup H, Javitch JA, and Gether U (2002) Zn(2+) site engineered at the oligomeric interface of the dopamine transporter. *FEBS Lett.* **524**:87-91.

Norregaard L, Frederiksen D, Nielsen EO, and Gether U (1998) Deliniation of an endogenous zinc-binding site in the human dopamine transporter. *EMBO J.* **17**:4266-4273.

Norregaard L, Visiers I, Loland CJ, Ballesteros J, Weinstein H, and Gether U (2000) Structural probing of a microdomain in the dopamine transporter by engineering of artificial Zn^{2+} binding sites. *Biochemistry* **39**:15836-15846.

Norregaard L, Loland CJ, and Gether U (2003) Evidence for distinct sodium-, dopamine-, and cocaine-dependent conformational changes in transmembrane segment 7 and 8 of the dopamine transporter. *J.Biol.Chem.* **278**:30587-30596.

O'Shea RD (2002) Roles and regulation of glutamate transporters in the central nervous system. *Clin.Exp.Pharmacol.Physiol.* **29**:1018-1023.

Olivares L, Aragon C, Gimenez C, and Zafra F (1997) Analysis of the transmembrane topology of the glycine transporter GLYT1. *J.Biol.Chem.* **272**:1211-1217.

Olson AL and Pessin JE (1996) Structure, function, and regulation of the mammalian facilitative glucose transporter gene family. *Annu.Rev.Nutr.* **16**:235-256.

Oulianova N and Berteloot A (1996) Sugar transport heterogeneity in the kidney: two independent transporters or different transport modes through an oligomeric Protein? 1. Glucose transport studies. *J.Membr.Biol.* **153**:181-194.

Pacholczyk T, Blakely RD, and Amara SG (1991) Expression cloning of a cocaine- and antidepressant-sensitive human noradrenaline transporter. *Nature* **350**:350-354.

Pantanowitz S, Bendahan A, and Kanner BI (1993) Only one of the charged amino acids located in the transmembrane alpha-helics of the gamma-aminobutyric transporter (subtype A) is essential for its activity. *J.Biol.Chem.* **268**:3222-3225.

Parson SM (2000) Transport mechanism in acetylcholine and monoamine storage. *FASEB J.* **14**:2434-2434.

Penado KM, Rudnick G and Stephan MM (1998) Critical Amino Acid Residues in Transmembrane Span 7 of the Serotonin Transporter Identified by Random Mutagenesis. *J.Biol.Chem.* **273**:28098-28106.

Petersen CI and DeFelice LJ (1999) Ionic interactions in the *Drosophila* serotonin transporter identify it as a serotonin channel. *Nat.Neurosci.* **2**:605-610.

Pifl C, Agneter E, Drobny H, Reither H, and Singer EA (1997) Induction by low Na^+ or Cl^- of cocaine sensitive carrier-mediated efflux of amines from cells transfected with the cloned human catecholamine transporters. *Br.J.Pharmacol.* **121**:205-212.

Pifl C and Singer EA (1999) Ion dependence of carrier-mediated release in dopamine or norepinephrine transporter-transfected cells questions the hypothesis of facilitated exchange diffusion. *Mol.Pharmacol.* **56**:1047-1054.

Pines G, Danbolt NC, Bjoras M, Zhang Y, Bendahan A, Eide L, Koepsell H, Storm-Mathisen J, Seeberg E, and Kanner BI (1992) Cloning and expression of a rat brain L-glutamate transporter. *Nature* **360**:464-467.

Qian Y, Galli A, Ramamoorthy S, Risso S, DeFelice LJ, and Blakely RD (1997) Protein kinase C activation regulates human serotonin transporters in HEK-293 cells via altered cell surface expression. *J.Neurosci.* **17**:45-57.

Ramamoorthy S, Bauman AL, Moore KR, Han H, Yangfeng T, Chang AS, Ganapathy V, and Blakely RD (1993) Antidepressant- and cocaine-sensitive human serotonin transporter-molecular-cloning, expression, and chromosomal localization. *Proc.Natl.Acad.Sci. USA* **90**:2542-2546.

Ravna AW and Edvardsen O (2001) A putative three-dimensional arrangement of the human serotonin transporter transmembrane helices: a tool to aid experimental studies. *J.Mol.Graph.Model.* **20**:133-144.

Ravna AW, Sylte I, and Dahl SG (2003a) Molecular mechanism of citalopram and cocaine interactions with neurotransmitter transporters. *J.Pharmacol.Exp.Ther.* **307**:34-41.

Ravna AW, Sylte I, and Dahl SG (2003b) Molecular model of the neural dopamine transporter. *J.Comput. Aided Mol.Des.* **17**:367-382.

Rios CD, Jordan BA, Gomes I, and Devi LA (2001) G-protein-coupled receptor dimerization: modulation of receptor function. *Pharmacol.Ther.* **92**:71-87.

Robinson MB and Dowd LA (1997) Heterogeneity and functional properties of subtypes of sodium-dependent glutamate transporters in the mammalian central nervous system. *Adv.Pharmacol.* **37**:69-115.

Rodriguez GJ, Roman DL, White KJ, Nichols DE, and Barker EL (2003) Distinct recognition of substrates by the human and *Drosophila* serotonin transporters. *J.Pharmacol.Exp.Ther.* **306**:338-346.

Roman DL, Walline CC, Rodriguez GJ, and Barker EL (2003a) Interactions of antidepressants with the serotonin transporter: a contemporary molecular analysis. *Eur.J.Pharmacol.* **479**:53-63.

Roman DL, Saldana SN, Nichols DE, Carroll FI, and Barker EL (2003b) Distinct molecular recognition of psychostimulant by human and *Drosophila* serotonin transporters. *J.Pharmacol.Exp.Ther.* in press.

Rosenberg MF, Velarde G, Ford RC, Martin C, Berridge G, Kerr ID, Callaghan R, Schmidlin A, Wooding C, Linton KJ, and Higgins CF (2001) Repacking of the transmembrane domains of P-glycoprotein during the transport ATPase cycle. *EMBO J.* **20**:5615-5625.

Roubert C, Cox PJ, Bruss M, Hamon M, Bonisch H, and Giros B (2001) Determination of residues in the norepinephrine transporter that are critical for tricyclic antidepressant affinity. *J.Biol.Chem.* **276**:8254-8260.

Rudnick G and Wall SC (1992a) para-Chloroamphetamine induces serotonin release through serotonin transporters. *Biochemistry* **31**:6710-6718.

Rudnick G and Wall SC (1992b) The molecular mechanism of ecstasy [3,4-methylenedioxy-methamphetamine (MDMA)] serotonin transporters are targets for MDMA-induced serotonin release. *Proc.Natl.Acad.Sci. USA* **89**:1817-1821.

Rudnick G and Wall SC (1993) Non-neurotoxic amphetamine derivatives release serotonin through serotonin transporters. *Mol.Pharmacol.* **44**:1227-1231.

Rudnick G (1998) Ion-coupled neurotransmitter transport: thermodynamic vs. kinetic determination stoichiometry. *Methods Enzymol.* **296**:233-247.

Saldana SN and Barker EL (2004) Temperature and 3,4-methylenedioxymethamphetamine alter human serotonin transporter-mediated dopamine uptake. *Neurosci.Lett.* **16**:209-212.

Saunders C, Ferrer JV, Shi L, Chen J, Merrill G, Lamb ME, Leeb-Lundberg LM, Carvelli L, Javitch JA, and Galli A (2000) Amphetamine-induced loss of human dopamine transporter activity: an internalization-dependent and cocaine-sensitive mechanism. *Proc.Natl.Acad.Sci. USA* **97**:6850-6855.

Schmid JA, Just H, and Sitte HH (2001a) Impact of oligomerization on the function of the human serotonin transporter. *Biochem.Soc.Trans.* **29**:732-736.

Schmid JA, Scholze P, Kudlacek O, Freissmuth M, Singer EA, and Sitte HH (2001b) Oligomerization of the human serotonin transporter and of the rat GABA transporter 1 visualized by fluorescence resonance energy transfer microscopy in living cells. *J.Biol.Chem.* **276**:3805-3810.

Scholze P, Zwach J, Kattinger A, Pifl C, Singer EA, and Sitte HH (2000) Transporter-mediated release: a superfusion study on human embryonic kidney cells stably expressing the human serotonin transporter. *J.Pharmacol.Exp.Ther.* **293**:870-878.

Scholze P, Freissmuth M, and Sitte HH (2002) Mutations within an intramembrane leucine heptad repeat disrupt oligomer formation of the rat GABA transporter 1. *J.Biol.Chem.* **277**:43682-43690.

Seal RP, Shigeri Y, Eliasof S, Leighton BH, and Amara SG (2001) Sulfhydryl modification of V449C in the glutamate transporter EAAT1 abolishes substrate transport but not the substrate-gated anion conductance. *Proc.Natl.Acad.Sci. USA* **98**:15324-15329.

Shirvan A, Laskar O, Steiner-Mordoch S, and Schuldiner S (1994) Histidine-419 plays a role in energy coupling in the vesicular monoamine transporter from rat. *FEBS Letts.* **12**:145-150.

Sitte HH, Huck S, Reither H, Boehm S, Singer EA, and Pifl C (1998) Carrier-mediated release, transport rates, and charge transfer induced by amphetamine, tyramine, and dopamine in mammalian cells transfected with the human dopamine transporter. *J.Neurochem.* **71**:1289-1297.

Sitte HH, Hiptmair B, Zwach J, Pifl C, Singer EA, and Scholze P (2001) Quantitative analysis of inward and outward transport rates in cells stably expressing the cloned human serotonin transporter: inconsistencies with the hypothesis of facilitated exchange diffusion. *Mol.Pharmacol.* **59**:1129-1137.

Sitte HH, Scholze P, Schloss P, Pifl C, and Singer EA (2000) Characterization of carrier-mediated efflux in human embryonic kidney 293 cells stably expressing the rat serotonin transporter: a superfusion study. *J.Neurochem.* **74**:1317-1324.

Slotboom DJ, Konings WN, and Lolkema JS (2001a) Cysteine-scanning mutagenesis reveals a highly amphipathic, pore-lining membrane-spanning helix in the glutamate transporter GltT. *J.Biol.Chem.* **276**:10775-10781.

Slotboom DJ, Konings WN, and Lolkema JS (2001b) Glutamate transporters combine transporter- and channel-like features. *Trends Biochem.Sci.* **26**:534-539.

Slotboom DJ, Sobczak I, Konings WN, and Lolkema JS (1999) A conserved serine-rich stretch in the glutamate transporter family forms a substrate-sensitive reentrant loop. *Proc.Natl.Acad.Sci. USA* **96**:14282-14287.

Sorkina T, Doolen S, Galperin E, Zahniser NR, and Sorkin A (2003) Oligomerisation of dopamine transporters visualized in living cells by fluorescence resonance energy transfer microscopy. *J.Biol.Chem.* **278**:28274-28283.

Stein WD (1986) Transport Difussion Across Cell Membrane, pp 231-237. American Press Inc, London.

Sten-Kurdsen O (1978) Passive transport processes, in Membrane Transport in Biology (Giebish G, Tosteson DC, and Ussing HH eds) pp 5-114, Springer-Verlag, New York.

Storck T, Schulte S, Hofmann K, and Stoffel W (1992) Structure, expression, and functional analysis of a Na(+)-dependent glutamate/aspartate transporter from rat brain. *Proc.Natl.Acad.Sci. USA* **89**:10955-10959.

Strader CD, Candelore MR, Hill WS, Sigal IS, and Dixon RA (1989) Identification of two serine residues involved in agonist activation of the beta-adrenergic receptor. *J.Biol.Chem.* **264**:13572-13578.

Sun H and Nathans J (2000) ABCR: rod photoreceptor-specific ABC transporter responsible for Stargardt disease. *Methods Enzymol.* **315**:879-897.

Sur C, Betz H, and Schloss P (1997) A single serine residue controls the cation dependence of substrate transport by the rat serotonin transporter. *Proc.Natl.Acad.Sci. USA* **94**:7639-7644.

Tamura S, Nelson H, Tamura A, and Nelson N (1995) Short external loops as potential substrate binding site of gamma-aminobutyric acid transporters. *J.Biol.Chem.* **270**:28712-28715.

Torres GE, Carneiro A, Seamans K, Fiorentini C, Sweeney A, Yao WD, and Caron MG (2003a) Oligomerization and trafficking of the human dopamine transporter - Mutational analysis identifies critical domains important for the functional expression of the transporter. *J.Biol.Chem.* **278**:2731-2739.

Torres GE, Gaintdinov RR, and Caron MG (2003b) Plasma membrane monoamine transporters: structure, regulation, and function. *Nat.Rev.Neurosci.* **4**:13-25.

Turk E, Kerner CJ, Lostao MP, and Wright EM (1996) Membrane topology of the human Na+/glucose cotransporter SGLT1. *J.Biol.Chem.* **271**:1925-1934.

Turner RJ and Moran A (1982) Heterogeneity of sodium-dependent D-glucose transport sites along the proximal tubule: evidence from vesicle studies. *Am.J.Physiol* **242**:F406-F414.

Vaughan RA, Gaffaney JD, Lever JR, Reith ME, and Dutta AK (2001) Dual incorporation of photoaffinity ligands on dopamine transporters implicated proximity of labeled domains. *Mol.Pharmacol.* **59**:1157-1164.

Waddell ID, Zomerschoe AG, Voice MW, and Burchell A (1992) Cloning and expression of a hepatic microsomal glucose transport protein. Comparison with liver plasma-membrane glucose-transport protein GLUT 2. *Biochem.J.* **286**:173-177.

Walker JE, Saraste M, Runswick MJ, and Gay NJ (1982) Distantly related sequences in the alpha- and beta-subunits of ATP synthase, myosin, kinases and other ATP-requiring enzymes and a common nucleotide binding fold. *EMBO J.* **1**:945-951.

Wall SC, Gu H, and Rudnick G (1995) Biogenic-amine flux mediated by cloned transporters stably expressed in cultured-cell lines - amphetamine specificity for inhibition and efflux. *Mol.Pharmacol.* **47**:544-550.

Walmsley AR, Barrett MP, Bringaud F, and Gould GW (1998) Sugar transporters from bacteria, parasites and mammals: structure-activity relationships. *Trends Biochem. Sci.* **23**:476-481.

Wardzala LJ, Cushman SW, and Salans LB (1978) Mechanism of insulin action on glucose transport in the isolated rat adipose cell. Enhancement of the number of functional transport systems. *J.Biol.Chem.* **253**:8002-8005.

Weihe E and Eiden LE (2000) Vesicular amine transporter expression in amine-handling cells of the nervous, endocrine, and inflammatory system. *FASEB J.* **14**:243-2449.

White FJ (1998) Cocaine and the serotonin saga. *Nature* **393**:118-119.

Zarbiv R, Grunewald M, Kavanaugh MP, and Kanner BI (1998) Cysteine scanning of the surroundings of an alkali-ion binding site of the glutamate transporter GLT-1 reveals a conformationally sensitive residue. *J.Biol.Chem.* **273**:14231-14237.

Zerangue N and Kavanaugh MP (1996) Flux coupling in a neuronal glutamate transporter. *Nature* **383**:634-637.

VITA

VITA

Gustavo J. Rodríguez born on November 5, 1976 to Andres Rodríguez and Mercedes Roman in Ponce, Puerto Rico. He is the younger of two children. During his years in the Thomas Armstrong High School, he worked with Ms. Marta Rivera Chamorro and Prof. Jose Rodríguez studying the distribution of termite populations in the Aguirre Forest. Gustavo presented the results of his studies in the International Science and Engineering Fair at Birmingham, AL representing his country. After graduating from High School, Gustavo attended The University of Puerto Rico-Mayagüez campus where he studied chemistry. At college, Gustavo MARC Fellow and worked for Drs. Cynthia Robledo and Marisol Vera in the Department was of Chemistry performing synthesis and spectroscopic analysis of dipeptides. In the summer of 1997, he participated in the Avon Summer program at the Cornell University School of Medicine in New York, NY. Gustavo presented his results in several meeting in Puerto Rico and The United States. After completing his undergraduate degree in June 1998, Gustavo moved to West Lafayette, IN where he continued a Ph.D. in Medicinal Chemistry and Molecular Pharmacology Department at Purdue University School of Pharmacy. Gustavo joined Dr. Eric L. Barker laboratory in January 1999 and spend the next 5 years investigating the molecular mechanism of serotonin translocation trough the serotonin transporter. Gustavo is the author or coauthor in two article published and several poster presentations. Gustavo was selected for the APA Minority Fellowship in Neuroscience (1999-2002) and the ASPET Minority Travel award (2003). Gustavo completed the requirements for the Ph.D. from Purdue University in January, 2004. He began his post-doctoral training with Dr. Theodore Wensel at the Baylor College of Medicine, Houston, TX in March 2004.